AD-A158 973 SHIFT-VARIANT MULTIDIMENSIONAL SYSTEMS(U) PITTSBURGH UNIV PA DEPT OF ELECTRICAL ENGINEERING N K BOSS 29 MAY 85 AFOSR-TR-85-0724 AFOSR-83-0038 1/2

UNCLASSIFIED F/G 12/1 NL

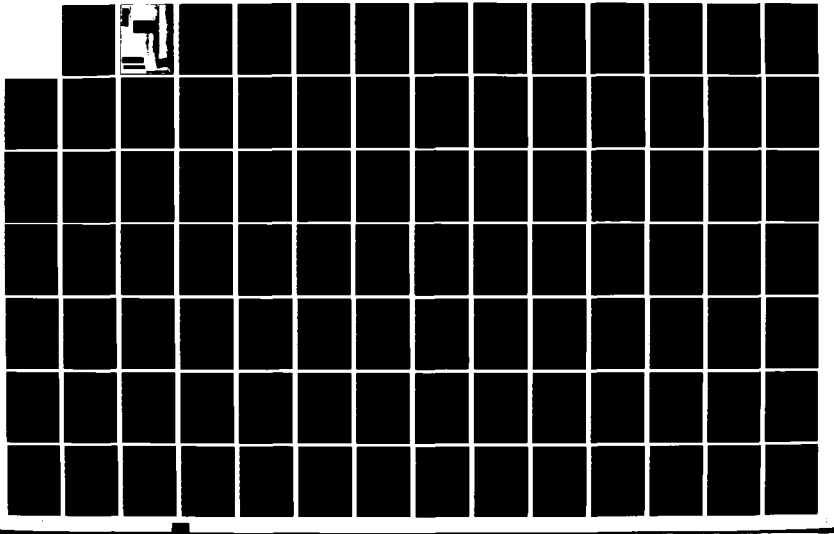

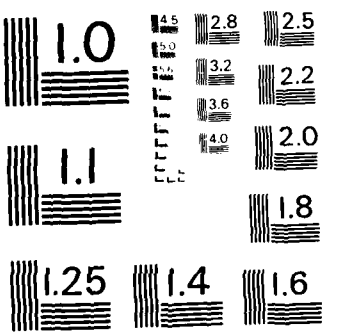

AFOSR-TR- 85-0724

Final Research Report

AFOSR Grant 83-0033

Period: 2-1-83 to 8-31-84

P.I.: Dr. N.F. Ness

85 09 029

Unclassified

SECURITY CLASSIFICATION OF THIS PAGE

REPORT DOCUMENTATION PAGE

1a. REPORT SECURITY CLASSIFICATION: Unclassified	1b. RESTRICTIVE MARKINGS
2a. SECURITY CLASSIFICATION AUTHORITY	3. DISTRIBUTION/AVAILABILITY OF REPORT: Approved for Public Release - Distribution Unlimited
2b. DECLASSIFICATION/DOWNGRADING SCHEDULE	
4. PERFORMING ORGANIZATION REPORT NUMBER(S)	5. MONITORING ORGANIZATION REPORT NUMBER(S): AFOSR-TR- 85-0724
6a. NAME OF PERFORMING ORGANIZATION: University of Pittsburgh; 6b. OFFICE SYMBOL (If applicable)	7a. NAME OF MONITORING ORGANIZATION: Air Force Office of Scientific Research
6c. ADDRESS (City, State and ZIP Code): Department of Electrical Engineering, University of Pittsburgh, Pittsburgh, PA 15261	7b. ADDRESS (City, State and ZIP Code): Division of Mathematical and Information Sciences; Bolling Air Force Base, Washington, DC 20332
8a. NAME OF FUNDING/SPONSORING ORGANIZATION: Air Force Office of Scientific Research; 8b. OFFICE SYMBOL (If applicable): AFOSR/NM	9. PROCUREMENT INSTRUMENT IDENTIFICATION NUMBER: Department of the Air Force Grant No. AFOSR-83-0038
8c. ADDRESS (City, State and ZIP Code): Division of Mathematical and Information Sciences; Bolling Air Force Base, Washington, DC 20332	10. SOURCE OF FUNDING NOS. — PROGRAM ELEMENT NO.: 61102F; PROJECT NO.: 2304; TASK NO.: A6; WORK UNIT NO.:
11. TITLE (Include Security Classification): Shift-Variant Multidimensional Systems	
12. PERSONAL AUTHOR(S): Professor N.K. Bose	
13a. TYPE OF REPORT: Final; 13b. TIME COVERED: FROM 2/1/83 TO 3/31/85	14. DATE OF REPORT (Yr., Mo., Day): 5/29/85; 15. PAGE COUNT:
16. SUPPLEMENTARY NOTATION	

17. COSATI CODES			18. SUBJECT TERMS (Continue on reverse if necessary and identify by block number)
FIELD	GROUP	SUB. GR.	Multidimensional systems; State-space model; Spatio-temporal processing; Image Restoration; Shift-variant systems; Bilinear degradation

19. ABSTRACT (Continue on reverse if necessary and identify by block number)

Procedures for compensating for effects which degrade the accuracy of remotely sensed datas by mathematically inverting some of the degrading phenomenon are required in biomedical, industrial, surveilance and earth and space applications. Images to be restored are often degraded by a linear spatially varying operation. Degradations due to motion blurring and optical system distortions often require the imaging systems to be analyzed by modeling the degradation as a linear shift-invariant motion blur, but counterparts of such techniques in the shift-variant case is severely handicapped by the required space-time computational complexity. Furthermore, a systematic approach for handling the analysis of multidimensional shift-variant systems remainsto be developed in view of some of the basic differences between the properties of shift-invariant and shift-variant systems. For example, the crucial factor of determining the best sampling rate in digital implementations of analog shift-variant systems is considerably complicated by the fact that for the shift-variant case, the output bandwidth can exceed the input band-

20. DISTRIBUTION/AVAILABILITY OF ABSTRACT: UNCLASSIFIED/UNLIMITED ☒ SAME AS RPT. ☐ DTIC USERS ☐	21. ABSTRACT SECURITY CLASSIFICATION: Unclassified
22a. NAME OF RESPONSIBLE INDIVIDUAL: Maj. Woodruff; Professor N.K. Bose, Principal Investigator	22b. TELEPHONE NUMBER (Include Area Code): (202) 767-5027; ~~412-624-5405~~
	22c. OFFICE SYMBOL: NM

DD FORM 1473, 83 APR EDITION OF 1 JAN 73 IS OBSOLETE.

SECURITY CLASSIFICATION OF THIS PAGE

width.

The research being reported was directed to the alleviation of the shortcomings referred to above. The following specific results have been obtained. For any 2-D discrete first quadrant quarter-plane causal linear shift-variant (LSV) system, whose impulse response is a K-th order degenerate sequence, a K-th order state-space model was obtained. This model is recursive and is based on a three-term recurrence formula relating any point in the state-space to its three closest neighboring points and the current input. The state-space model was extended in order to model 2-D discrete LSV systems with support on a causality cone. Subsequently, the 2-D quarter-plane causal and weakly causal discrete models were generalized to the n-D(n>2) case. The resulting state-space models are recursive and are based on a (2^n-1)-points recurrence formula, which for the causal case uses the (2^n-1)-closest neighboring points in addition to the input in order to compute any current output state. For the weakly causal case, the (2^n-1) computed outputs required are not, in general, the closest neighbors to the output presently being computed. Conditions for the existence of a 2-D state-space model for the inverse system were obtained and with these conditions satisfied, a state-space model of the inverse system is readily derivable from the original one. Models for the 2-D LSV system and its inverse can be used to perform analysis and deconvolution problems very efficiently. This was substantiated from derived expressions for space-time computational complexities.

Examples of physically motivated applications making use of the theoretical results developed have been worked out. These applications include effects of 1-D LSV motion blur and the blurring due to Seidel aberration of a lens; in particular, the 2-D LSV coma aberration was studied in detail. The reconstruction of the original object from the LSV blurred image was carried out successfully by means of the state-space model for the inverse system. For the construction of the state-space model, the impulse responses of the blurring phenomena were approximated in a degenerate form via series expansion using orthogonal functions.

The problem of restoring images degraded by phenomena, which can be modeled by linear shift-invariant systems, has been discussed above. Sometimes, the degrading phenomena may not be accurately modeled by systems that are restricted to be linear. In such cases, the incorporation of the second-order term of a Volterra series (characterizing the input/output behavior of the nonlinear system), which forms a class of bilinear systems, improves substantially the measure of adequacy for the model. This type of bilinear system occurs in imaging through turbulent atmosphere, coherent imaging through systems with time-varying pupils, etc. Recent research results on bilinearly distorted images are available based on finite impulse response linear digital filtering and Bayesian methods. Here, additional methods have been investigated for restoring images, which are distorted by a system that is describable by the second-order term of the Volterra series. When the blurring phenomenon is nonlinear and can be modeled either by a shift-invariant of shift-variant bilinear system, the data restoration problem can be most conveniently formulated as a special system of linear equations with nonnegative coefficients whose solution is required to satisfy constraints like nonnegativity in addition to being factorable with the factors having a certain characterizing property. An algorithm implementing this objective along with another important alternative applicable to a specialized model are discussed in the research report.

TABLE OF CONTENTS

Items

A-1

b. Research Objectives

To a great extent the techniques for analysis and restoration of images has been developed under the assumption that the system is linear shift-invariant (LSI). These techniques are successful in some cases because a system which is diffraction-limited or a system whose object plane undergoes uniform linear motion perpendicular to the system reference axis does indeed satisfy these assumptions. However, LSI systems are singled out for study mainly because of the widespread understanding of the Fourier Transform theory along with well-known fast algorithms for its implementation. In comparison with LSI systems, very little work has been done on linear shift-variant (LSV) systems. Most of the research on two dimensional (2-D) LSV systems has been done on restoration techniques by means of coordinate transformations. This technique, decomposes the LSV system into a distortion of the input plane followed by a shift-invariant operation and terminated by a distortion of the output plane. Essentially, the shift-variant problem is transformed into a shift-invariant one and the deconvolution or inverse filtering is done with the well-known shift-invariant methods for this purpose. The main drawback of image restoration by coordinate transformation is that it can only be applied to a limited class of LSV systems. For one dimensional (1-D) LSV systems, there has been some research activity and most of the work has to do with the reconstruction of motion degraded images. Besides the already mentioned approaches to image restoration based on

coordinate transformations, some methods have used 1-D state-space models for a class of LSV systems. At present the technique for analysis and deconvolution of LSV systems are either applicable to the 1-D case or to a very restrictive class of 2-D LSV systems. It is important to note that the characterization of a LSV system by means of the superposition integral or the superposition sum holds in general, but it is completely impractical for the analysis and the deconvolution of LSV systems. Therefore, we can conclude that there is a great need for an efficient and convenient model for LSV systems which will permit the analysis and deconvolution in a simple form.

One of the primary objectives of this research has been to provide not only a mathematical structure for the state-space modeling of discrete LSV systems but to apply this model to the problems of efficient analysis and deconvolution of multidimensional systems. It is expected that the state-space model will be useful in system analysis and synthesis. The state-space model should be useful in solving the problem of deconvolution very efficiently. In fact, for the noise-free case the deconvolution scheme developed from the state-space model is considerably more efficient from space as well as time computational complexity standpoints than other techniques which are currently available.

A portion of the time for the proposed research was also devoted to the approximation problem of specified 2-D linear shift-variant impulse responses by K-th order degenerate approximants.

Several applications require the restoration of bilinearly degraded images. For example, in coherent optical image processing, the bilinear term in the Volterra series expansion plays an important role due to the nonlinear nature of partially coherent image formation. The problem of restoration of images distorted by nonlinear nonzero-spread systems, which appear quite frequently in real world problems have not been systematically tackled. Therefore, portion

of the research effort was directed to the development of algorithms for digital restoration of bilinearly degraded images (shift-invariant as well as shift-variant).

c. Details of Research Results Obtained

The primary outcomes of the research effort are in the following two categories:

1. Linear shift-variant multidimensional systems.
2. Restoration of bilinearly degraded images.

Detailed documentation of results obtained in the above mentioned areas are contained in the succeeding pages of this report.

LINEAR SHIFT-VARIANT MULTIDIMENSIONAL SYSTEMS[†]

H. M. Valenzuela and N. K. Bose
348 Benedum Hall
University of Pittsburgh
Pittsburgh, PA 15261
U.S.A.

[†]This work was based on research conducted under AFOSR Grant #83-0038 and is to appear as a chapter in the book "Multidimensional Systems Theory: Progress, Directions, and Open Problems" to be published by D. Reidel Publishing Company, Dordecht, Holland.

Chapter 5

LINEAR SHIFT-VARIANT MULTIDIMENSIONAL SYSTEMS

5.1 Introduction

The study of 1-D time-varying systems, now well-documented in the literature, was motivated to a great extent by the need to design adaptive control systems, where the parameters of the controller are adjusted to counterbalance the fluctuations in process dynamics stemming from changes in environment. For example, variations of flight conditions (including flight speed) of supersonic aircrafts and missiles during rapid ascent through the atmosphere introduce time-varying parameter variations. In space flight, relevant problems that had to be tackled included those [5.1] of transferring a space vehicle from one orbit to another, rendezvous and interplanetary guidance. The development of the rigid-body equations of motion of artificial satellites requires accounting for cyclic variations of inertial torques that occur as the vehicle progresses in its orbit. Similarly, successful solution of the satellite rendezvous problem requires dealing with the combined complexity of both mass and orbital variations, for with both the target and interceptor in orbit, the interceptor must expend fuel-mass in maneuvering; further, the kinematics of interceptor guidance introduce additional time-varying parameters forcing the characterizing differential equations to have both periodic and aperiodic coefficients. Also of interest is a class of problems which relate to the gyroscopic stabilization of orbiting satellites. In circuit and systems

theory specific applications concerned with the theory of modulators, parametric amplifiers and harmonic generators use linear circuits with periodically varying parameters [5.2].

The developed tools of multidimensional systems theory, as documented in [5.3], provide scopes for considerable applications in a broad range of problems. However, over the last few years, it is fair to say that the theory of linear shift-invariant (LSI) two or more dimensional systems have been well understood. However, with the increased activities in the area of image processing (optical and digital) many physical problems are charaterizable by a 2-D linear integral operator,

$$g(x,y) = \int_{-\infty}^{\infty} \int_{-\infty}^{\infty} f(u,v)\, h(x,y;u,v)\, dv$$

where g(x,y), f(x,y) are, respectively, the output and input while h(x,y;u,v) is the system response at (x,y) to an unit impulse applied at (u,v). The presence of additive noise in the preceding input-output model of a physical process could also be expected. In 1977, Goodman state that "the type of coherent optical processing which is by far the least explored to date is that of linear space-variant filtering" [5.4], and the importance of overcoming this deficiency was realized because space-variant processing is required in various optical and digital data processing applications including restoration of images degraded either by space-variant aberrations or space-variant motion blur, restoration of radiographs blurred by a space-variant source penumbra, restoration of rotation blur of 2-D patterns where different objects

suffer from different blur according to their distance from the center of rotation and also their angular positions [5.5], and performance of particular transformations (like the Mellin transform and Abel transform). Also, emerging applications in areas like robotic vision, have necessitated the development of techniques suitable for recognition patterns which may be subjected to the effects of unknown rotation and scaling. One such technique is based on the use of scaled transform (a modified Fourier transform), which have been shown to be equivalent to a class of linear shift-variant (LSV) filters, referred to as the class of "form-invariant" filters [5.6].

Actually, the problem of 2-D images degraded by spatially varying point spread functions has been tackled since about the early seventies. Sawchuk [5.7] transformed the spatially varying problem to a spatially invariant one via coordinate transformations and as a result some generality in the approach had to be sacrificed, especially with the presence of additive noise. In that situation, however, statistics of the noise and object random processes could change under a geometrical coordinate transformation. The usual assumption of the minimum mean-square error estimation (MMSE) method is that these statistics are jointly stationary, and this may not be valid in many cases. Frieden [5.8] developed a positive (an incoherent object scene is a spatial radiance distribution and cannot be negative) restoring formula from a statistical communication theory model of image formation by which the optimal restored object from a set of candidate objects is required to obey a principle of maximum entropy. Frieden's approach, though

The particular structure of the matrices in (5.34) to (5.36) will allow us to perform the summation in (5.32) by means of a (2^k-1)-point recursion. This recursion will be a generalization to k-dimensions ($k > 2$) of the recursion in (5.10) and the justification will be developed next. To do this, the following definitions are, first, introduced.

Definition 5.3: The $\prod_{j=1}^{k}(n_j+1)$ row-vector $\underline{\delta}_k^{i_1 i_2 \ldots i_k}$ is defined as

$$\underline{\delta}_k^{i_1 i_2 \ldots i_k} \triangleq [\underline{0}\ \underline{0}\ \ldots\ \underline{0}\ \underline{\delta}_{k-1}^{i_2 i_3 \ldots i_k}\ \underline{0}\ \ldots\ \underline{0}], \quad (5.37)$$

(i_1+1)-th block position from the right

where $\underline{0}$ is a $\prod_{j=2}^{k}(n_j+1)$ row-vector of zeros, there are n_1 such $\underline{0}$ vectors, and the position of the remaining nonzero row-vector is indicated above. Furthermore, the (n_k+1) row-vector $\underline{\delta}_1^{i_k}$ is defined as

$$\underline{\delta}_1^{i_k} \triangleq [0\ \ 0\ \ldots\ 0\ \ 1\ \ 0\ \ldots\ 0]. \quad (5.38)$$

(i_k+1)-th position from the right

Definition 5.4: $\underline{\delta}_k(j) \triangleq$ sum of all $\binom{k}{j}$ distinct vectors $\underline{\delta}_k^{i_1 i_2 \ldots i_k}$ with $i_\ell = \begin{matrix}0\\ \text{or}\\ 1\end{matrix}$ $(\ell=1,2,\ldots,k)$ and $i_1+i_2+\ldots+i_k=j$.

Definition 5.5: $\underline{\delta}_{k+1}^{i}(j) \triangleq$ sum of all $\binom{k}{j}$ distinct vectors

where,

$$\underline{B}^{i_1..i_\ell}_{i,k-\ell}(n_{\ell+1},..,n_k) = \begin{bmatrix} \underline{B}^{i_1..i_\ell 0}_{i,k-\ell-1}(n_{\ell+2},..,n_k) & & \\ \underline{B}^{i_1..i_\ell 0}_{i,k-\ell-1}(n_{\ell+2},..,n_k) & \underline{B}^{i_1..i_\ell 1}_{i,k-\ell-1}(n_{\ell+2},..,n_k) & \\ \vdots & \vdots & \\ \underline{B}^{i_1..i_\ell 0}_{i,k-\ell-1}(n_{\ell+2},..,n_k) & \underline{B}^{i_1..i_\ell 1}_{i,k-\ell-1}(n_{\ell+2},..,n_k) & \cdots \ \underline{B}^{i_1..i_\ell n_{\ell+1}}_{i,k-\ell-1}(n_{\ell+2},..,n_k) \end{bmatrix}, \quad (5.35)$$

$$\ell=1,2,\ldots,k-2,\ i_j=0,1,\ldots,n_j,\ j=1,2,\ldots,\ell$$

5.16

$$\underline{B}^{i_1..i_{k-2}\,r}_{i,1}(n_k) = \begin{bmatrix} B_i(i_1,..,i_{k-2},r,0) & & \\ B_i(i_1,..,i_{k-2},r,0) & B_i(i_1,..,i_{k-2},r,1) & \\ \vdots & \vdots & \\ B_i(i_1,..,i_{k-2},r,0) & B_i(i_1,..,i_{k-2},r,1) & \cdots \ B_i(i_1,..,i_{k-2},r,n_k) \end{bmatrix}. \quad (5.36)$$

$$r=0,1,\ldots,n_{k-1}$$

5.15

$$\underline{B}_{i,k}(n_1,..,n_k) = \begin{bmatrix} \underline{B}^0_{i,k-1}(n_2,..,n_k) & & \\ \underline{B}^0_{i,k-1}(n_2,..,n_k) & \underline{B}^1_{i,k-1}(n_2,..,n_k) & \\ \vdots & \vdots & \\ \underline{B}^0_{i,k-1}(n_2,..,n_k) & \underline{B}^1_{i,k-1}(n_2,..,n_k) & \cdots \quad \underline{B}^{n_1}_{i,k-1}(n_2,..,n_k) \end{bmatrix}, \quad (5.34)$$

where $\alpha_i(n_1,..,n_k)$ $(i=1,2,...,K)$ and $\beta_i(m_1,..,m_k)$ $(i=1,2,...,K)$ are, respectively, linearly independent functions of $(n_1,n_2,...,n_k)$ and $(m_1,m_2,...,m_k)$.

Substituting (5.30) in (5.29), after carrying out some manipulations analogous to the ones in Section 5.2, we have

$$y(n_1,...,n_k) = \sum_{i=1}^{K} \alpha_i(n_1,...,n_k) x_i(n_1,...,n_k), \quad (5.31)$$

where

$$x_i(n_1,..,n_k) = \sum_{m_1=0}^{n_1} ... \sum_{m_k=0}^{n_k} \beta_i(m_1,..,m_k) \cdot u(m_1,..,m_k). \quad (5.32)$$
$$i=1,2,...,K$$

The expression in (5.32) can be written in matrix form

$$\underline{x}_k^i = \underline{B}_{i,k}(n_1,..,n_k) \cdot \underline{u}_k \ , \ i=1,2,..,K, \quad (5.33)$$

where $\underline{x}_k^i$ and $\underline{u}_k$ are vectors of order $([(n_1+1)\cdot(n_2+1)...(n_k+1)] \times 1)$ obtained, respectively, by ordering the k-dimensional arrays $\{x_i(i_1,i_2,...,i_k)\}$ and $\{u(i_1,i_2,...,i_k)\}$ $(i_j=0,1,...,n_j; j=1,2,...k)$ by means of a lexicographic ordering, described next. The element $u(j_1,j_2,...,j_k)$ occurs in row

$$\sum_{i=1}^{k-1} j_i \prod_{\ell=i}^{k-1} (n_{\ell+1} + 1) + (j_k+1),$$

for $j_i=0,1,...,n_i$, $i=1,2,...,k$, of the vector $\underline{u}_k$. A similar lexicographical ordering is given to the elements $\{x_i(j_1,j_2,...,j_k)\}$ to form the vector $\underline{x}_k^i$, $i=1,2,...,K$. $\underline{B}_{i,k}(n_1,..,n_k)$ in (5.33) is a square matrix of order $((n_1+1)\cdot(n_2+1)...(n_k+1))$, given by

into its components and summing over them in equation (5.9). This derivation, even though simple, cannot be easily extended to higher dimensions. In this section, the particular structure of a matrix will be used to our advantage in obtaining a k-D recursive model. First, this will be done for the case when the impulse response sequence has support in a positive cone and, subsequently, weakly causal LSV systems will be tackled.

5.3.1 k-D Positive Cone Causal State-Space Model

A k-D positive cone causal discrete LSV system can be characterized by the superposition sum

$$y(n_1,..,n_k) = \sum_{m_1=0}^{n_1} \cdots \sum_{m_k=0}^{n_k} h(n_1,..,n_k;m_1,..,m_k)u(m_1,..,m_k) , \tag{5.29}$$

where $u(\underline{m})$ is the input at coordinate point $\underline{m}=(m_1,m_2,\ldots,m_k)$, $y(\underline{n})$ is the output at coordinate point $\underline{n} = (n_1,n_2,\ldots,n_k)$ and $h(\underline{n},\underline{m})$ is the response of the system at the point $\underline{n}$ to a unit impulse at the point $\underline{m}$. At this point, a definition, which is a natural extension of Definition 3.1, is given.

Definition 5.2: A sequence $\{h(n_1,n_2,..,n_k;m_1,m_2,..,m_k)\}$, is K-th order degenerate if it can be expressed as

$$h(n_1,..,n_k;m_1,..,m_k) = \sum_{i=1}^{K} \alpha_i(n_1,..,n_k)\beta_i(m_1,..,m_k), \tag{5.30}$$

$$\hat{\underline{x}}(n_1,n_2) = \hat{\underline{A}}_1(n_1,n_2)\hat{\underline{x}}(n_1-1,n_2) + \hat{\underline{A}}_2(n_1,n_2)\hat{\underline{x}}(n_1,n_2-1) - \hat{\underline{A}}_3(n_1,n_2)\hat{\underline{x}}(n_1-1,n_2-1) + \hat{\underline{b}}(n_1,n_2)u(n_1,n_2), \tag{5.22}$$

$$y(n_1,n_2) = \hat{\underline{c}}(n_1,n_2)\hat{\underline{x}}(n_1,n_2), \tag{5.23}$$

where

$$\hat{\underline{A}}_1(n_1,n_2) = \underline{T}(n_1,n_2) \cdot \underline{T}^{-1}(n_1-1,n_2), \tag{5.24}$$

$$\hat{\underline{A}}_2(n_1,n_2) = \underline{T}(n_1,n_2) \cdot \underline{T}^{-1}(n_1,n_2-1), \tag{5.25}$$

$$\hat{\underline{A}}_3(n_1,n_2) = \underline{T}(n_1,n_2) \cdot \underline{T}^{-1}(n_1-1,n_2-1), \tag{5.26}$$

$$\hat{\underline{b}}(n_1,n_2) = \underline{T}(n_1,n_2)\underline{b}(n_1,n_2), \tag{5.27}$$

$$\hat{\underline{c}}(n_1,n_2) = \underline{c}(n_1,n_2)T^{-1}(n_1,n_2). \tag{5.28}$$

From the above, we can say that the state-space representation in (5.22) to (5.28) is related to the state-space model in (5.12) to (5.16) by the transformation matrix in (5.21).

5.3 k-D State-Space Model

Now, the results obtained in sections 5.2 will be extended to the k-dimensional (k > 2) case. The state-space model in Section 5.2 was obtained by making use of a geometric argument which consists of splitting a 2-D grid

$$\underline{x}(-1,n_2) = \underline{0} \quad \text{for} \quad n_2 = 0,1,\ldots,N_2, \tag{5.20}$$

The state-space model introduced in (5.12)-(5.16) is based on a three term recursion, which means that in order to generate the state vector $\underline{x}(n_1,n_2)$ at a point (n_1,n_2) we need to have previously computed the state vectors at the points (n_1-1,n_2), (n_1,n_2-1) and (n_1-1,n_2-1) in addition to the current input. See Figure 5.2.

From (5.10), it is easy to see that the states are decoupled; this is a nice feature which permits parallel computation of the states.

The state-space model introduced here has a structure similar to the Fornasini-Marchesini state-space representation [5.3]. The main difference between these two models, is that in (5.12) and (5.13) some of the matrices are non-constant.

The state-space model in (5.12) to (5.16) is not a unique state-space model representation of the system.

Let $\hat{\underline{x}}(n_1,n_2)$ be a new state vector defined by

$$\hat{\underline{x}}(n_1,n_2) = \underline{T}(n_1,n_2)\underline{x}(n_1,n_2). \tag{5.21}$$

Let the transformation matrix $\underline{T}(n_1,n_2)$ be nonsingular for all points (n_1,n_2) in the region S, defined in (5.18). Making use of this transformation, equations (5.12) to (5.16), become

where

$$\underline{x}(n_1,n_2) = \begin{bmatrix} x_1(n_1,n_2) \\ x_2(n_1,n_2) \\ \vdots \\ x_K(n_1,n_2) \end{bmatrix} , \qquad (5.14)$$

$$\underline{b}(n_1,n_2) = \begin{bmatrix} \beta_1(n_1,n_2) \\ \beta_2(n_1,n_2) \\ \vdots \\ \beta_K(n_1,n_2) \end{bmatrix} , \qquad (5.15)$$

$$\underline{c}(n_1,n_2) = [\alpha_1(n_1,n_2),\ \alpha_2(n_1,n_2),\ldots,\alpha_K(n_1,n_2)] . \qquad (5.16)$$

The initial conditions for the model above are:

$$\underline{x}(n_1,-1) = \underline{0} , \ \underline{x}(-1,n_2) = \underline{0} \quad n_1,n_2 = 0,1,2,\ldots \qquad (5.17)$$

If the input array $\{u(n_1,n_2)\}$ has a finite support

$$S = \{(n_1,n_2),\ 0 \le n_1 \le N_1,\ 0 \le n_2 \le N_2\} , \qquad (5.18)$$

and we are interested in computing the output $y(n_1,n_2)$ on S, then we only require a finite set of boundary conditions, which is given by

$$\underline{x}(n_1,-1) = \underline{0} \quad \text{for} \quad n_1 = 0,1,\ldots,N_1 , \qquad (5.19)$$

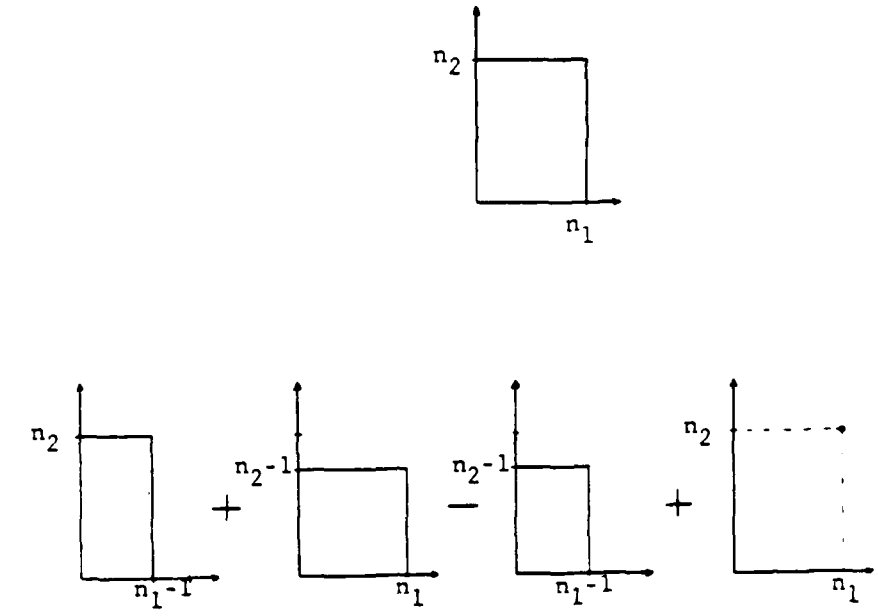

Figure 5.1: Decomposition of rectangular grid for obtaining recursion

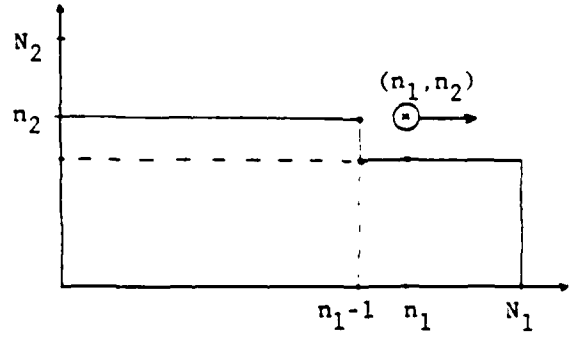

Figure 5.2: Neighbors of (n_1,n_2) required to compute state at (n_1,n_2) by the state-space model

Let us consider $x_i(n_1,n_2)$ for an arbitrary but fixed i, i=1,2,...,K. Splitting the summation in (5.8) according to the masks in Figure 5.1, we have

$$x_i(n_1,n_2) = \sum_{m_1=0}^{n_1-1}\sum_{m_2=0}^{n_2} \beta_i(m_1,m_2)u(m_1,m_2) + \sum_{m_1=0}^{n_1}\sum_{m_2=0}^{n_2-1} \beta_i(m_1,m_2)u(m_1,m_2) - \sum_{m_1=0}^{n_1-1}\sum_{m_2=0}^{n_2-1} \beta_i(m_1,m_2)u(m_1,m_2) + \beta_i(n_1,n_2)u(n_1,n_2) . \quad (5.9)$$

Substituting (5.8) in (5.9) and making use of (5.7), we have

$$x_i(n_1,n_2) = x_i(n_1-1,n_2) + x_i(n_1,n_2-1) - x_i(n_1-1,n_2-1) + \beta_i(n_1,n_2)u(n_1,n_2) \qquad i=1,2,\ldots,K . \quad (5.10)$$

$$y(n_1,n_2) = \sum_{i=1}^{K} \alpha_i(n_1,n_2)x_i(n_1,n_2) . \quad (5.11)$$

Equations (5.10) and (5.11) can be rewritten as

$$\underline{x}(n_1,n_2) = \underline{x}(n_1-1,n_2) + \underline{x}(n_1,n_2-1) - \underline{x}(n_1-1,n_2-1) + \underline{b}(n_1,n_2)u(n_1,n_2) , \quad (5.12)$$

$$y(n_1,n_2) = \underline{c}(n_1,n_2)\underline{x}(n_1,n_2) , \quad (5.13)$$

Let $h(n_1,n_2;\ m_1,m_2)$ be the impulse response of a 2-D first quadrant quarter-plane causal discrete LSV system, and let $u(n_1,n_2)$ be the input to the system with support in the first quadrant. Then,

$$h(n_1,n_2;\ m_1,m_2) = 0 \quad \text{for } n_1 < m_1 \text{ or } n_2 < m_2, \tag{5.3}$$

and

$$u(n_1,n_2) = 0 \quad \text{for } n_1 < 0 \text{ or } n_2 < 0. \tag{5.4}$$

Substituting (5.3) and (5.4) in (5.1) the input-output relation is given by

$$y(n_1,n_2) = \sum_{m_1=0}^{n_1} \sum_{m_2=0}^{n_2} h(n_1,n_2;\ m_1,m_2)u(m_1,m_2). \tag{5.5}$$

If the impulse response $h(n_1,n_2;\ m_1,m_2)$ is a K-th order degenerate sequence given by (5.2), then, substituting (5.2) in (5.5) we have

$$y(n_1,n_2) = \sum_{m_1=0}^{n_1} \sum_{m_2=0}^{n_2} \Big(\sum_{i=1}^{K} \alpha_i(n_1,n_2)\beta_i(m_1,m_2) \Big) u(m_1,m_2). \tag{5.6}$$

After some manipulations involving the interchanging of summations, we obtain

$$y(n_1,n_2) = \sum_{i=1}^{K} \alpha_i(n_1,n_2)x_i(n_1,n_2), \tag{5.7}$$

where

$$x_i(n_1,n_2) = \sum_{m_1=0}^{n_1} \sum_{m_2=0}^{n_2} \beta_i(m_1,m_2)u(m_1,m_2). \tag{5.8}$$

$$i=1,2,\ldots,K$$

Linear Shift-Invariant systems the sum in (5.1) gets transformed into the standard 2-D convolution and there are very efficient techniques for calculating the 2-D discrete convolution. These techniques include transform domain methods that make use of fast algorithms and there are also state-space models for recursive implementation in the spatial domain [ch. 4 in 5.3].

For LSV systems; the transform domain techniques cannot be used in general and, in addition to this, there are, as yet no state-space recursive models for 2-D LSV systems. Some very restrictive 1-D state-space models for LSV systems have appeared in the literature. They permit the analysis of 1-D LSV systems under very strong restrictions imposed on the impulse response [5.16], [5.17].

5.2 2-D Quarter Plane Causal State-Space Model

In order to develop a state-space model, the following definition has to be introduced as a natural extension of the 1-D case [5.14].

Definition 5.1: A sequence $\{h(n_1,n_2;\ m_1,m_2)\}$ is a K-th order degenerate sequence if it can be expressed as

$$h(n_1,n_2;\ m_1,m_2) = \sum_{i=1}^{K} \alpha_i(n_1,n_2)\beta_i(m_1,m_2)\,, \qquad (5.2)$$

where $\alpha_i(n_1,n_2)$ $(i=1,2,\ldots,K)$ and $\beta_i(m_1,m_2)$ $(i=1,2,\ldots,K)$ are, respectively, linearly independent functions of (n_1,n_2) and (m_1,m_2).

(where the impulse response sequence was assumed to be either expressible or approximated in k-th order degenerate form) domains. In this chapter attention will be focused on the development of a state-space model for a k-D LSV system whose impulse response is expressible in K-th order degenerate form. For convenience in exposition, the development of the model will be initiated for the 2-D quarter-plane causal case and a complete proof for the feasibility of extension to the k-D ($k > 2$) case based on a (2^k-1)-point recursion will be given. The possibility of generalizing the model to cover multi-dimensional weakly causal LSV systems will be substantiated. The model for the inverse system will be derived and applied to problems in deconvolution. Nontrivial physically motivated examples will be included.

A two dimensional discrete LSV system can be described by the discrete sum

$$y(n_1,n_2) = \sum_{m_1=-\infty}^{\infty} \sum_{m_2=-\infty}^{\infty} h(n_1,n_2;\, m_1,m_2)u(m_1,m_2), \quad (5.1)$$

where $u(\underline{m})$ is the input at coordinate point $\underline{m}=(m_1,m_2)$, $y(\underline{n})$ is the output at coordinate point $\underline{n}=(n_1,n_2)$ and $h(n_1,n_2;\, m_1,m_2)$ is the response of the sytem at the point $\underline{n}$ to a unit impulse at the point $\underline{m}$.

The input-output relation in (5.1) is far from being very convenient because it is not recursive and, therefore, the amount of computational time required for implementing the relation will be very large. In the case of 2-D discrete

sufficiently general, poses some dimensionality problems in implementation, in spite of the fact that the restorations besides being positive are spatially smooth and not overly sensitive to noise in the image data at object points that are near the background radiance. Then, there is the class of iterative methods based on gradient type [5.9] and conjugate gradient type [5.10] of optimization procedures. Iterative methods are not very suited for image restoration because of the problem of noise suppression. If the blurred image to be processed includes a noise, then this noise strongly deteriorates the quality of the restored image as the number of iterations increase. Thus, a method is desired that enables one to suppress noise amplification more efficiently, while restoring the image sharply. The three ways to suppress noise amplification are: (1) stop the iterations at a moderate iteration number; (2) introduce constraints; and (3) reblur the blurred image as done in [5.11] for LSI systems. In spite of these efforts, the general problem of space-time computational complexity has limited the use of practically all methods (including those already cited and others [5.12], [5.13]), in shift-variant multidimensional problems.

A more general approach than that permitted via use of coordinate transformation was pursued recently in [5.14], where the analysis was restricted to one-dimensional (1-D) discrete LSV systems. Investigations, however, were carried out both in the frequency (using the discrete version of Zadeh's generalized transfer function introduced in the discussion of continuous time systems [5.15]) and time

$\underline{\delta}_{k+1}^{ii_2i_3\ldots i_{k+1}}$ with $i = \begin{cases} 0 \\ \text{or} \\ 1 \end{cases}$, $i_\ell = \begin{cases} 0 \\ \text{or} \\ 1 \end{cases}$ $(\ell=2,3,\ldots,k+1)$ and

$i_2+i_3+\ldots+i_{k+1}=j$.

Therorem 5.1: Given the matrices in (5.34) to (5.36), then for any integer $k \geq 1$, we have

$$\underline{\delta}_k^{00\ldots0}\ \underline{B}_{i,k}(n_1,\ldots,n_k) = \sum_{j=1}^{k}(-1)^{j+1}\underline{\sigma}_k(j)\underline{B}_{i,k}(n_1,\ldots,n_k) + \underline{\delta}_k^{00\ldots0}\ \beta_i(n_1,\ldots,n_k). \qquad (5.39)$$

Proof: (by induction)

For k=1

$$\underline{B}_{i,1}(n_1) = \begin{bmatrix} \beta_i(0) & & & \\ \beta_i(0) & \beta_i(1) & & \\ \vdots & \vdots & & \\ \beta_i(0) & \beta_i(1) & \ldots & \beta_i(n_1) \end{bmatrix}. \qquad (5.40)$$

The last row of $\underline{B}_{i,1}(n_1)$ in (5.40) can be expressed as

$$[\beta_i(0)\ \beta_i(1)\ \ldots\ \beta_i(n_1)] = [\beta_i(0)\ \beta_i(1)\ \ldots\ \beta_i(n_1-1)0] + [0\ \ 0\ \ldots\ 0\ \ 1]\beta_i(n_1). \qquad (5.41)$$

Making use of Definitions 5.3 and 5.4, the expression in (5.41) can be written as

$$\underline{\delta}_1^{0}\ \underline{B}_{i,1}(n_1) = \underline{\sigma}_1(1)\ \underline{B}_{i,1}(n_1) + \underline{\delta}_1^{0}\ \beta_i(n_1), \qquad (5.42)$$

which corresponds to the expression in (5.39) for k=1.

From the matrices in (5.34) to (5.36), for any integer $k \geq 1$, we can write

$$[\underline{0}\ \ \underline{0}\ \ldots\ \underline{0}\ \ \underline{\delta}_k^{i_2 i_3 \ldots i_{k+1}}\ \underline{B}_{i,k}^{n_1}(n_2,n_3,\ldots,n_{k+1})]$$
$$= (\underline{\delta}_{k+1}^{0 i_2 i_3 \ldots i_{k+1}} - \underline{\delta}_{k+1}^{1 i_2 i_3 \ldots i_{k+1}})\underline{B}_{i,k+1}(n_1,n_2,\ldots,n_{k+1}). \tag{5.43}$$

If we now assume that the hypothesis is valid for a fixed integer k, with n_1 fixed, we can write

$$\underline{\delta}_k^{00\ldots0}\ \underline{B}_{i,k}^{n_1}(n_2,\ldots,n_{k+1}) = \sum_{j=1}^{k}(-1)^{j+1}\ \underline{\sigma}_k(j)\underline{B}_{i,k}^{n_1}(n_2,\ldots,n_{k+1})$$
$$+\ \underline{\delta}_k^{00\ldots0}\ \beta_i(n_1,n_2,\ldots,n_{k+1}). \tag{5.44}$$

Also from (5.43), after setting $i_2=i_3=\ldots=i_{k+1}=0$, we have

$$\underline{\delta}_{k+1}^{00\ldots0}\ \underline{B}_{i,k+1}(n_1,\ldots,n_{k+1}) = \underline{\delta}_{k+1}^{100\ldots0}\ \underline{B}_{i,k+1}(n_1,\ldots,n_{k+1})$$
$$+\ [\underline{0}\ \underline{0}\ \ldots\ \underline{0}\ \underline{\delta}_k^{0\,0\ldots0}\ \underline{B}_{i,k}^{n_1}(n_2,\ldots,n_{k+1})]\ . \tag{5.45}$$

Substituting (5.44) in (5.45), we have

$$\underline{\delta}_{k+1}^{00\ldots0}\ \underline{B}_{i,k+1}(n_1,\ldots,n_{k+1}) = \underline{\delta}_{k+1}^{10\ldots0}\ \underline{B}_{i,k+1}(n_1,\ldots,n_{k+1})$$
$$+\ \sum_{j=1}^{k}(-1)^{j+1}[\underline{0}\ \underline{0}\ldots\underline{\sigma}_k(j)\underline{B}_{i,k}^{n_1}(n_2,\ldots,n_{k+1})]$$
$$+\ [\underline{0}\ \underline{0}\ldots\underline{0}\ \underline{\delta}_k^{00\ldots0}\ \beta_{k+1}(n_1,\ldots,n_{k+1})]\ . \tag{5.46}$$

From (5.43), making use of Definitions 5.4 and 5.5, we obtain

$$[\underline{0}\ \underline{0}\ldots\underline{0}\ \underline{\sigma}_k(j)\ \underline{B}_{i,k}^{n_1}(n_2,\ldots,n_{k+1})]$$
$$= (\underline{\sigma}_{k+1}^{0}(j) - \underline{\sigma}_{k+1}^{1}(j))\underline{B}_{i,k+1}(n_1,..,n_{k+1}). \qquad (5.47)$$

Also, from Definition 5.3, we have

$$[\underline{0}\ \underline{0}\ldots\underline{0}\ \underline{\beta}_{k+1}(n_1,..,n_{k+1})] = \underline{\delta}_{k+1}^{00..0}\beta_{k+1}(n_1,..,n_{k+1}). \qquad (5.48)$$

Substituting (5.47) and (5.48) in (5.46), we have

$$\underline{\delta}_{k+1}^{00..0}\ \underline{B}_{i,k+1}(n_1,..,n_{k+1}) =$$
$$[\underline{\delta}_{k+1}^{10..0} + \sum_{j=1}^{k}(-1)^{j+1}(\underline{\sigma}_{k+1}^{0}(j)-\underline{\sigma}_{k+1}^{1}(j))]\underline{B}_{i,k+1}(n_1,..,n_{k+1})$$
$$+ \underline{\delta}_{k+1}^{00..0}\ \underline{B}_{i,k+1}(n_1,..,n_{k+1}). \qquad (5.49)$$

From Definition 5.4, it is straight forward to show that

$$\underline{\varepsilon}_{k+1}(j) = \begin{cases} \underline{\delta}_{k+1}^{10..0} + \underline{\sigma}_{k+1}^{0}(1), & j=1 \\ \underline{\sigma}_{k+1}^{0}(j) + \underline{\sigma}_{k+1}^{1}(j-1), & j=2,3,\ldots,k \\ \underline{\sigma}_{k+1}^{1}(k), & j=k+1 \end{cases} \qquad (5.50)$$

Consider now the expression in square brackets in (5.49),

$$\underline{\delta}_{k+1}^{10..0} + \sum_{j=1}^{k} (-1)^{j+1} (\underline{\sigma}_{k+1}^{0}(j) - \underline{\sigma}_{k+1}^{1}(j))$$

$$= \underline{\delta}_{k+1}^{100..0} + \underline{\sigma}_{k+1}^{0}(1) + \sum_{j=2}^{k} (-1)^{j+1} (\underline{\sigma}_{k+1}^{0}(j) + \underline{\sigma}_{k+1}^{1}(j-1))$$

$$+ (-1)^{(k+1)+1} \underline{\sigma}_{k+1}^{1}(k) \quad . \tag{5.51}$$

Substituting (5.50) in (5.51), we have

$$\underline{\delta}_{k+1}^{100..0} + \sum_{j=1}^{k} (-1)^{j+1} (\underline{\sigma}_{k+1}^{0}(j) - \underline{\sigma}_{k+1}^{1}(j))$$

$$= \sum_{j=1}^{k+1} (-1)^{j+1} \underline{\sigma}_{k+1}(j) \, . \tag{5.52}$$

Substituting (5.52) in (5.49), we have

$$\underline{\delta}_{k+1}^{00..0} \underline{B}_{i,k+1}(n_1,\ldots,n_{k+1})$$

$$= \sum_{j=1}^{k+1} (-1)^{j+1} \underline{\sigma}_{k+1}(j) \underline{B}_{i,k+1}(n_1,\ldots,n_{k+1})$$

$$+ \underline{\delta}_{k+1}^{00..0} \beta_{k+1}(n_1,\ldots,n_{k+1}) \quad , \tag{5.53}$$

which corresponds to the hypothesis for k+1. Therefore, by the principle of mathematical induction, the proof is now complete.

The following definition has to be introduced at this point:

Definition 5.6: Define,

$$x_i^j(n_1,n_2,\ldots,n_k) = \sum_{s=1}^{\binom{k}{j}} x_i[n_1-r_s(1),\ n_2-r_s(2),\ldots,n_k-r_s(k)]$$

where $\sum_{i=1}^{k} r_s(i)=j$, $r_s(i)=0$ or 1 for each i and the sets $\{r_s(1),\ r_s(2),\ldots,\ r_s(k)\}$, $s=1,2,\ldots,\binom{k}{j}$ are mutually distinct.

Theorem 5.2: Given a k-D, ($k \geq 1$), positive cone causal LSV system whose impulse response is a K-th order degenerate sequence characterized by expression (5.30). Then, the superposition sum in (5.29) can be implemented by a K-th order state-space model. This state-space model is based on a (2^k-1)-point recursion described by,

$$x_i(n_1,..,n_k) = \sum_{j=1}^{k} (-1)^{j+1} x_i^j(n_1,..,n_k) + \beta_i(n_1,..,n_k)u(n_1,..,n_k) \qquad i=1,2,\ldots,K, \qquad (5.54)$$

$$y(n_1,..,n_k) = \sum_{i=1}^{K} \alpha_i(n_1,..,n_k)x_i(n_1,..,n_k). \qquad (5.55)$$

Proof: From expressions (5.33) to (5.36), making use of Definition 5.3, we have

$$x_i(n_1-i_1,n_2-i_2,..,n_k-i_k) = \underline{\delta}_k^{i_1 i_2 .. i_k} \underline{B}_{i,k}(n_1,..,n_k)\underline{u}_k \qquad i=1,2,\ldots,K. \qquad (5.56)$$

Substituting the expression (5.39) of Theorem 5.1 in (5.56), after setting $i_1=i_2=\ldots=i_k=0$,

$$x_i(n_1,..,x_k) = \sum_{j=1}^{k} (-1)^{j+1} \underline{\varepsilon}_k(j) \underline{B}_{i,k}(n_1,..,n_k) \underline{u}_k + \underline{\delta}_k^{00..0} \beta_i(n_1,..,n_k) \underline{u}_k \quad . \tag{5.57}$$

From (5.56), making use of Definitions 5.4 and 5.6, we have

$$x_i^j(n_1,..,n_k) = \underline{\varepsilon}_k(j) \ \underline{B}_{i,k}(n_1,..,n_k) \underline{u}_k \quad . \tag{5.58}$$

From the ordering defined for the vector $\underline{u}_k$, we have

$$u(n_1,..,n_k) = \underline{\delta}_k^{00..0} \ \underline{u}_k \quad . \tag{5.59}$$

Substituting (5.58) and (5.59) in (5.57), we obtain the expression in (5.54) The recursion is based on ℓ-points, where

$$\ell = \sum_{j=1}^{k} \binom{k}{j} = 2^k - 1 \quad . \tag{5.60}$$

The proof is now complete.

The example below serves to clarify the various notations introduced in the preceding discussion. For brevity in exposition, this example tackles the k=2 case, for which the 3-point recursion arrived at in section 5.2 is verified as a special case of the general result.

Example 5.1 Consider (5.32) for the case, k=2. Then, the expression

$$x_i(n_1,n_2) = \sum_{m_1=0}^{n_1} \sum_{m_2=0}^{n_2} \beta_i(m_1,m_2)u(m_1,m_2),$$

is considered for the case when $n_1=n_2=2$. Then counterpart of the matrix form representation in (5.33) is given below in expanded form. Note that the lexicographical ordering described has been adopted. It is clear that in the k=2 case, this ordering results from a row-by-row scan of each of the arrays $\{x_i(i_1,i_2)\}$ and $\{u(i_1,i_2)\}$.

$$\begin{bmatrix} x_i(0,0) \\ x_i(0,1) \\ x_i(0,2) \\ x_i(1,0) \\ x_i(1,1) \\ x_i(1,2) \\ x_i(2,0) \\ x_i(2,1) \\ x_i(2,2) \end{bmatrix} = \begin{bmatrix} \beta_i(0,0) & & & & & & & & \\ \beta_i(0,0) & \beta_i(0,1) & & & & & & & \\ \beta_i(0,0) & \beta_i(0,1) & \beta_i(0,2) & & & & & & \\ \beta_i(0,0) & & & \beta_i(1,0) & & & & & \\ \beta_i(0,0) & \beta_i(0,1) & & \beta_i(1,0) & \beta_i(1,1) & & & & \\ \beta_i(0,0) & \beta_i(0,1) & \beta_i(0,2) & \beta_i(1,0) & \beta_i(1,1) & \beta_i(1,2) & & & \\ \beta_i(0,0) & & & \beta_i(1,0) & & & \beta_i(2,0) & & \\ \beta_i(0,0) & \beta_i(0,1) & & \beta_i(1,0) & \beta_i(1,1) & & \beta_i(2,0) & \beta_i(2,1) & \\ \beta_i(0,0) & \beta_i(0,1) & \beta_i(0,2) & \beta_i(1,0) & \beta_i(1,1) & \beta_i(1,2) & \beta_i(2,0) & \beta_i(2,1) & \beta_i(2,2) \end{bmatrix} \begin{bmatrix} u(0,0) \\ u(0,1) \\ u(0,2) \\ u(1,0) \\ u(1,1) \\ u(1,2) \\ u(2,0) \\ u(2,1) \\ u(2,2) \end{bmatrix} \tag{5.61a}$$

Specializing the representation in (5.33) to this case, (5.61a) can be written as,

$$\underline{x}_2^i = \underline{B}_{i,2}(n_1,n_2)\underline{u}_2,$$

where,

$$\underline{B}_{i,2}(n_1,n_2)=\begin{bmatrix} \underline{B}_{i,1}^0(n_2) & & \\ \underline{B}_{i,1}^0(n_2) & \underline{B}_{i,1}^1(n_2) & \\ \underline{B}_{i,1}^0(n_2) & \underline{B}_{i,1}^1(n_2) & \underline{B}_{i,1}^2(n_2) \end{bmatrix}, \qquad (5.61b)$$

and

$$\underline{B}_{i,1}^j(n_2) = \begin{bmatrix} \beta_i(j,0) & & & \\ \beta_i(j,0) & \beta_i(j,1) & & \\ \vdots & \vdots & \ddots & \\ \beta_i(j,0) & \beta_i(j,1) & \cdots & \beta_i(j,n_2) \end{bmatrix}. \qquad (5.61c)$$

Clearly, (5.61b) and (5.61c) give the relevant specializations of the matrices in (5.34)-(5.36). Applying Definitions 5.3 and 5.4 to the case under consideration, we have

$$\underline{\delta}_2^{00} = [000 \mid 000 \mid 001],$$

$$\underline{\delta}_2^{10} = [000 \mid 001 \mid 000],$$

$$\underline{\delta}_2^{01} = [000 \mid 000 \mid 010],$$

$$\underline{\delta}_2^{11} = [000 \mid 010 \mid 000],$$

$$\underline{\sigma}_2(1) = \underline{\delta}_2^{01} + \underline{\delta}_2^{10},$$

$$\underline{\sigma}_2(2) = \underline{\delta}_2^{11}.$$

Let $\underline{r}_j$ denote the j-th row in the matrix $\underline{B}_{i,2}$ of (5.61a), j=1,2,...,9. Clearly

$$\underline{r}_9 = \underline{r}_8 + \underline{r}_6 - \underline{r}_5 + [0\ 0\ \ldots\ 0\ \beta_i(2,2)]$$

the above equation can be rewritten in the form,

$$\begin{aligned}\underline{\delta}_2^{00}\ \underline{B}_{i,2}(n_1,n_2) &= \underline{\delta}_2^{01}\ \underline{B}_{i,2}(n_1,n_2) + \underline{\delta}_2^{10}\underline{B}_{i,2}(n_1,n_2)\\ &\quad - \underline{\delta}_2^{11}\ \underline{B}_{i,2}(n_1,n_2) + \underline{\delta}_2^{00}\ \beta_i(2,2)\\ &= \underline{\sigma}_2(1)\underline{B}_{i,2}(n_1,n_2) - \underline{\sigma}_2(2)\underline{B}_{i,2}(n_1,n_2)\\ &\quad + \underline{\delta}_2^{00}\ \beta_i(2,2)\ ,\end{aligned} \tag{5.62}$$

which is the relevant specialization of (5.39).

Note that,

$$x_i(n_1-i,n_2-j) = \underline{\delta}_2^{ij}\ \underline{B}_{i,2}(n_1,n_2)\cdot\underline{u}_2. \tag{5.63}$$

Multiplying (5.62) from the right by $\underline{u}_2$ and using (5.63), we get

$$\begin{aligned}x_i(n_1,n_2) &= x_i(n_1,n_2-1) + x_i(n_1-1,n_2)\\ &\quad - x_i(n_1-1,n_2-1) + \beta_i(n_1,n_2)u(n_1,n_2).\end{aligned} \tag{5.64}$$

Applying Definition 5.6,

$$x_i^1(n_1,n_2) = x_i(n_1-1,n_2) + x_i(n_1,n_2-1), \tag{5.65a}$$

$$x_i^2(n_1,n_2) = x_i(n_1-1,n_2-1). \tag{5.65b}$$

Substituting (5.65a) and (5.65b) in (5.64) we get

$$x_i(n_1,n_2) = x_i^1(n_1,n_2) - x_i^2(n_1,n_2) + \beta_i(n_1,n_2)u(n_1,n_2),$$

which is the relevant specialization of (5.54).

5.3.2 Extension of the k-D State-Space Model to a Causality Hypercone

The state-space model developed in Section 5.3.1 for a k-dimensional positive cone (or hypercone) causal discrete LSV system, can be naturally extended in order to represent a k-dimensional (k > 2) weakly causal discrete LSV system. Definitions 5.7 and 5.8 given next, are introduced in order to reach the desired goal.

Definition 5.7: A k-dimensional causality hypercone C_c; is the intersection of k half hyperplanes $Hp_{i1},p_{i2},\ldots,p_{ik}$ (i=1,2,...,k), where

$$Hp_{i1},p_{i2},\ldots,p_{ik} = \{(x_1,\ldots,x_k) \mid (x_1,\ldots,x_k) \in R^k,$$

$$p_{i1}x_1 + \ldots + p_{ik}x_k \geq 0\}$$

$$(i=1,2,\ldots,k)$$

and $p_{ij}(i,j=1,2,\ldots,k)$ are non-negative integers, satisfying

$$\det \Phi = 1,$$

where

$$\Phi \triangleq \begin{bmatrix} p_{11} & p_{12} & \cdots & p_{1k} \\ \vdots & & & \\ p_{k1} & p_{k2} & \cdots & p_{kk} \end{bmatrix}, \qquad (5.66)$$

It is important to note that in a k-dimensional causality cone C_c, any vector $\underline{v}$ going from the origin to a point P in C_c can be expressed as a linear combination of the

vectors g_i, i=1,2,...,k. These vectors are called the generator of the causality cone and it can be shown that the generator g_i, i=1,2,...,k corresponds to the i-th column of the adjoint of the unimodular transformation matrix Φ.

Definition 5.8: A k-D discrete LSV system with impulse response $h(n_1,\ldots,n_k;m_1,\ldots,m_k)$, is causal on a causality hypercone C_c if and only if

$$h(n_1,\ldots,n_k;m_1,\ldots,n_k) \equiv 0 \quad \text{for } (\ell_1,\ldots,\ell_k) \notin C_c,$$

with $\ell_i = n_i - m_i$ (i=1,2,...,k).

The one-to-one and onto mapping ϕ, defined in (5.66), maps any integer point in C_c onto a unique integer point in the positive cone Q_1

$$\phi: C_c \cap Z^k \longrightarrow Q_1 \cap Z^k \text{ and } \phi[(0,0,..,0)]=(0,0,..,0),$$

Given a k-D discrete LSV system with a K-th order degenerate impulse response, which is causal in C_c, then use of the mapping ϕ defined in (5.66) and its inverse, a state-space model can be derived. The resulting K-th order state-space model will be based on a (2^k-1)-points recursion. For the sake of clarity and brevity in exposition, the procedure is described for the 2-D case, from which the k-D (k > 2) counterpart can be obtained as a direct generalization.

Let

$$y(n_1,n_2) = \sum_{(m_1,m_2)\in C_c} \sum_{(n_1,n_2)\in C_c} h(n_1,n_2;\, m_1,m_2)u(m_1,m_2), \tag{5.67}$$

be the input-output relation of a discrete LSV system, and let $\{h(n_1,n_2;\, m_1,m_2)\}$ be causal in C_c. In addition to this, assume that $\{h(n_1,n_2;\, m_1,m_2)\}$ is a K-th order degenerate sequence expressed as in (5.2). Using the map Φ in (5.66) with k=2, we map the input, the output and the impulse response in (5.67), as follows

$$\hat{u}(\hat{m}_1,\hat{m}_2) = u(m_1,m_2)\Big|_{\binom{m_1}{m_2} = \Phi^{-1}\cdot\binom{\hat{m}_1}{\hat{m}_2}}, \tag{5.68a}$$

$$\hat{y}(\hat{n}_1,\hat{n}_2) = y(n_1,n_2)\Big|_{\binom{n_1}{n_2} = \Phi^{-1}\cdot\binom{\hat{n}_1}{\hat{n}_2}}, \tag{5.68b}$$

and

$$\hat{h}(\hat{n}_1,\hat{n}_2;\hat{m}_1,\hat{m}_2) = h(n_1,n_2;m_1,m_2)\Big|_{\substack{\binom{m_1}{m_2} = \Phi^{-1}\binom{\hat{m}_1}{\hat{m}_2} \\ \binom{n_1}{n_2} = \Phi^{-1}\binom{\hat{n}_1}{\hat{n}_2}}}. \tag{5.68c}$$

Then, $\hat{h}(\hat{n}_1,\hat{n}_2;\, \hat{m}_1,\hat{m}_2)$ is first quadrant quarter plane causal. The input array $\hat{u}(\hat{m}_1,\hat{m}_2)$ and the output array $\hat{y}(\hat{n}_1,\hat{n}_2)$ have support on Q_1. In addition to this, from

(5.2) and (5.68c) $\hat{h}(\hat{n}_1,\hat{n}_2;\hat{m}_1,\hat{m}_2)$ is a K-th order degenerate sequence, and it can be written as

$$\hat{h}(\hat{n}_1,\hat{n}_2;\ \hat{m}_1,\hat{m}_2) = \sum_{i=1}^{K} \hat{\alpha}_i(\hat{n}_1,\hat{n}_2)\hat{\beta}_i(\hat{m}_1,\hat{m}_2)\ , \qquad (5.69)$$

where

$$\hat{\alpha}_i(\hat{n}_1,\hat{n}_2) = \alpha_i(n_1,n_2)\Big|_{\binom{n_1}{n_2} = \Phi^{-1}\binom{\hat{n}_1}{\hat{n}_2}}\ , \qquad (5.70a)$$

$$\hat{\beta}_i(\hat{m}_1,\hat{m}_2) = \beta_i(m_1,m_2)\Big|_{\binom{m_1}{m_2} = \Phi^{-1}\binom{\hat{m}_1}{\hat{m}_2}}\ . \qquad (5.70b)$$

From (5.67) and (5.68), we have

$$\hat{y}(\hat{n}_1,\hat{n}_2) = \sum_{m_1=0}^{\hat{n}_1}\sum_{m_2=0}^{\hat{n}_2} \hat{h}(\hat{n}_1,\hat{n}_2;\ \hat{m}_1,\hat{m}_2)\hat{u}(\hat{m}_1,\hat{m}_2)\ . \qquad (5.71)$$

For the first quadrant quarter plane causal LSV system in (5.71), with its impulse response given by (5.69), we can now write, using equations (5.12) to (5.16), a state-space model with support on Q_1.

$$\begin{aligned} \underline{x}(\hat{n}_1,\hat{n}_2) &= \underline{x}(\hat{n}_1-1,\hat{n}_2) + \underline{x}(\hat{n}_1,\hat{n}_2-1) \\ &\quad - \underline{x}(\hat{n}_1-1,\hat{n}_2-1) + \underline{\hat{b}}(\hat{n}_1,\hat{n}_2)\hat{u}(\hat{n}_1,\hat{n}_2)\ , \\ \hat{y}(\hat{n}_1,\hat{n}_2) &= \underline{\hat{c}}(\hat{n}_1,\hat{n}_2)\underline{x}(\hat{n}_1,\hat{n}_2)\ , \end{aligned} \qquad (5.72)$$

where

$$\underline{\hat{b}}(\hat{n}_1,\hat{n}_2) = \begin{bmatrix} \hat{\beta}_1(\hat{n}_1,\hat{n}_2) \\ \vdots \\ \hat{\beta}_K(\hat{n}_1,\hat{n}_2) \end{bmatrix} . \tag{5.73a}$$

$$\underline{\hat{c}}(\hat{n}_1,\hat{n}_2) = [\hat{\alpha}_1(\hat{n}_1,\hat{n}_2),\ldots,\hat{\alpha}_K(\hat{n}_1,\hat{n}_2)] . \tag{5.73b}$$

The initial conditions are:

$$\underline{\hat{x}}(\hat{n}_1,-1) = 0,\ \underline{\hat{x}}(-1,n_2) = 0 \quad n_1,n_2 = 0,1,2,\ldots \tag{5.73c}$$

Mapping back to C_c the state-space equation described in (5.72) and (5.73), (for notational brevity, replace $p_{11},p_{12},p_{21},p_{22}$ in (5.66) by p, r, q, t, respectively)

$$\underline{x}(n_1,n_2) = \underline{x}(n_1-t,n_2+q) + \underline{x}(n_1+r,n_2-p) - \underline{x}(n_1+r-t,n_2+q-p) + \underline{b}(n_1,n_2)u(n_1,n_2),\ (n_1,n_2) \in C_c , \tag{5.74a}$$

$$y(n_1,n_2) = \underline{c}(n_1,n_2)\underline{x}(n_1,n_2),\ (n_1,n_2) \in C_c, \tag{5.74b}$$

where

$$\underline{b}(n_1,n_2) = \begin{bmatrix} \beta_1(n_1,n_2) \\ \vdots \\ \beta_K(n_1,n_2) \end{bmatrix} , \tag{5.75a}$$

$$\underline{c}(n_1,n_2) = [\alpha_1(n_1,n_2), \ldots, \alpha_K(n_1,n_2)] . \tag{5.75b}$$

The initial conditions are:

$$\underline{x}(tn+r,-qn-p) = 0,\ \underline{x}(-rn-t,pn+q) = 0 \quad n=0,1,\ldots \tag{5.75c}$$

$$h(r_i,\theta_i;r_o,\theta_o) = \frac{1}{r_o^4}\, h_0\left(\frac{r_i\cos(\theta_i-\theta_o)-r_o}{r_o^2}+1,\ \frac{r_o\sin(\theta_i-\theta_o)}{r_o^2}\right), \quad (5.90)$$

where the function $h_0(x_i,y_i)$ is the response to an impulse at $r_o=1$, $\theta_o=0$. The form of $h_0(\cdot)$ for several special cases such as spherical and coma aberrations are derived in [5.20]. For Cartesian coordinates (x_1,x_2) and (τ_1,τ_2) of the image and object planes, respectively, we have

$$\begin{aligned} x_1 &= r_i\cos\theta_i & \tau_1 &= r_o\cos\theta_o \ , \\ x_2 &= r_i\sin\theta_i & \tau_2 &= r_o\sin\theta_o \ . \end{aligned} \quad (5.91)$$

Substituting (5.91) in (5.90), the impulse response in Cartesian coordinates, $h(x_1,x_2;\tau_1,\tau_2)$, for the coma aberration becomes

$$h(x_1,x_2;\tau_1,\tau_2) = \frac{1}{\tau_1^2+\tau_2^2}\, h_0\left(\frac{x_1\tau_1+x_2\tau_2}{\tau_1^2+\tau_2^2},\ \frac{x_2\tau_1-x_1\tau_2}{\tau_1^2+\tau_2^2}\right), \quad (5.92)$$

where $h_0(x_1,x_2)$ is the response to an impulse at $\tau_1=1$, $\tau_2=0$; that is, $h_0(x_1,x_2) = h(x_1,x_2;1,0)$, is given by

$$h_0(x_1,x_2) = \begin{cases} \dfrac{2C}{\sqrt{x_1^2-3x_2^2}} & \text{for } (x_1,x_2)\ \varepsilon\ \text{I} \ , \\ \dfrac{C}{\sqrt{x_1^2-3x_2^2}} & \text{for } (x_1,x_2)\ \varepsilon\ \text{II} \ , \end{cases} \quad (5.93)$$

derived in (5.88)-(5.89), a state-space model of the inverse system was implemented.

The (32x32)-points original object, shown in Figure (5.4a) was blurred by the simulated motion blur described in (5.86) with the parameters in (5.87) and (5.84) taken typically as T=1, α=2, a=1 and ϵ=.2. The resulting motion blurred image is shown in Figure (5.4b). From the motion blurred image in Figure (5.4b) by using a $(2\cdot K+1)$-th, (K=10), state-space model of the inverse system, the original object was reconstructed. The reconstructed object is shown in Figure (5.4c), From Figure (5.4c), we can conclude that for a fairly low order state-space model, the reconstruction is very accurate.

5.5.2 Coma Aberration

Within the geometrical optics model of image formation, aberrations are described by the ray aberration function which is a vector in the image (output) plane from the Gaussian image point to the point where the ray actually intersects the image plane. The Gaussian image point is the image in the output plane of a point in the input plane in absence of optical aberrations. Let (r_i, θ_i) and (r_o, θ_o) denote, respectively, the polar coordinates of the image and object planes. It has been shown in a paper by Robbins and Huang [5.19] that the impulse response, $h(r_i, \theta_i; r_o, \theta_o)$, for coma aberration is given by

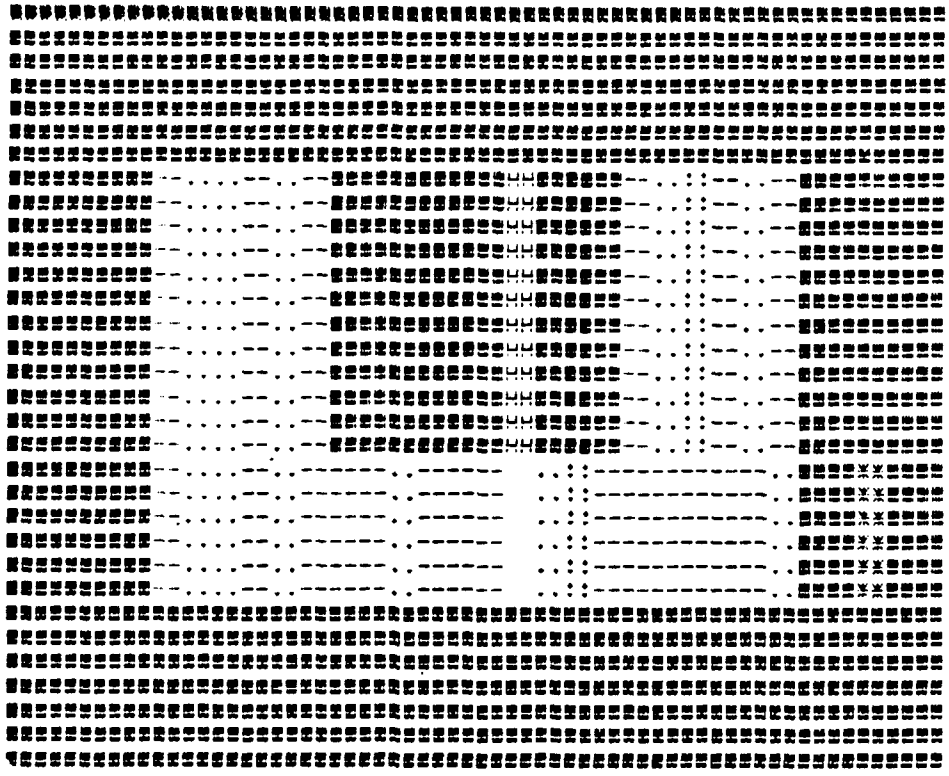

Figure 5.4c: Restored object from motion blurred image

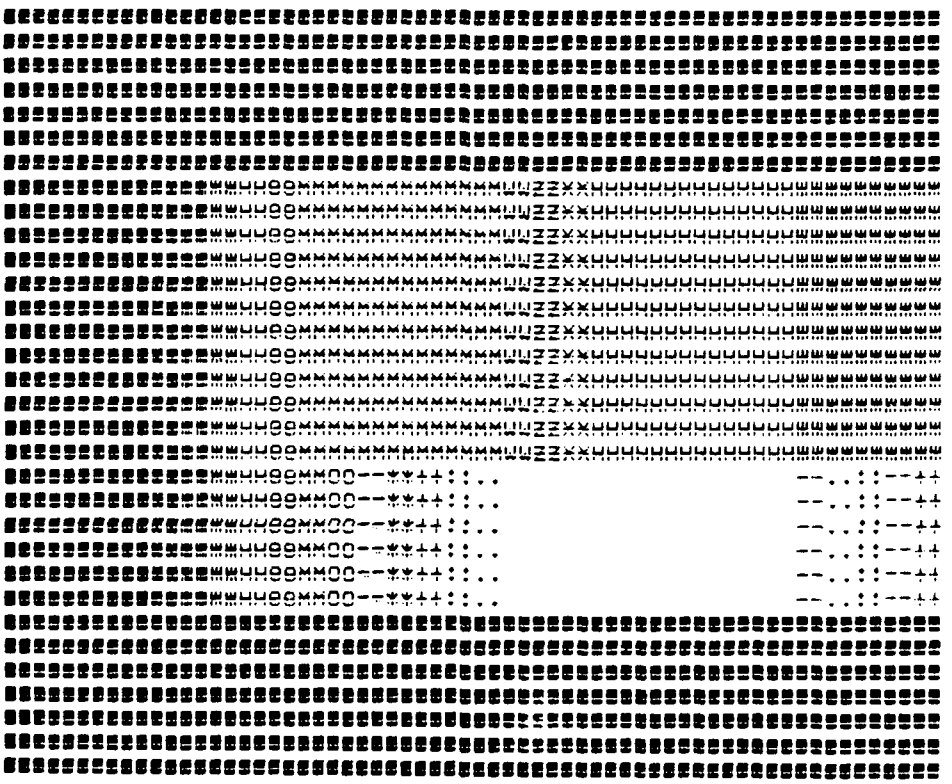

Figure 5.4b: Motion blurred image

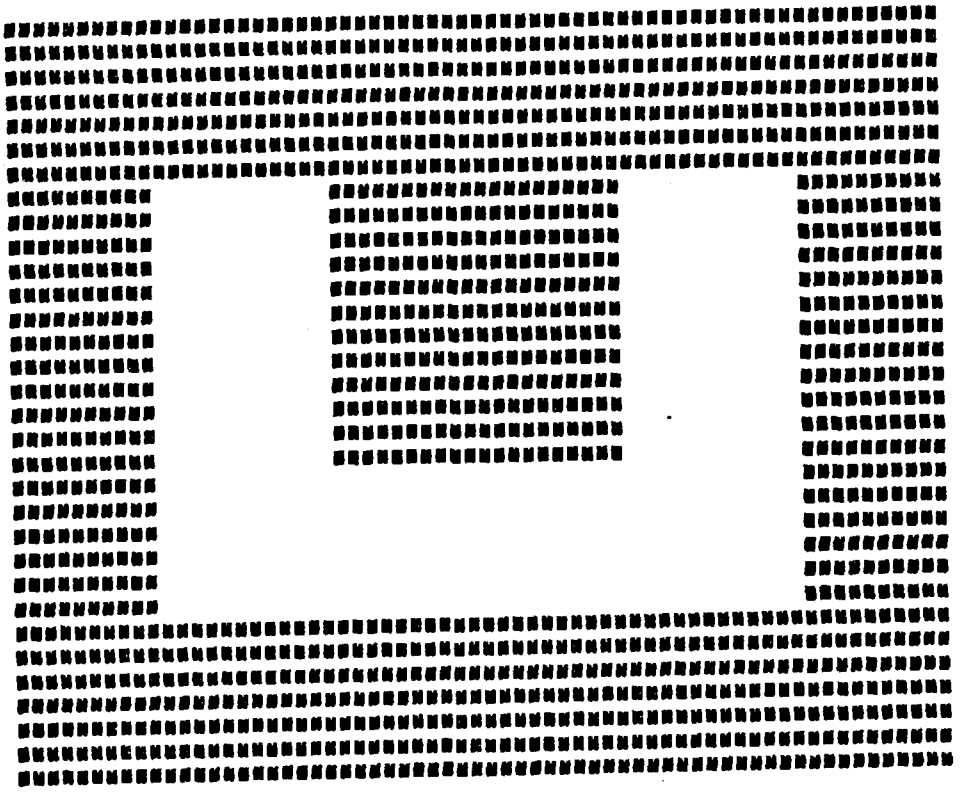

Figure 5.4a: Original Object

(NxN) of the input array. The discrete motion blurring is carried out, line by line, by means of the following expression

$$y(n_1,n_2) = \sum_{m_1=0}^{n_1} \hat{h}_D(n_1,m_1)u(m_1,n_2) \quad . \qquad (5.86)$$

$$n_i=0,1,\ldots,N-1, \quad i=1,2$$

Analogously, before implementing a discrete state-space model for the inverse system, the approximated impulse response $h^*(x,u)$ in (5.84), has to be discretized, and the resulting discrete impulse response $h_D^*(n,m)$ is given by

$$h_D^*(n,m) = h^*(n\cdot\Delta, m\cdot\Delta) , \qquad (5.87)$$

where Δ has been previously defined. Then, from (5.87) and (5-84)-(5.85), we have

$$h_D^*(n,m) = \sum_{i=0}^{2\cdot K} \alpha_i(n)\beta_i(m) , \qquad (5.88)$$

where

$$\alpha_0(n) = 1 \quad , \quad \beta_0(m) = a_0(m\Delta) , \qquad (5.89a)$$

$$\alpha_i(n) = \cos(n\cdot\frac{2\pi}{T_p} i\cdot\Delta) \quad . \quad \beta_i(m) = a_i(m\Delta), \; i=1,\ldots,K , \qquad (5.89b)$$

$$\alpha_i(n) = \sin(n\cdot\frac{2\pi}{T_p} i\Delta), \; \beta_i(m) = b_i(m\Delta), \; i=K+1,\ldots,2K , \qquad (5.89c)$$

From the $(2\cdot K+1)$-th order degenerate sequence, $\{h_D^*(n,m)\}$

$$b_k(u) = \begin{cases} \frac{a}{(u+\alpha)} \cdot \{\alpha_k \cos(w_k(u_2-d_2))\cos(w_k d) + \frac{1}{k\pi}\cos(w_k u_1)\}, \\ \qquad \frac{1}{D_2} \neq \frac{2k}{T} \qquad (5.85c) \\ \frac{a}{(u+\alpha)} \cdot \{\beta_k \cos(w_k(u_2-d))\cos(w_k d) + \frac{1}{k\pi}\cos(w_k u_1) \\ \qquad - \frac{d}{T}\sin(\frac{\pi}{D_2}u_2) \ , \ \frac{1}{D_2} = \frac{2k}{T} \\ \qquad k=1,2,\ldots \ , \end{cases}$$

where

$$w_k = \frac{2k\pi}{T} \ ,$$

$$\alpha_k = 2\left(\frac{w_k}{T(w_k^2 - (\frac{\pi}{D_2})^2} - \frac{1}{2k\pi}\right) ,$$

$$\beta_k = 2\left(\frac{1}{2\cdot T(w_k + \frac{\pi}{D_2})} - \frac{1}{2k\pi}\right) ,$$

$$d = D_2/2 \ .$$

In order to simulate the motion blurring phenomenon on a digital computer, the impulse response $\hat{h}(x,u)$ in (5.83) was discretized and $\hat{h}_D(n,m)$ corresponds to the discrete version of (5.83), where

$$\hat{h}_D(n,m) = \hat{h}(n\Delta, m\Delta) \ ,$$

for a fixed Δ, such that $U = (N-1)\cdot\Delta$. The constant U has been previously defined and N corresponds to the size

$$T_p > U_2 - U + D_1,$$

where

$$U_2 = \frac{T+a}{a} U + \frac{\alpha T}{a} ,$$

and D_1 will be defined to be $T_p/4$. Under this assumption $\hat{h}(x,u)$ can be expanded in a Fourier series, which is truncated to yield,

$$h^*(x,u) = a_0(u) + \sum_{k=1}^{K} \{a_k(u)\cos(\frac{2\pi}{T_p}kx) + b_k(u)\sin(\frac{2\pi}{T_p}kx)\}. \tag{5.84}$$

The $a_k(u)$'s and $b_k(u)$'s in (5-13), obtained in closed form, are

$$a_0(u) = \frac{a}{T(u+\alpha)} (u_2 - u_1 - d_2), \tag{5.85a}$$

$$a_k(u) = \begin{cases} \frac{a}{(u+\alpha)} \cdot \{\alpha_k \sin(w_k(u_2-d))\cos(w_k d) - \frac{1}{k\pi}\sin(w_k u_1)\}, \\ \qquad \frac{1}{D_2} \neq \frac{2k}{T} , \\ \frac{a}{(u+\alpha)} \cdot \{\beta_k \sin(w_k(u_2-d))\cos(w_k d) - \frac{1}{k\pi}\sin(w_k u_1) \\ \qquad - \frac{d}{T}\cos(\frac{\pi}{D_2}u_2) , \frac{1}{D_2} = \frac{2k}{T} \\ \qquad k=1,2,\ldots , \end{cases} \tag{5.85b}$$

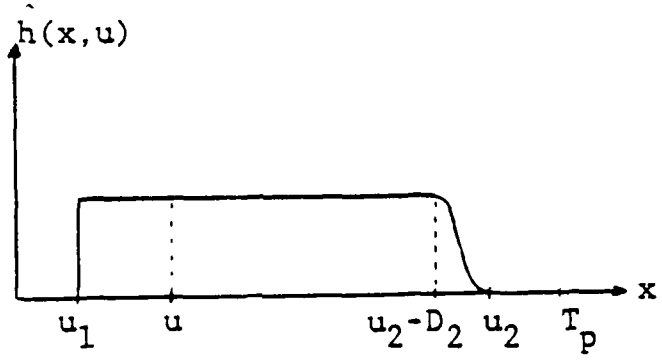

Figure 5.3: The impulse response of LSV system modeling motion blur

over these superfluous points. The discontinuity at $x = \frac{T+a}{a} u + \frac{\alpha T}{a}$, will be slightly smoothed for better results in the approximation. From the above, the function to be approximated, $\hat{h}(x,u)$, is

$$\hat{h}(x,u) = \begin{cases} \frac{a}{u+\alpha} & u_1 \le x \le u_2 - D_2 , \\ \frac{a}{u+\alpha} \cdot w(x) & u_2 - D_2 \le x \le u_2 , \\ 0 & \text{elsewhere} , \end{cases} \qquad (5.83)$$

where

$$u_1 = u - D_1 ,$$

$$u_2 = \frac{T+a}{a} u + \frac{\alpha T}{a} ,$$

$$D_2 = (u_2 - u)/10 ,$$

$w(x)$ is a Hanning window, given as

$$w(x) = .5(1 - \cos(\frac{\pi}{D_2} (x-u_2)).$$

The constant D_1 will be defined later in this section. The function, $\hat{h}(x,u)$, is plotted, for a fixed but arbitrary value of u, in Figure 5.3.

The u variable will take values over a finite interval, $[0,U]$; then, for any arbitrary but fixed $u \in [0,U]$, we can consider $\hat{h}(x,u)$ to be periodic in x for a sufficiently large period, T_p.

5.5 Examples of Applications

In this section, two examples are presented which illustrate the application of the state-space model for the inverse system to the restoration of a degraded image, where the degradation is modeled by a LSV system describable by (5.10) to (5.17). In section 5.5.1, the physical phenomenon responsible for image degradation is motion blur while in section 5.5.2 the degradation is due to a type of optical aberration, referred to as coma.

5.5.1. Space-Variant Motion Blur

Consider the one-dimensional motion [5.18]

$$u = g(x;t) = \frac{ax-\alpha t}{t+a} \qquad a,\alpha,u > 0 \quad t \in [0,T], \tag{5.81}$$

Using Sawchuk's analysis, this motion is modeled by a LSV system whose impulse response is:

$$h(x,u) = \begin{cases} \frac{a}{u+\alpha}, & u \leq x \leq \frac{T+a}{a}u + \frac{\alpha T}{a}, \\ 0 & \text{elsewhere}, \end{cases} \tag{5.82}$$

In order to obtain a 1-D state-space model for this blurring, the impulse response in (5.82) will be approximated in degenerate form. Before carrying out the approximation, it is important to note that the state-space model is causal and, therefore, it will not evaluate the impulse response, $h(x,u)$, at points $x < u$; this will be used to our advantage in extending $h(x,u)$

$$h(n_1,n_2;n_1,n_2) \neq 0 \text{ for all } 0 \leq n_i \leq N \text{ , } i=1,2. \qquad (5.79)$$

5.4.2 Weakly Causal Case

The inverse of the system described in (5.74)-(5.75) is easily shown to be:

$$\underline{z}(n_1,n_2) = \underline{A}_I(n_1,n_2)[\underline{z}(n_1-t,n_2+q) + \underline{z}(n_1+r,n_2-p) - \underline{z}(n_1+r-t,n_2+q-p)] + \underline{b}_I(n_1,n_2)y(n_1,n_2) \qquad (5.80a)$$

$$u(n_1,n_2) = \underline{c}_I(n_1,n_2)[\underline{z}(n_1-t,n_2+q) + \underline{z}(n_1+r,n_2-p) - \underline{z}(n_1+r-t,n_2+q-p)] + \underline{d}_I(n_1,n_2)y(n_1,n_2), \qquad (5.80b)$$

with initial conditions

$$\underline{z}(tn+r,-qn-p) = \underline{0} \text{ , } z(-rn-t,pn+q) = \underline{0} \text{ , } n=0,1,\ldots \qquad (5.80c)$$

where $\underline{A}_I(n_1,n_2)$, $\underline{b}_I(n_1,n_2)$ $\underline{c}_I(n_1,n_2)$ and $\underline{d}_I(n_1,n_2)$ have been defined in (5.77).

The necessary and sufficient condition for the existence of the state-space model, in (5.80) is,

$$\underline{c}_I(n_1,n_2) \cdot \underline{b}_I(n_1,n_2) \neq 0 \text{ for all } (n_1,n_2) \in C_c \text{ ,}$$

or, equivalently,

$$h(n_1,n_2;n_1,n_2) \neq 0 \text{ for all } (n_1,n_2) \in C_c \text{ ,}$$

$$\underline{z}(n_1,-1) = \underline{0}\ ,\ z(-1,n_2) = \underline{0} \text{ for } n_i=0,1,\ldots,N\ ,\ i=1,2\ , \quad (5.76c)$$

where

$$\underline{A}_I(n_1,n_2) = I_K - \underline{b}(n_1,n_2)[\underline{c}(n_1,n_2)\underline{b}(n_1,n_2)]^{-1}\ \underline{c}(n_1,n_2), \quad (5.77a)$$

and I_K is the K-th order identity matrix,

$$\underline{b}_I(n_1,n_2) = \underline{b}(n_1,n_2)[\underline{c}(n_1,n_2)\underline{b}(n_1,n_2)]^{-1}, \quad (5.77b)$$

$$\underline{c}_I(n_1,n_2) = -[\underline{c}(n_1,n_2)\underline{b}(n_1,n_2)]^{-1}\ \underline{c}(n_1,n_2)\ , \quad (5.77c)$$

$$\underline{d}_I(n_1,n_2) = [c(n_1,n_2)\underline{b}(n_1,n_2)]^{-1}. \quad (5.77d)$$

It is important to note at this stage, that the state-space model of the inverse system, given in equations (5.76) and (5.77), is based also on a three point recursion. Therefore, it will provide a very efficient deconvolution procedure. In addition to this, for a reasonably low order state-space model, there will be no storage problem because the state-vector is only two dimensional and there is no need to store it over the entire input mask.

The state-space model, considered here, for the inverse system exists if and only if

$$\underline{c}(n_1,n_2)\underline{b}(n_1,n_2) \neq 0 \text{ for } 0 \leq n_i \leq N\ ,\ i=1,2, \quad (5.78)$$

or equivalently, by substituting (5.15) and (5.16) in (5.78) and making use of (5.2), we have that the condition in (5.78) is equivalent to

From the above equations, we can see that the state-space model in (5.74) and (5.75) preserves the three point recursion. It is important to emphasize that in this case the recursion in (5.74a) does not depend on the closest past neighbors of the point currently under consideration.

5.4 State-Space Model for the Inverse System

In section 5.4.1, the state-space model for the inverse of the system described in (5.10)-(5.17) is first given. In section 5.4.2, the counterpart in the weakly causal case is considered.

5.4.1 First Quadrant Quarter-Plane Case

Consider the state-space model of the first quadrant quarter-plane discrete LSV system described in (5.10)-(5.17). The state-space model of the inverse system, whose state-vector, input and output at the point (n_1,n_2) are, respectively, $\underline{z}(n_1,n_2)$, $y(n_1,n_2)$ and $u(n_1,n_2)$ is:

$$\underline{z}(n_1,n_2) = \underline{A}_I(n_1,n_2)[\underline{z}(n_1-1,n_2) + \underline{z}(n_1,n_2-1) - \underline{z}(n_1-1,n_2-1)] + \underline{b}_I(n_1,n_2)y(n_1,n_2), \quad (5.76a)$$

$$u(n_1,n_2) = \underline{c}_I(n_1,n_2)[\underline{z}(n_1-1,n_2) + \underline{z}(n_1,n_2-1) - \underline{z}(n_1-1,n_2-1)] + \underline{d}_I(n_1,n_2)y(n_1,n_2), \quad (5.76b)$$

with initial conditions

where C is a constant and the regions I and II are clearly defined in Figure 5.5.

The impulse response $h(x_1,x_2;\tau_1,\tau_2)$ for the coma aberration in (5.92) is, in general, non-causal, but by imposing some constraint on the radius R_0 in the pattern of the impulse response $h_0(x_1,x_2)$ in (5.93) as shown in Figure 5.5, it is possible to perform the deconvolution, recursively. The restriction on R_0 corresponds to a limitation in the amount of coma aberration to be tolerated, which can be made very small depending on the quality of the lens.

In order to perform the deconvolution, the input plane will be divided into its four quadrants and the deconvolution will be carried out for each one of them. The final reconstructed object is obtained by superimposing the four resulting arrays. For this procedure to be valid, without loss of generality, an object point outside Q_1 should not affect an image point on Q_1. This condition is illustrated in Figure 5.6, and it will be used to determine a bound for R_0.

From Figure 5.6, the inequality $d_v < |\hat{y}|$ is sufficient to guarantee that the object point (τ_1,τ_2) will not affect any image point on Q_1. Simple calculations enable one to get the maximum allowable R_0 required to recursively restore an (NxN) input array to be

$$R_{0_{max}} = \frac{1}{(\frac{1}{3})^{\frac{1}{2}}\,(N-1) - 2} \qquad (5.94)$$

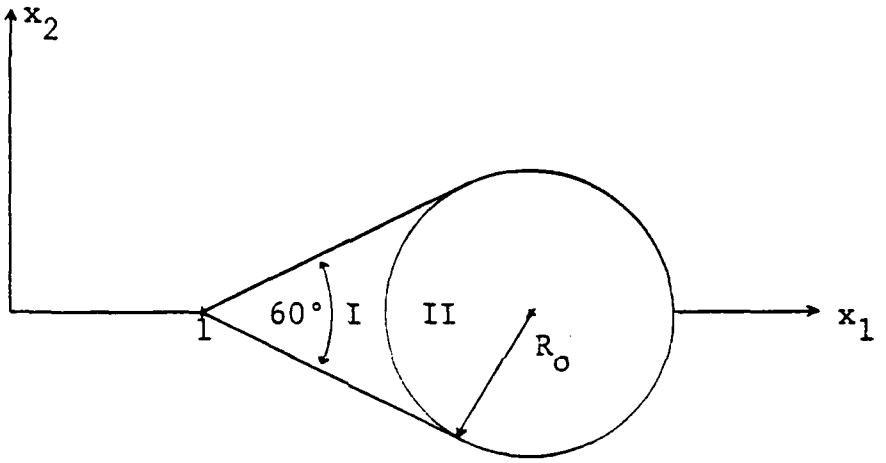

Figure 5.5: The shape of impulse response of LSV system modeling coma aberration

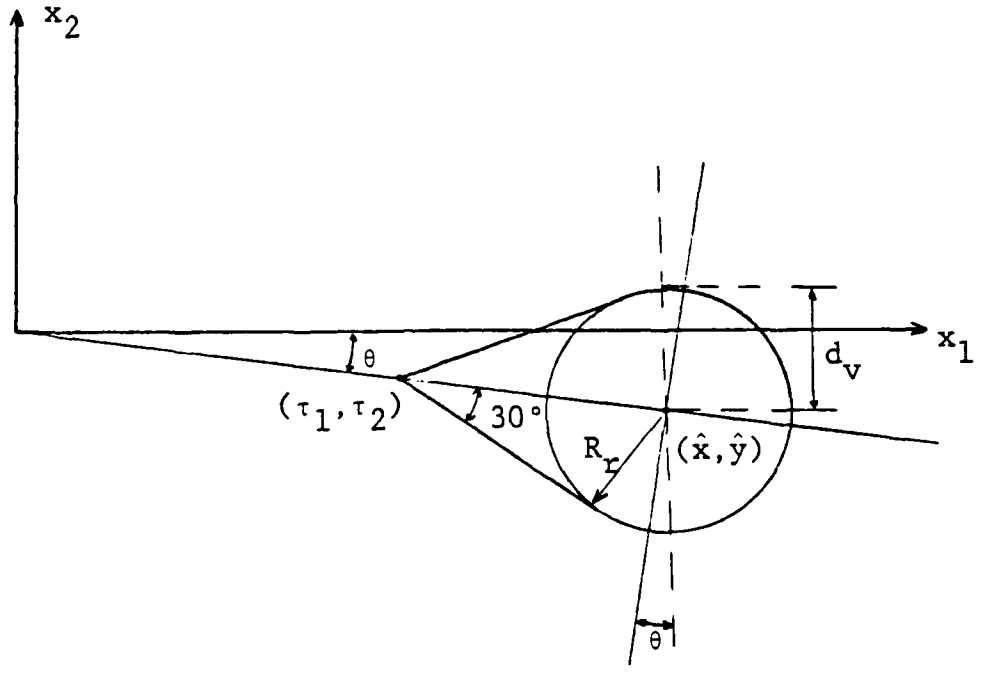

Figure 5.6: Diagram to determine a maximum value of the radius of the coma pattern

As an example, a (31x31)-point original object $u(n_1,n_2)$, $-15 \le n_i \le 15$, $i=1,2$, which is the counterpart of the (32x32)-point original object in Figure 5.4a was blurred by the coma aberration. For this object size, N=31, and $R_{D_{max}} = .065$. The blurred image $y(n_1,n_2)$, $-15 \le n_i \le 15$, $i=1,2$ was obtained by performing the summation,

$$y(n_1,n_2) = \sum_{m_1=-15}^{15} \sum_{m_2=-15}^{15} \hat{h}_D(n_1,n_2;m_1,m_2)u(m_1,m_2)$$
$$-15 \le n_i \le 15, \quad i=1,2$$

where

$$\hat{h}_D(n_1,n_2;m_1,m_2) = h(n_1\Delta,n_2\Delta;m_1\Delta,m_2\Delta)$$
$$-15 \le n_i \le 15, \quad -15 \le m_i \le 15, \quad i=1,2$$

and

$$\Delta = 1/15$$

The resulting blurred image is shown in Figure 5.7. In order to implement the state-space model, the impulse response, $\hat{h}_D(n_1,n_2;m_1,m_2)$, was exactly represented as a degenerate sequence by means of the DFT of $h_D(n_1,n_2;m_1,m_2)$ for each pair (m_1,m_2), $-15 \le m_i \le 15$. This procedure is explained in [5.21]. The symmetry of the impulse response of the coma blurring was used in reducing the amount of DFT's required for this representation. A state-space model of the inverse system was obtained and used in the deconvolution. The deconvolved image matched exactly the original image.

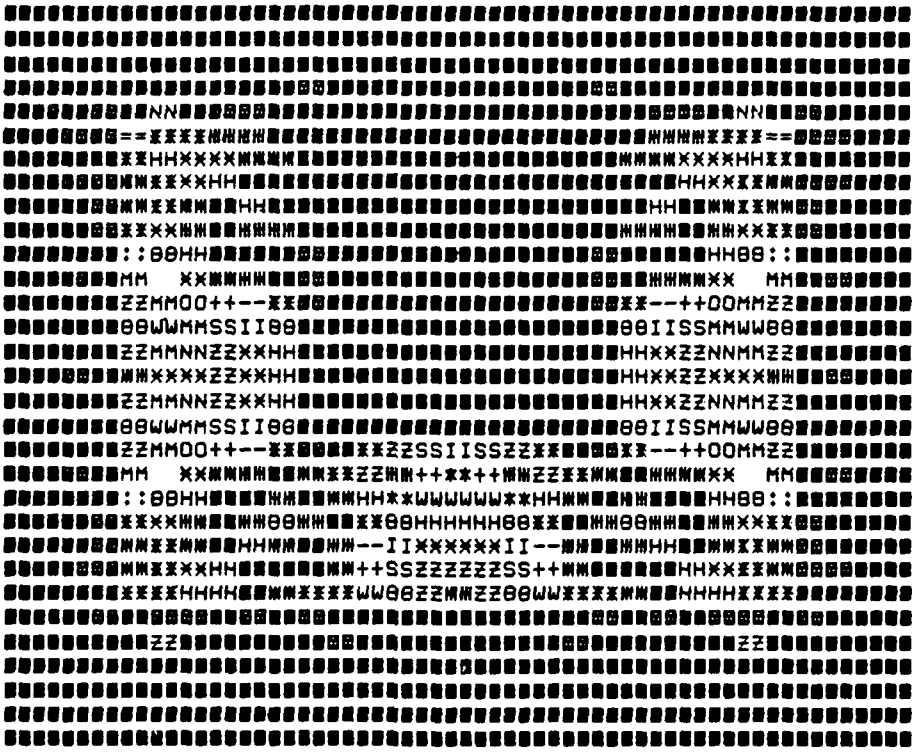

Figure 5.7: Image blurred by coma aberration

5.6 Conclusions

Procedures for compensating for effects which degrade the accuracy of remotely sensed datas by mathematically inverting some of the degrading phenomenon are required in biomedical, industrial, surveillance and earth and space applications. Images to be restored are often degraded by a linear spatially varying operation. Degradations due to motion blurring and optical system distortions often require the imaging systems to be analyzed by modeling the degradation as a linear shift-variant operation. High speed digital computers have been primarily responsible for the development of techniques for image restoration of shift-invariant motion blur, but counterparts of such techniques in the shift-variant case are severely handicapped by the required space-time computational complexity. Attention has been directed to the alleviation of this shortcoming and the results arrived at are, first, briefly summarized and then directions for research in the immediate future are provided.

For any 2-D discrete first quadrant quarter-plane causal linear shift-variant (LSV) system, whose impulse response is a K-th order degenerate sequence a K-th order state-space model was obtained. This model is recursive and is based on a three-term recurrence formula relating any point in the state-space model to its three closest past points and the current input. The state-space model was extended in order to model 2-D discrete LSV systems with support on a causality cone. Subsequently, the 2-D quarter-plane causal and weakly causal discrete models were extended to the n-D ($n > 2$) case.

The resulting state-space models are recursive and based on a (2^n-1)-points recurrence formula, which for the causal case used the (2^n-1)-closest neighboring past points in addition to the input in order to compute any current output state. For the weakly causal case, the (2^n-1) computed points required are not, in general, the closest neighbors to the present output, which is being computed. Conditions for the existence of a 2-D state-space model for the inverse system are readily derivable from the original one. Models for the 2-D LSV system and its inverse can be used to perform analysis and deconvolution problems very efficiently. This can be substantiated from dervided expressions for space-time computational complexities [5.21].

Examples of physically motivated applications making use of the theoretical results developed have been worked out. These applications include effects of 1-D LSV motion blur and the blurring due to Seidel aberrations of a lens; in particular, the 2-D LSV coma aberration was studied in detail. The reconstruction of the original object from the LSV blurred image was carried out successfully by means of the state-space model for the inverse system. For the construction of the LSV model, the impulse responses of the blurring phenomena were approximated in degenerate form via series expansions using orthogonal functions. For details regarding this, see [5.21].

The possibility of using the state-space model of the inverse system for the restoration of the original object from a LSV blurred image in the presence of additive noise is currently under investigation. A causal, discrete counterpart of the integral equation in Phillips [5.22] was implemented, and for various signal-to-noise-ratios (SNR) the deconvolution was performed. It is interesting to note that in this case, there were no large oscillations and as the SNR increased the difference between the original sequence and the deconvolved one decreased. Also the deconvolution of motion blurred and coma blurred images corrupted by noise was performed for different SNR. The restored objects, for a SNR=100 or larger, were easily recognized in the case of objects with well defined edges, such as a white letter on a black background. The reconstruction of the original object was very poor in the case when the object did not have sharply defined edges

Since the state-space model developed works very efficiently to deblur images affected by 2-D linear shift-varying blurs, its use, in presence of noise needs to be examined. An obvious approach would be to filter out the additive noise, and, subsequently, obtain, recursively, the restored object using the state-space model of the inverse system, already developed. Specifically, let $x(k_1,k_2)$ be the blurred image with additive noise,

$$x(k_1,k_2) = s(k_1,k_2) + n(k_1,k_2) \qquad (5.95)$$

where $s(k_1,k_2)$ is the spatially-variant blurred image and $n(k_1,k_2)$ is the additive noise. We want to filter out

$n(k_1,k_2)$ or in other words we want a satisfactory estimate, $\hat{s}(k_1,k_2)$, of the blurred image. From this obtained estimate, $\hat{s}(k_1,k_2)$, the deconvolution can be implemented, recursively, via the developed state-space model. Some assumptions are necessary before $n(k_1,k_2)$ may be filtered out to satisfaction. A stationary noise, $\{n(k_1,k_2)\}$, which is uncorrelated with $\{s(k_1,k_2)\}$ and having known mean as well as correlation may be assumed. The sequence, $\{s(k_1,k_2)\}$ originates from a spatially blurred object and, therefore, it is inherently nonstationary. We will assume that $\{s(k_1,k_2)\}$ is nonstationary in the mean and also in the autocorrelation. Under these assumptions, we feel that a solution to the filtering problem could be obtained and a possible approach is outlined.

It is possible to transform $\{x(k_1,k_2)\}$ into an approximately stationary process, $\{\bar{x}(k_1,k_2)\}$, given by [5.23],

$$\bar{x}(k_1,k_2) = \bar{s}(k_1,k_2) + \bar{n}(k_1,k_2) \qquad (5.96)$$

where $\{\bar{s}(k_1,k_2)\}$ and $\{\bar{n}(k_1,k_2)\}$ are stationary and uncorrelated and the mean and correlation of $\{\bar{n}(k_1,k_2)\}$ are computable from those of $\{n(k_1,k_2)\}$. From the process, $\{\bar{x}(k_1,k_2)\}$, an estimate, $\hat{\bar{s}}(k_1,k_2)$, of $\bar{s}(k_1,k_2)$ is obtained. This is possible to do via use of Wiener filtering theory. Next, an inverse transformation to that employed in order to arrive at (5.96) is applied to $\{\hat{\bar{s}}(k_1,k_2)\}$ and an estimate $\hat{s}(k_1,k_2)$ of the original image $s(k_1,k_2)$ is obtained. It is pointed out that if the noise is nonstationary, further assumptions are necessary (like local stationarity) before a satisfactory solution to the problem is expected.

Linear Restoration of Bilinearly Distorted Image: Several applications require restoration of bilinearly (a special type of nonlinear map) distorted images. Some of these applications and a procedure to restore bilinearly distorted image in the presence of additive noise, by linear filtration is considered in [5.24]. It is also known how 1-D bilinear transformation (shift-invariant or special shift-variant) can be computed by use of 2-D linear optical processors [5.25]. It has also been pointed out in [2, p. 219] that properties of n-D bilinear systems can be inferred from the investigation of similar properties in a 2n-D linear system. These inter-relations between a bilinear and a higher dimensional linear system suggest the necessity of investigating into the possibility of restoring bilinearly distorted images using the developed state-space model (of appropriate spatial dimension) for linear shift variant systems.

REFERENCES

[5.1] H. D'Angelo, "Linear Time-Varying Systems: Analysis and Synthesis," Allyn and Bacon, Inc. Boston, 1970.

[5.2] D. G. Tucker, "Circuits with Periodically-Varying Parameters," Van Nostrand Co., Inc., London, 1964.

[5.3] N. K. Bose, "Applied Multidimensional Systems Theory," Van Nostrand Reinhold Co., New York, 1982.

[5.4] J. W. Goodman, "Operations achievable with coherent optical information processing systems," Proc. of IEEE, Jan. 1977, 65, pp. 29-38.

[5.5] R. Bamler and J. Hofer-Alfeis, "Optical restoration for rotation blur by sequence deconvolution," Tenth Int. Optical Comp. Conf., M.I.T., Cambridge, MA, April 1983, pp. 146-149.

[5.6] C. Braccini, "Scale-invariant, image processing by means of scaled transforms or form-invariant, linear shift-variant filters," Optics Letters, vol. 8, no. 7, July 1983, pp. 392-394.

[5.7] A. A. Sawchuk, "Space-variant image restoration by coordinate transformation," J. Opt. Soc. Am., 64, 1974, pp. 133-144.

[5.8] B. R. Frieden, "Restoring with maximum likelihood and maximum entropy," J. Opt. Soc. Am., 62, April 1972, pp. 511-518.

[5.9] C. K. Rushforth and R. L. Frost, "Comparison of some algorithms for constructing space-limited images," J. Op. Soc. Am., 70, Dec. 1980, pp. 1539-1543.

[5.10] E. S. Angel and A. K. Jain, "Restoration of images degraded by spatially varying point spread functions by a conjugate gradient method," Applied Optics, 17, July 1978, pp. 2186-2190.

[5.11] S. Kavata and Y. Ichioka, "Iterative image restoration for linearly degraded images 2: Reblurring procedure," J. Opt. Soc. Am., 70, July 1980, pp. 768-772.

[5.12] S. C. Sahasrabudhe and A. D. Kulkarni, "Shift variant image degradation and restoration using SVD," Computer Graphics and Image Proc., 9, March 1979, pp. 203-212.

[5.13] E. B. Barrett and R. N. Devich, "Linear programming compensation for space-variant image degradation," Abstract in J. Op. Soc. Am., 66, Feb. 1976, p. 172.

[5.14] N. Huang and J. K. Aggarwal, "On linear shift-variant digital filters," IEEE Trans. Circuits & Systems, 27, 1980, pp. 672-678.

[5.15] L. Zadeh, "Frequency analysis of variable networks," Proc. of IRE, 7, March 1950, pp. 290-299.

[5.16] E. W. Hansen and A. Jablokow, "State variable representation of a class of linear shift-variant systems," IEEE Transactions on Acoustics, Speech and Signal Processing, vol. ASSP-30, No. 6, December 1982, pp. 874-880.

[5.17] A. O. Aboutalib and L. M. Silverman, "Restoration of motion degraded images," IEEE Transactions on Circuits and Systems, vol. CAS-22, No. 3, March 1975, pp. 278-286.

[5.18] A. A. Sawchuk, "Space-variant motion degradation and restoration," Proc. of IEEE, 60, July 1972, pp. 854-861.

[5.19] G. M. Robbins and T. S. Huang, "Inverse filtering for linear shift-variant imaging systems," Proceedings of IEEE, 60, July 1972, pp. 862-872.

[5.20] G. M. Robbins, "Impulse response for a lens with Seidel aberrations," Res. Lab. Electroncis Quarterly Progress Report 93, M.I.T., Cambridge, MA, April 1969.

[5.21] H. M. Valenzuela, "Modeling of multidimensional linear shift-variant systems with applications," Ph.D. Dissertation (based on research conducted under the supervision of N. K. Bose), University of Pittsburgh, Pittsburgh, PA, 1983.

[5.22] D. L. Phillips, "A technique for the numerical solution of certain integral equations of the first kind," JACM, vol. 9, 1962, pp. 84-97.

[5.23] Rosenfeld, A., ed., Image Modeling, "Nonstationary Statistical Image Models and Their Application to Image Data Compression," by B. R. Hunt, Academic Press, New York, 1981

[5.24] B. E. A. Saleh and W. D. Goeke, "Linear restoration of bilinearly distorted images," J. Op. Soc. Am., 70, May 1980, pp. 506-515.

[5.25] B. E. A. Saleh, "Bilinear processing of 1-D signals by using linear 2-D coherent optical processors," Applied Optics, 21, Nov. 1978, pp. 3408-3411.

$$\underline{g} \triangleq [g(0),g(1),\cdots,g(N-1)]^T \tag{3.10}$$

hen, the bilinear system description in (1.1), or (3.2), can be written as

$$B\underline{x} = \underline{g} \tag{3.11}$$

herefore, the image restoration problem of interest here requires the finding of the onnegative vector $\underline{f}$ which satisfies (3.7), (3.8) and (3.11).

Fact 3.1 : Let $Q^{(n)}$, $\underline{h}^{(n)}$, n=0,1,•••,N−1, B, $\underline{f}$, and $\underline{g}$ be, respectively, as in (3.4), (3.5), (3.6), 3.3), and (3.10) and $\underline{h}^{(n)}$, n=0,1,•••,N−1 and $\underline{f}$, $\underline{g}$ be nonnegative. Define an N×1 vector $\underline{w}$, /hose elements are given by,

$$(\underline{w})_i = \sqrt{(\underline{g})_i} \tag{3.12}$$

nd also define an N×N matrix U

$$U \triangleq \begin{bmatrix} \underline{h}^{(0)T} \\ \underline{h}^{(1)T} \\ \vdots \\ \underline{h}^{(N)T} \end{bmatrix} . \tag{3.13}$$

' $\underline{f}$ is a solution of

$$U\underline{f} = \underline{w} \tag{3.14}$$

hen $\underline{x}$ obtained from $\underline{f}$ via (3.7) and (3.8) will be a solution of

$$B\underline{x} = \underline{g}. \tag{3.15}$$

et the linear subspace $R(B^T)$ be defined as

$$R(B^T) \triangleq \{\underline{z} : \underline{z}=B^T\underline{y},\ \underline{y}\epsilon R^N\} \tag{3.16}$$

/here R^N denotes the N-dimensional Euclidean space. Then, the projection, $\hat{\underline{x}}$, of $\underline{x}$ on (B^T) will satisfy

$$< (B)_i^T, \hat{\underline{x}} > = (\underline{g})_i, \quad i=1,2,\cdots,N \tag{3.17}$$

Proof : (3.14) implies that

$$<\underline{h}^{(i-1)},\underline{f}> = (\underline{w})_i.$$

3. Image Restoration From Noncausal Bilinear Blurring

In this section, the problem of restoring an image which is blurred by the bilinear system described by (1.1), will be discussed. The (N×N) nonnegative matrix, $Q^{(n)}$, is, first defined.

$$Q^{(n)} \triangleq \begin{bmatrix} q(n;0,0) & q(n;0,1) & \cdots & q(n;0,N-1) \\ q(n;1,0) & q(n;1,1) & \cdots & q(n;1,N-1) \\ \vdots & \vdots & \cdots & \vdots \\ q(n;N-1,0) & q(n;N-1,1) & \cdots & q(n;N-1,N-1) \end{bmatrix} \qquad n=0,1,\cdots,N-1 \tag{3.1}$$

Then, $Q^{(n)}$, $n=0,1,\cdots,N-1$, are symmetric matrices if $\gamma(m_1,m_2)$ in (1.2) is symmetric. Assume that $\gamma(m_1,m_2)$ is symmetric [4, 6, 7, 13] throughout this section. With $Q^{(n)}$ in (3.1), equation (1.1) can be rewritten by

$$g(n) = \underline{f}^T Q^{(n)} \underline{f}, \qquad n=0,1,\cdots,N-1 \tag{3.2}$$

where

$$\underline{f} = [f(0),f(1),\cdots,f(N-1)]^T \tag{3.3}$$

If the system is completely coherent, then

$$Q^{(n)} = \underline{h}^{(n)} \underline{h}^{(n)T}, \qquad n=0,1,\cdots,N-1 \tag{3.4}$$

where

$$\underline{h}^{(n)} = [h(n;0),h(n;1),\cdots,h(n;N-1)]^T, \qquad n=0,1,\cdots,N-1 \tag{3.5}$$

Let $(A)_i$ denote the i^{th}-row of A. Let,

$$(B)_i \triangleq [(Q^{(i-1)})_1,(Q^{(i-1)})_2,\cdots,(Q^{(i-1)})_N], \qquad i=1,2,\cdots,N \tag{3.6}$$

$$X = \underline{f}\underline{f}^T \tag{3.7}$$

and

$$\underline{x} = [(X)_1,(X)_2,\cdots,(X)_N]^T \tag{3.8}$$

Then, using the usual Euclidean innerproduct notation, $<\cdot,\cdot>$, (3.2) is expresseible as,

$$g(n) = < (B)_{n+1}^T, \underline{x} >, \qquad n=0,1,\cdots,N-1 \tag{3.9}$$

Let

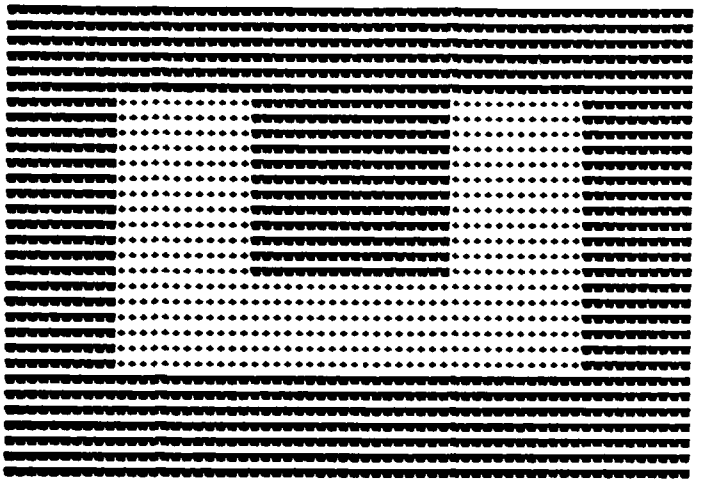

(a) Original Image

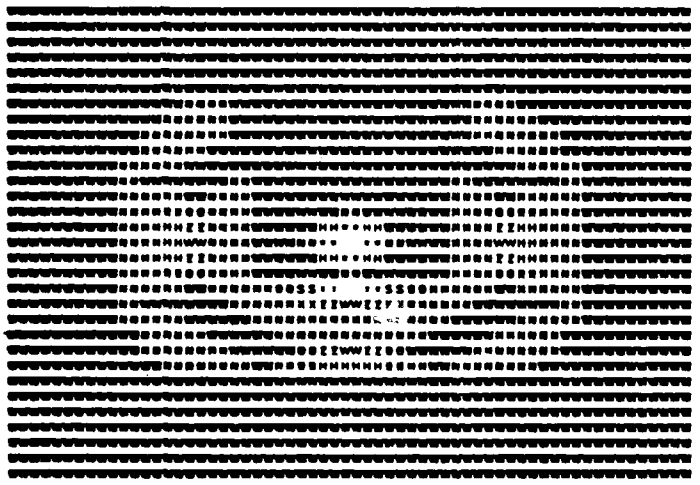

(b) Blurred Image

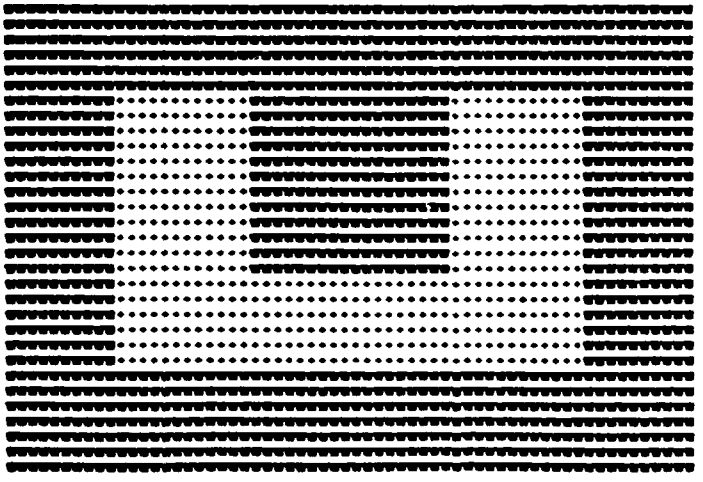

(c) Restored Image

'igure - 5. Bilinearly Blurred Image Restoration Simulation (Causal)

has been done in [17]. For a (31×31) image, $R_0 \leq 0.0065$ guarantees the occurrence of the desired effect and for each segmented region, the support of $h_c(n_1,n_2;m_1,m_2)$ is obtained from:

$$h_c(n_1,n_2;m_1,m_2) = \begin{cases} \text{nonzero} , & m_1 \leq n_1 \text{ and } m_2 \leq n_2 \\ 0 , & \text{otherwise} \end{cases} \tag{2.21}$$

Then, each segmented image is blurred bilinearly by using (2.13). Figure-5(a) shows the original 31×31 image and Figure-5(b) shows the blurred image. To simulate the blurred image, Δ in (2.19) has been chosen as 0.254. Also $\gamma_2(m_1,m_2,\ell_1,\ell_2)$ in (1.2) is given by

$$\gamma_2(m_1,m_2,\ell_1,\ell_2) = \text{sinc}[(m_1-\ell_1)/N_h]\text{sinc}[(m_2-\ell_2)/N_h] \tag{2.22}$$

where N_h is the maximum possible support width of $h_c(n_1,n_2;m_1,m_2)$ for any (n_1,n_2). The system's coherent impulse response is given by

$$h_2(n_1,n_2;m_1,m_2) = \sqrt{h_c(n_1,n_2;m_1,m_2)} \tag{2.23}$$

Each function has been chosen to ensure the nonnegativity of the resulting DIR. By applying the algorithm in Figure-1 to each segmented output quadrant image and by combining those results, the original image is recovered as in Figure-5(c).

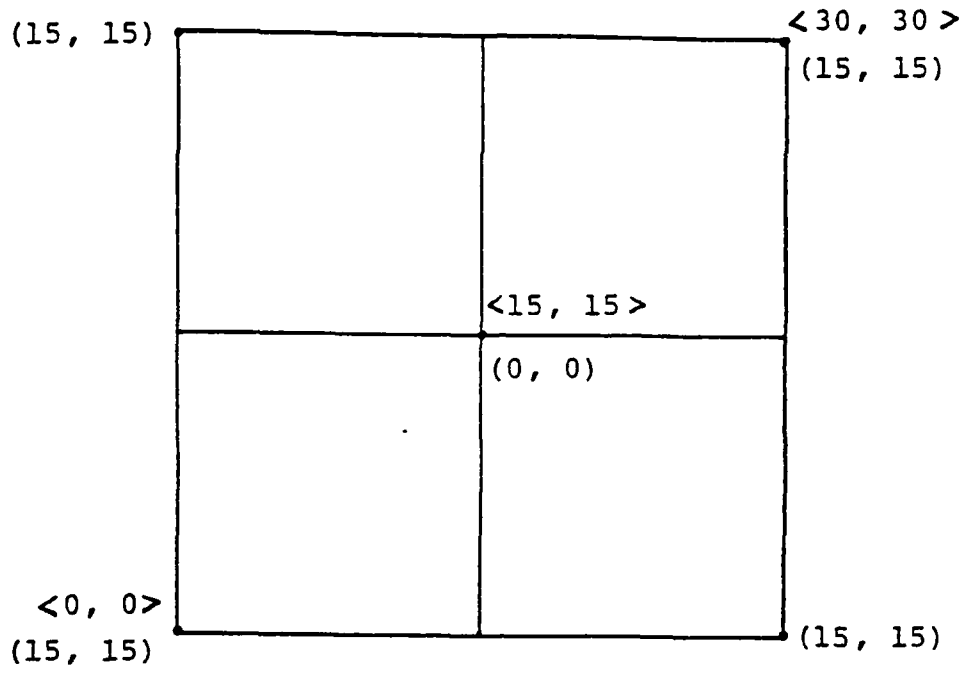

Figure - 3. Image Segmentation and Indexing in Coma Blur

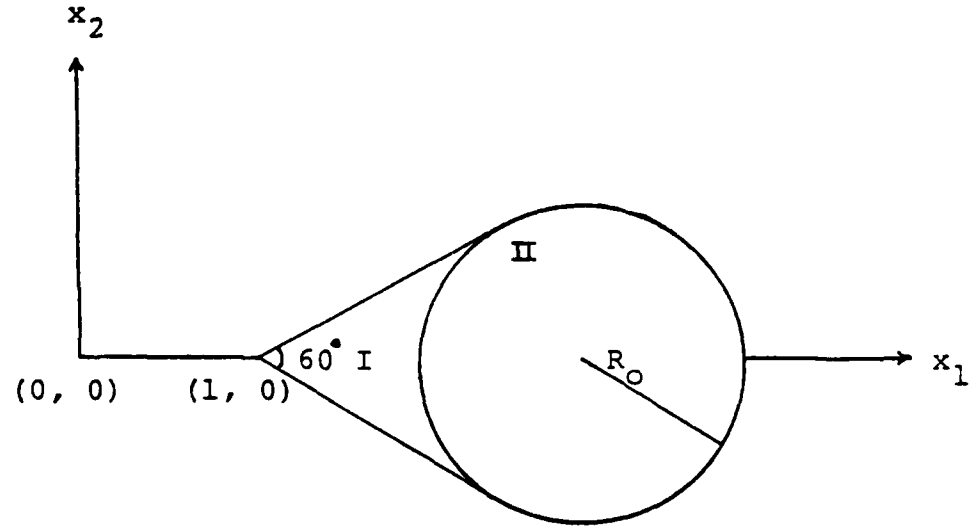

Figure - 4. The Shape of Impulse Response of the Coma Aberration

The recursive implementation analogous to (2.8), (2.9) and (2.10) also can be obtained. Since (2.13) characterizes a quarterplane 2-D discrete system, row-by-row recursion, i.e., $(n_1,n_2) \rightarrow (n_1+1,n_2) \rightarrow \cdots \rightarrow (N-1,n_2) \rightarrow (0,n_2+1) \rightarrow (1,n_2+1) \rightarrow \cdots$, and the column-by-column recursion are two of several possibilities for implementing the recursion. The next equation provides the input/output description of 2-D discrete bilinear system whose DIR has support in a nonsymmetric half-plane on (m_1,m_2)-plane or (ℓ_1,ℓ_2)-plane.

$$y(n_1,n_2) = \sum_{m_1=0}^{n_1}\sum_{m_2=0}^{N-1}\sum_{\ell_1=0}^{n_1}\sum_{\ell_2=0}^{N-1} q_2(n_1,n_2;m_1,m_2,\ell_1,\ell_2)u(m_1,m_2)u(\ell_1,\ell_2) \qquad (2.17)$$

or,

$$y(n_1,n_2) = \sum_{m_1=0}^{N-1}\sum_{m_2=0}^{n_2}\sum_{\ell_1=0}^{N-1}\sum_{\ell_2=0}^{n_2} q_2(n_1,n_2;m_1,m_2,\ell_1,\ell_2)u(m_1,m_2)u(\ell_1,\ell_2) \qquad (2.18)$$

(2.17) can be solved recursively column-by-column, and (2.18) row-by-row.

To simulate the proposed algorithm, we synthesize a special type of noncausal bilinear system by employing a coma type lens aberration as the system's coherent impulse response. The coma aberration is described in [17, 23]. It will be briefly described here.

In the rectangular coordinate system, it is easy to explain this coma aberration by segmenting the input support region into 4 quadrants as in Figure-3. And for each segmented quadrant the index will be reordered the center point of the original input as the origin, i.e., (0,0), of the each segmented image. In Figure-3, $<m_1,m_2>$ denotes the original index of (31×31) original image and (m_1,m_2) the new index for each segmented part. The point spread function, $h_C(n_1,n_2;m_1,m_2)$, of the lens coma aberration is given by [17]

$$h_C(n_1,n_2;m_1,m_2) = [1/\{(m_1\Delta)^2+(m_2\Delta)^2\}]h_0(x_1,x_2) \qquad (2.19)$$

where Δ denotes the sampling distance and

$$x_1 \triangleq (m_1n_1+m_2n_2)/(m_1^2+m_2^2)$$

$$x_2 \triangleq (m_1n_2-m_2n_1)/(m_1^2+m_2^2)$$

$$h_0(x_1,x_2) = \begin{cases} (2C)/\sqrt{x_1^2-3x_2^2}, & (x_1,x_2)\in I \\ C/\sqrt{x_1^2-3x_2^2}, & (x_1,x_2)\in II \end{cases} \qquad (2.20)$$

and regions I and II are defined in Figure-4. From Figure-4, it is clear that by constraining R_0 to be less than a certain value, it is possible to ensure that the i^{th}-quadrant input, i=1,2,3,4, does not affect the j^{th}-quadrant ($i\neq j$) output. This analysis

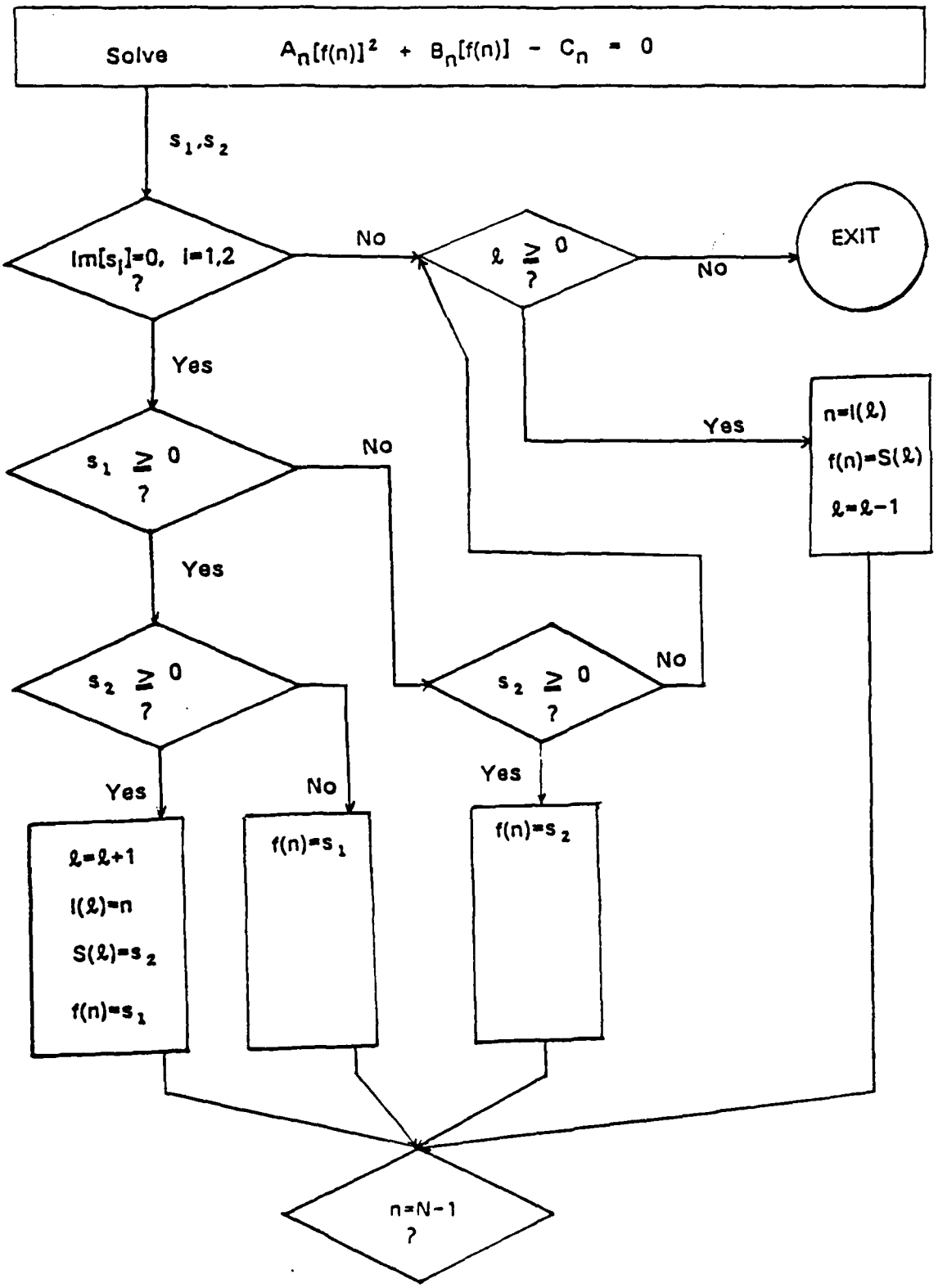

Figure-2. Added Algorithm for Real DIR Case

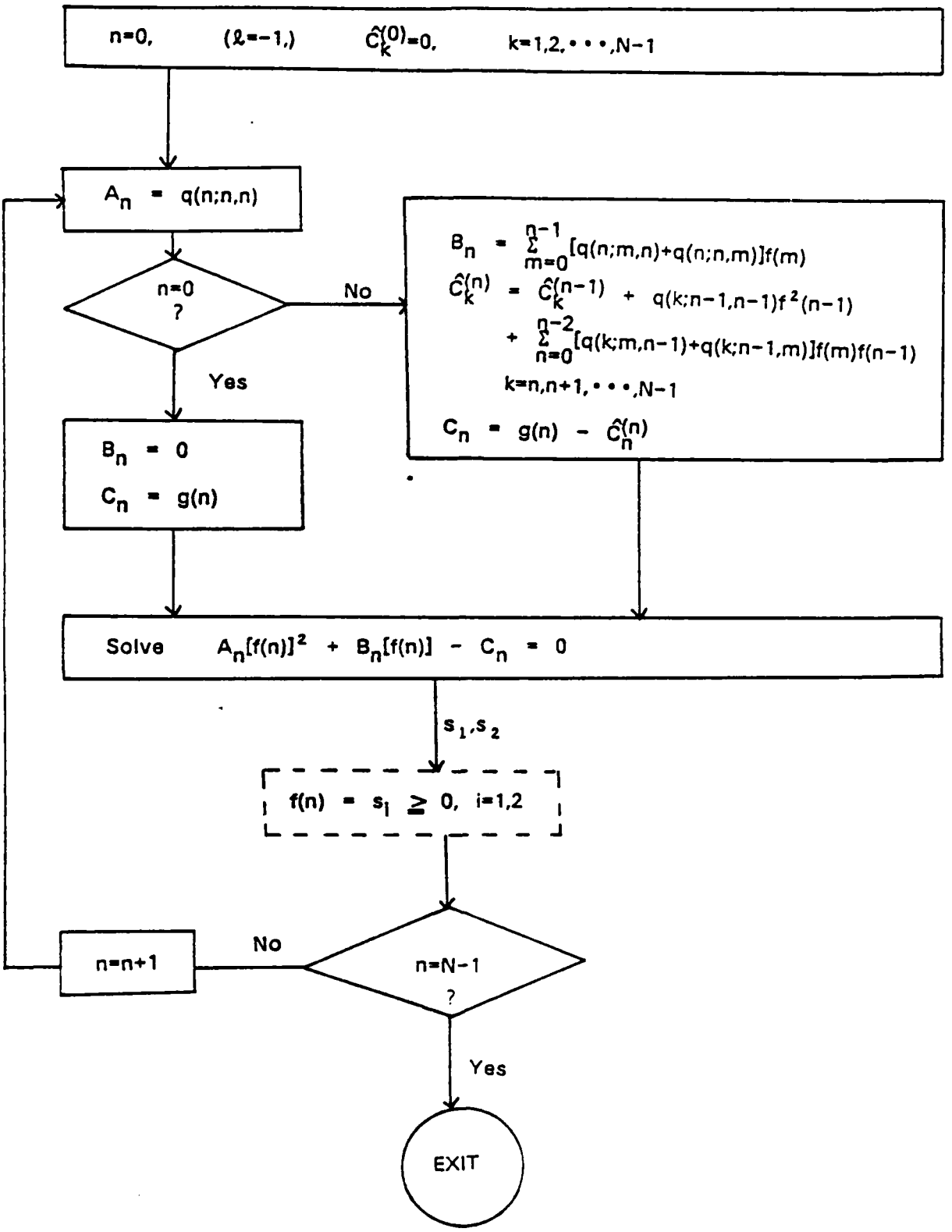

Figure-1. Recursive Restoration Algorithm for Nonnegative DIR Case

Suppose the values for f(m), m=0,1,•••,n−1, are known; then, A_n, B_n and C_n can be computed by using (2.5), (2.6) and (2.7). Hence, f(n) may be obtained by solving (2.12). Since all the coefficients, A_n, B_n and C_n, in (2.12) are nonnegative, the equation (2.12) has two real solutions, one of which is nonnegative and the other is negative. The nonnegative solution is assigned to f(n) and the recursion is continued. The flowchart for this is given in the Figure−1. In the Figure−1, the initialization $\ell=-1$ will not be necessary in this case. After recursion is completed, the desired nonnegative output, f(m), m=0,1,•••,N−1, is uniquely obtained.

Next, suppose that the elements of the DIR, are not all nonnegative. Then, the inequalities (2.3) and (2.4) may not hold. To proceed, it is assumed that $q(0;0,0)>0$. The flowchart in Figure−2, when embedded appropriately in the hatched box of Figure−1 provides a brute-force implementation of the solution f(m), m=0,1,•••,N−1, when this solution exists.

For a 2−D discrete bilinear system, the counterpart of the expression in (2.1) is

$$y(n_1,n_2) = \sum_{m_1=0}^{n_1}\sum_{m_2=0}^{n_2}\sum_{\ell_1=0}^{n_1}\sum_{\ell_2=0}^{n_2} q_2(n_1,n_2;m_1,m_2,\ell_1,\ell_2)u(m_1,m_2)u(\ell_1,\ell_2) \qquad (2.13)$$

where all the notations are self-evident. The counterparts of (2.5), (2.6), (2.7) in this case are given below.

$$A_{n_1,n_2} \triangleq q_2(n_1,n_2;n_1,n_2,n_1,n_2) \qquad (2.14)$$

$$\begin{aligned} B_{n_1,n_2} \triangleq & \sum_{m_1=0}^{n_1-1}\sum_{m_2=0}^{n_2-1}\{q_2(n_1,n_2;m_1,m_2,n_1,n_2)+q_2(n_1,n_2;n_1,n_2,m_1,m_2)\}u(m_1,m_2) \\ & +\sum_{m=0}^{n_1-1}\{q_2(n_1,n_2;m,n_2,n_1,n_2)+q_2(n_1,n_2;n_1,n_2,m,n_2)\}u(m,n_2) \\ & +\sum_{m=0}^{n_2-1}\{q_2(n_1,n_2;n_1,m,n_1,n_2)+q_2(n_1,n_2;n_1,n_2,n_1,m)\}u(n_1,m) \end{aligned} \qquad (2.15)$$

$$\begin{aligned} C_{n_1,n_2} \triangleq & \; y(n_1,n_2-\sum_{m_1=0}^{n_1-1}\sum_{m_2=0}^{n_2-1}\sum_{\ell_1=0}^{n_1-1}\sum_{\ell_2=0}^{n_2-1} q_2(n_1,n_2;m_1,m_2,\ell_1,\ell_2)u(m_1,m_2)u(\ell_1,\ell_2) \\ & -\sum_{m_1=0}^{n_1-1}\sum_{m_2=0}^{n_2-1}\sum_{\ell=0}^{n_1-1}\{q_2(n_1,n_2;m_1,m_2,\ell,n_2)+q_2(n_1,n_2;\ell,n_2,m_1,m_2)\}u(m_1,m_2)u(\ell,n_2) \\ & -\sum_{m_1=0}^{n_1-1}\sum_{m_2=0}^{n_2-1}\sum_{\ell=0}^{n_2-1}\{q_2(n_1,n_2;m_1,m_2,n_1,\ell)+q_2(n_1,n_2;n_1,\ell,m_1,m_2)\}u(m_1,m_2)u(n_1,\ell) \\ & -\sum_{m=0}^{n_1-1}[\sum_{\ell=0}^{n_1-1}q_2(n_1,n_2;m,n_2,\ell,n_2)u(\ell,n_2)+\sum_{\ell=0}^{n_2-1}q_2(n_1,n_2;m,n_2,n_1,\ell)u(n_1,\ell)]u(m,n_2) \\ & -\sum_{m=0}^{n_2-1}[\sum_{\ell=0}^{n_1-1}q_2(n_1,n_2;n_1,m,\ell,n_2)u(\ell,n_2)+\sum_{\ell=0}^{n_2-1}q_2(n_1,n_2;n_1,m,n_1,\ell)u(n_1,\ell)]u(n_1,m) \end{aligned} \qquad (2.16)$$

2. Image Restoration From Causal Bilinear Blurring (Noise-Free Case)

An 1-D discrete causal bilinear system will be represented by,

$$g(n) = \sum_{m_1=0}^{n}\sum_{m_2=0}^{n} q(n;m_1,m_2)f(m_1)f(m_2). \tag{2.1}$$

The case of nonnegative DIR will be considered first. Suppose that we are given g(n), n=0,1,•••,N-1 and q(n;m_1,m_2), $0 \leq m_1,m_2 \leq n$, n=0,1,•••,N-1, and these are nonnegative. The nonnegative input f(m), m=0,1,•••,N-1, is to be recovered. This can be done by rewriting (2.1) as

$$\begin{aligned} g(n) = {} & q(n;n,n)f^2(n) + [\sum_{m=0}^{n-1}\{q(n;m,n)+q(n;n,m)\}f(m)]f(n) \\ & + \sum_{m_1=0}^{n-1}\sum_{m_2=0}^{n-1} q(n;m_1,m_2)f(m_1)f(m_2). \end{aligned} \tag{2.2}$$

Since, for the noise-free case, $q(n;m_1,m_2) \geq 0$ and $f(m) \geq 0$, therefore

$$q(n;n,n)f^2(n) + [\sum_{m=0}^{n-1}\{q(n;m,n)+q(n;n,m)\}f(m)]f(n) \geq 0. \tag{2.3}$$

From (2.2) and (2.3), the inequality in (2.4) follows.

$$g(n) - \sum_{m_1=0}^{n-1}\sum_{m_2=0}^{n-1} q(n;m_1,m_2)f(m_1)f(m_2) \geq 0. \tag{2.4}$$

Let,

$$A_n \triangleq q(n;n,n) \tag{2.5}$$

$$B_n \triangleq \sum_{m=0}^{n-1}\{q(n;m,n)+q(n;n,m)\}f(m) \tag{2.6}$$

$$C_n \triangleq C_n^{(n)} = g(n) - \sum_{m_1=0}^{n-1}\sum_{m_2=0}^{n-1} q(n;m_1,m_2)f(m_1)f(m_2) \tag{2.7}$$

$C_n^{(n)}$ can be obtained by implementing the following recursion.

$$\hat{C}_k^{(0)} = 0, \qquad k=0,1,\bullet\bullet\bullet,n \tag{2.8}$$

$$\begin{aligned} \hat{C}_n^{(k)} = {} & \hat{C}_n^{(k-1)} + [\sum_{m=0}^{k-2}\{q(n;m,k-1)+q(n;k-1,m)\}f(m)]f(k-1) \\ & + q(n;k-1,k-1)f^2(k-1), \quad k=1,2,\bullet\bullet\bullet,n \end{aligned} \tag{2.9}$$

$$C_n^{(n)} = g(n) - \hat{C}_n^{(n)} \tag{2.10}$$

From (2.4), (2.5), (2.6) and (2.7)

$$A_n \geq 0, \quad B_n \geq 0, \quad C_n \geq 0. \tag{2.11}$$

The expression (2.2) can be rewritten in terms of A_n, B_n, and C_n by

$$A_n f^2(n) + B_n f(n) - C_n = 0. \tag{2.12}$$

$$h(n;m) = \begin{cases} \text{nonzero} , & m \leq n \\ 0 , & \text{otherwise,} \end{cases} \tag{1.12}$$

then it is easy to see that the system DIR will be of the form

$$q(n;m_1,m_2) = \begin{cases} \text{nonzero} , & m_1 \leq n \text{ and } m_2 \leq n \\ 0 , & \text{otherwise.} \end{cases} \tag{1.13}$$

For the incoherent imaging system of patterns on the translucent scattering substrates, the causality of the lens irradiance spread function and the substrate scattering function will result in the system DIR of the form in (1.13). A physical realization of the causal scattering substrate has not yet been reported. However, the example of the lens irradiance spread function of the type in (1.12) can be formed as we shall see in section 2 by considering the lens coma aberration [17]. Since the irradiance spread function, $h_c(n;m)$, of the lens is related to the system's coherent impulse response, from(1.4), by

$$h_c(n;m) = |h(n;m)|^2, \tag{1.14}$$

one can say that the support of $h(n;m)$ is the same as that of $h_c(n;m)$.

In this paper, we will mainly study the original image intensity restoration from the image intensity blurred by the system described by (1.1). For the restoration of the bilinearly blurred images, nonlinear [18, 19] as well as linear methods [12, 20, 21, 22] have been considered. The linear methods used for the restoration of a bilinearly blurred image are successful in the incoherent case, but the restoration becomes poor [18, 20, 21, 22] as the blurring system approaches the completely coherent case. The nonlinear method [19] has been successfully applied to restore only those images which are of low contrast following blurring by a coherent system.

A procedure to restore images blurred by completely coherent systems is described in section 3. In several applications including the imaging system of patterns on the translucent scattering substrate [13] and a portion of the diffraction-limited imaging system [7], the characterizing DIR is nonnegative. Except in section 2 this nonnegativity property of the DIR is assumed to hold. In section 2, a recursive scheme for restoring a class of bilinearly blurred images is developed. In section 3, a technique for restoring a wider class of bilinearly blurred images is considered. In section 4, the effect on the quality of restoration due to the presence of additive noise is analysed.

$$g(n) = \sum_{m=0}^{N-1} |h(n;m)|^2 |f(m)|^2 \tag{1.4}$$

where $g(n)$ and $|f(m)|^2$ represent, respectively, the image intensity at n and the object intensity at m. For the completely coherent case, in which the field's coherence function is given by [4, 6]

$$\gamma(m_1,m_2) = 1 , \quad \text{for all } m_1 \text{ and } m_2 \tag{1.5}$$

we have

$$g(n) = |\sum_{m=0}^{N-1} h(n;m)f(m)|^2. \tag{1.6}$$

The region falling between the two extremes of complete incoherence and complete coherence is the region of partial coherence and the partially coherent system is described by (1.1) and (1.2). When the following condition holds,

$$\gamma(m_1,m_2) = \gamma^*(m_2,m_1) \tag{1.7}$$

the field's coherence function is said to be symmetric and in that case the DIR $q(n;m_1,m_2)$ is also symmetric. This implies that,

$$q(n;m_1,m_2) = q^*(n;m_2,m_1). \tag{1.8}$$

When (1.8) holds and the input sequence is real, (1.1) is a hermitian form and, therefore, can be written as

$$g(n) = \sum_{m_1=0}^{N-1} \sum_{m_2=0}^{N-1} \mathrm{Re}[q(n;m_1,m_2)]f(m_1)f(m_2). \tag{1.9}$$

Hence, the imaginary part of the system's DIR doesn't contribute to the image formation.

In the imaging system of patterns on translucent scattering substrates [13], the DIR can be given by

$$q(n;m_1,m_2) = [1/2][M(m_1,m_2)S(n;m_1)+M(m_2,m_1)S(n;m_2)] \tag{1.10}$$

where $M(m_1,m_2)$ represents the substrate scattering function at surface point m_1 resulting from a small illumination spot of unit power at surface point m_2 and $S(n;m)$ is the lens irradiance spread function. From (1.10), we have

$$q(n;m_1,m_2) = q(n;m_2,m_1) \tag{1.11}$$

and $q(n;m_1,m_2)$ always takes the real, positive value [13].

For the partially coherent imaging system, if the system's coherent impulse response has the following support

1. Introduction

A 1-D continuous bilinear transformation arises in the second order term of the Volterra series representations of the nonlinear system [1, 2, 3, 4]. In the discrete domain, the 1-D bilinear transformation with the finite support range input can be described as

$$g(n) = \sum_{m_1=0}^{N-1} \sum_{m_2=0}^{N-1} q(n;m_1,m_2) f(m_1) f(m_2) \tag{1.1}$$

where $\{g(n)\}$ and $\{f(m)\}$ are, respectively, the output and input sequences, assumed real, $q(n;m_1,m_2)$ represents the system response at the output coordinate n due to two impulses at the input coordinates $m=m_1$ and $m=m_2$, and N is the size of the input support.

Recently, in the optical image processing area, this bilinear transformation has been studied extensively to analyze the optical imaging system. These areas include the partially coherent imaging system [4, 5, 6, 7, 8, 9], the magnification type X-ray imaging system [10, 11, 12], and the incoherent imaging patterns on translucent scattering substrates [13]. Ref[4] describes the general properties of the optical bilinear transformation in detail. The relationship between the 1-D bilinear transformation and the 2-D linear transformation has been studied in [4, 14, 15, 16].

In the partially coherent imaging system and the projection type imaging system [10, 11], the double impulse response (DIR), $q(n;m_1,m_2)$, of equation (1.1) can be represented by

$$q(n;m_1,m_2) = h^*(n;m_1) h(n;m_2) \gamma(m_1,m_2) \tag{1.2}$$

where $h^*(n;m)$ denotes the complex conjugate of $h(n;m)$, $h(n;m)$ represents the system's coherent impulse response at n due to the impulse at m and $\gamma(m_1,m_2)$ is the field's coherence function. The term $\gamma(m_1,m_2)$ represents the correlation-like coefficient between the object intensities at m_1 and m_2. The derivation of the expression (1.2) and the further detailed informations about $\gamma(m_1,m_2)$ can be obtained in [6, 7, 8] and various other related materials.

For the completely incoherent case, the light from each point in the object is assumed to be statistically independent of light from every other point [6]. Therefore, in this case [4, 6],

$$\gamma(m_1,m_2) = \begin{cases} 1, & m_1=m_2 \\ 0, & \text{otherwise} \end{cases} \tag{1.3}$$

and, from (1.1),(1.2) and (1.3), we obtain

BILINEARLY BLURRED IMAGE RESTORATION

On squaring both sides of the preceding equation, and then using successively (3.12), (3.4) and (3.11), one obtains

$$\begin{aligned}(\underline{g})_i &= \underline{f}^T \underline{h}^{(i-1)} [\underline{h}^{(i-1)}]^T \underline{f} \\ &= \underline{f}^T Q^{(i-1)} \underline{f} \\ &= <(B)_i^T, \underline{x}> \end{aligned} \tag{3.18}$$

Therefore, if $\underline{f}$ is a solution of (3.14), then $\underline{g}$ is a solution of (3.15).

To prove (3.17), $\underline{x}$ is decomposed as,

$$\underline{x} = \hat{\underline{x}} + \tilde{\underline{x}} \tag{3.19}$$

where $\hat{\underline{x}} \epsilon R(B^T)$ and $\tilde{\underline{x}} \epsilon N(B)$, where N(B) is defined as,

$$N(B) \triangleq \{\underline{y} : B\underline{y}=0,\ \underline{y} \epsilon R^{N^2}\} \tag{3.20}$$

since $R(B^T)$ in (3.16) and N(B) are orthogonal complementary spaces with respect to R^{N^2}. Premultiplying B on both sides of (3.19),

$$B\underline{x} = B\hat{\underline{x}} + B\tilde{\underline{x}} = B\hat{\underline{x}} \tag{3.21}$$

But, by (3.15) the left-hand side is $\underline{g}$. Hence,

$$B\hat{\underline{x}} = \underline{g} \tag{3.22}$$

and $\hat{\underline{x}}$ satisfies (3.17).

The above Fact says that if the each row of the matrix B satisfies (3.4), (3.5) and (3.6), then by forming a nonnegative vector $\underline{w}$ from $\underline{g}$ as in (3.12) and solving (3.14) for $\underline{f}$, one can restore the original image. When the nonnegative vector $\underline{w}$ is formed by (3.12), there are 2^N possible ways to set the value $(\underline{w})_i$ from $(\underline{g})_i$, i=1,2,•••,N. But the negative sign of any elements in $\underline{w}$ will violate the necessary condition for $\underline{f}$ to be nonnegative in (3.14). Hence, $\underline{w}$ may be formed uniquely from $\underline{g}$ without violating the necessary condition that $\underline{f}$ be nonnegative, by using (3.12). If $\underline{h}^{(i)}$, i=0,1,•••,N-1, are linearly independent, the nonnegative solution $\underline{f}$ will be unique. For the completely coherent case, the matrix B in (3.11) satisfies the condition in the Fact 3.1 by (1.2), (1.5) and (3.1). Therefore, one can exactly recover the original image for this case provided that $\underline{h}^{(i)}$, i=0,1,•••,N-1, are linearly independent.

Due to the Fact 3.1, if the projection, $\hat{\underline{x}}$, on $R(B^T)$ of $\underline{x}$ is known, where B can be

represented by (3.4), (3.5) and (3.6), then the null space component, $\tilde{\underline{x}}$ of $\underline{x}$ can be obtained from $\hat{\underline{x}}$ so that $\underline{x}$ can satisfy (3.7) and (3.8). However, for the partially coherent system, the matrix B generally does not satisfy the conditions in (3.4), (3.5) and (3.6). The Fact 3.1 will be adapted for use in the partially coherent case, by approximating the basis of $R(B^T)$ to the form in (3.4), (3.5) and (3.6). To do this a few terminologies and well-known Lemmas will be introduced.

Definition 3.1 : The Euclidean matrix norm of the matrix D will be denoted by $\|D\|$ and defined as

$$\|D\| \triangleq \sqrt{Tr[D^T D]} \tag{3.23}$$

where TrA denotes the trace of the square matrix A.

Definition 3.2 : Let S be the set of the matrices satisfying

$$S = \{D: D=\underline{d}\underline{d}^T, \underline{d}\epsilon R^N\} \tag{3.24}$$

Then, we mean by "the best approximation of a matrix Q on S" the matrix D^* which satisfies

$$\|Q-D^*\| = \min_{D\epsilon S}\|Q-D\| \tag{3.25}$$

The above two definitions can be explained in other way. Let

$$\underline{a} = [(Q)_1,(Q)_2,\cdots,(Q)_N]^T \tag{3.26}$$

$$\underline{e} = [(D)_1,(D)_2,\cdots,(D)_N]^T \tag{3.27}$$

where $D=\underline{d}\underline{d}^T$, $\underline{d}\epsilon R^N$. Then, the best approximation of a matrix Q on S is seeking the vector $\underline{e}^*$ which has the form in (3.27) and minimizing the usual Euclidean vector norm of $[\underline{a}-\underline{e}]$.

Definition 3.3 : A matrix E is said to be idempotent if $E^2=E$.

The following Lemma 3.1 is well-known [26] and its proof will be omitted.

Lemma 3.1 : Let Q be a N×N symmetric matrix with distinct real eigenvalues, $\lambda_1,\cdots,\lambda_r$ Then, the idempotents E_i, i=1,2,$\cdots$,r having the properties

1) $E_iE_j = 0$ if $i\neq j$

2) $\sum_{i=1}^{r} E_i = I_N$

3) $Q = \sum_{i=1}^{r} \lambda_i E_i$

exist, where I_N denotes the N×N identity matrix. Moreover, E_i, i=1,2,•••,r are unique and $E_i=\underline{v}_i\underline{v}_i^T$, where $\underline{v}_i$ is the eigenvector of Q corresponding to λ_i, i=1,2,•••,r.

Lemma 3.2 : If E is idempotent, rank E = Tr E.

Proof : Since E is invariant under the square operation, the eigenvalues of E are 1 and 0. Hence, the multiplicity of the 1 is the rank of E. But the sum of the eigenvalues of any matrix is the trace of the matrix. Therefore, Tr E = rank E.

Then, we state the Theorem 3.1 and present its proof.

Theorem 3.1 : Let S be the set as in (3.24). Then, the best approximation, D^*, of a symmetric nonnegative N×N matrix Q on S is given by

$$D^* = \lambda_1 E_1 = \lambda_1 \underline{v}_1 \underline{v}_1^T \tag{3.28}$$

where λ_1 and $\underline{v}_1$ are, respectively, the dominant eigenvalue and the dominant eigenvector of the matrix Q and E_1 denotes the dominant eigenspace of Q.

Proof : Suppose the rank of Q be r. Let the positive eigenvalues of Q be ordered in such a way that

$$\lambda_1 \geq \lambda_2 \geq \cdots \geq \lambda_p \tag{3.29}$$

where p is the number of the positive eigenvalue, and the negative eigenvalues in such a way that

$$\lambda_{p+1} \geq \lambda_{p+2} \geq \cdots \geq \lambda_r \tag{3.30}$$

Then,

$$\lambda_{r+1} = \cdots = \lambda_N = 0 \tag{3.31}$$

Now, suppose that $\underline{v}_i$ denote the orthonormalized eigenvectors of Q corresponding to λ_i i=1,2,•••,N. Then, $\underline{v}_1,\cdots,\underline{v}_N$ form an orthonormal basis of R^N. Let $\underline{d}$ be the vector which minimizes

$$\|Q-\underline{d}\underline{d}^T\| \tag{3.32}$$

Then, $\underline{d}$ can be expressed as a linear combination of $\underline{v}_i$, i=1,2,•••,N.

$$\underline{d} = \sum_{i=1}^{N} \alpha_i \underline{v}_i \tag{3.33}$$

Now,

$$\|Q-\underline{d}\underline{d}^T\|^2 = \mathrm{Tr}[(Q-\underline{d}\underline{d}^T)^T(Q-\underline{d}\underline{d}^T)]$$
$$= \mathrm{Tr}Q^2 - \mathrm{Tr}[Q(\underline{d}\underline{d}^T)] - \mathrm{Tr}[(\underline{d}\underline{d}^T)Q] + \mathrm{Tr}[\underline{d}\underline{d}^T]^2.$$

Since

$$\mathrm{Tr}[Q(\underline{d}\underline{d}^T)] = \mathrm{Tr}[(\underline{d}\underline{d}^T)Q],$$
$$\|Q-\underline{d}\underline{d}^T\|^2 = \mathrm{Tr}Q^2 - 2\mathrm{Tr}[Q(\underline{d}\underline{d}^T)] + \mathrm{Tr}(\underline{d}\underline{d}^T)^2. \tag{3.34}$$

By the Lemma 3.1,

$$\mathrm{Tr}Q^2 = \mathrm{Tr}[\sum_{i=1}^{r} \lambda_i E_i]^2 = \mathrm{Tr}[\sum_{i=1}^{r} \lambda_i^2 E_i].$$

Hence, by the Lemma 3.2,

$$\mathrm{Tr}Q^2 = \sum_{i=1}^{r} \lambda_i^2 \mathrm{Tr}E_i = \sum_{i=1}^{r} \lambda_i^2 \tag{3.35}$$

For the second term in (3.34),

$$\mathrm{Tr}[Q(\underline{d}\underline{d}^T)] = \mathrm{Tr}(\sum_{i=1}^{r} \lambda_i \underline{v}_i \underline{v}_i^T)(\sum_{j=1}^{N} \alpha_j \underline{v}_j)(\sum_{k=1}^{N} \alpha_k \underline{v}_k^T)$$
$$= \mathrm{Tr}(\sum_{i=1}^{r} \lambda_i \alpha_i \underline{v}_i)(\sum_{k=1}^{N} \alpha_k \underline{v}_k^T)$$
$$= \sum_{i=1}^{r}\sum_{k=1}^{N} \lambda_i \alpha_i \alpha_k \mathrm{Tr}[\underline{v}_i \underline{v}_k^T]$$

Since

$$\mathrm{Tr}[\underline{v}_i \underline{v}_k^T] = (\underline{v}_i, \underline{v}_k) = \begin{cases} 1, & i=k, \\ 0, & \text{otherwise}, \end{cases}$$
$$\mathrm{Tr}[Q(\underline{d}\underline{d}^T)] = \sum_{i=1}^{r} \lambda_i \alpha_i^2. \tag{3.36}$$

For the third term in (3.34),

$$\mathrm{Tr}(\underline{d}\underline{d}^T)^2 = \mathrm{Tr}[(\sum_{i=1}^{N} \alpha_i \underline{v}_i)(\sum_{j=1}^{N} \alpha_j \underline{v}_j^T)(\sum_{k=1}^{N} \alpha_k \underline{v}_k)(\sum_{\ell=1}^{N} \alpha_\ell \underline{v}_\ell^T)]$$
$$= \sum_{i=1}^{N}\sum_{j=1}^{N}\sum_{\ell=1}^{N} \alpha_i \alpha_j^2 \alpha_\ell \mathrm{Tr}[\underline{v}_i \underline{v}_\ell^T]$$
$$= \sum_{i=1}^{N}\sum_{j=1}^{N} \alpha_i^2 \alpha_j^2$$

$$= (\sum_{i=1}^{N} \alpha_i^2)^2. \tag{3.37}$$

By substituting (3.35), (3.36) and (3.37) into (3.34), one obtains

$$\|Q-\underline{d}\underline{d}^T\|^2 = \sum_{i=1}^{r}(\lambda_i-\alpha_i^2)^2 + [\sum_{i=r+1}^{N}\lambda_i^4 + \sum_{j=1}^{N}\sum_{k=1}^{N}\alpha_j^2\alpha_k^2(1-\delta_{jk})]$$

Let

$$\varepsilon_1 \triangleq \sum_{i=1}^{r}(\lambda_i-\alpha_i^2)^2 \geq 0 \tag{3.38}$$

$$\varepsilon_2 \triangleq \sum_{i=r+1}^{N}\alpha_i^4 + \sum_{j=1}^{N}\sum_{k=1}^{N}\alpha_j^2\alpha_k^2(1-\delta_{jk}) \geq 0 \tag{3.39}$$

Then,

$$\|Q-\underline{d}\underline{d}^T\|^2 = \varepsilon_1 + \varepsilon_2 \tag{3.40}$$

ε_1 can be rewritten by

$$\varepsilon_1 = \sum_{i=1}^{p}(\lambda_i-\alpha_i^2)^2 + \sum_{i=p+1}^{r}(\lambda_i-\alpha_i^2)^2. \tag{3.41}$$

Let

$$\underline{\alpha} = [\alpha_1^2,\alpha_2^2,\cdots,\alpha_N^2]^T \geq 0 \tag{3.42}$$

By varying $\underline{\alpha}$ from $[0,0,\cdots,0]^T$, one can set the $\underline{\alpha}^*$ which minimizes $\varepsilon_1+\varepsilon_2$. Starting from $[0,0,\cdots,0]^T$, ε_2 is *nondecreasing function of* $\underline{\alpha}$ as $\|\underline{\alpha}\|$ *increases.* However, ε_1 is decreasing monotonically as $\|\underline{\alpha}\|$ increases from $[0,0,\cdots,0]^T$ until $\underline{\alpha}$ reaches

$$\underline{\alpha} = [\lambda_1,\lambda_2,\cdots,\lambda_p,0,\cdots,0]^T$$

Then, ε_1 is increasing monotonically as $\|\underline{\alpha}\|$ increases. Based on these facts, one can conclude that the optimal $\underline{\alpha}^*$ minimizing $\|Q-\underline{d}\underline{d}^T\|$ exists within the region formed by $[0,0,\cdots,0]^T$ and $[\lambda_1,\lambda_2,\cdots,\lambda_p,0,0,\cdots,0]^T$.

Suppose $\underline{\alpha}^{(1)}=[\lambda_1,0,\cdots,0]^T$. Then,

$$[\varepsilon_1+\varepsilon_2]^{(1)} = \sum_{i=1}^{r}\lambda_i^2-\lambda_1^2.$$

Let

$$\underline{\alpha}^{(2)} = [0,\lambda_2,0,\cdots,0]^T.$$

Then,

$$[\varepsilon_1+\varepsilon_2]^{(2)} = \sum_{i=1}^{r}\lambda_i^2-\lambda_2^2.$$

By checking in this way, one obtains

$$[\epsilon_1+\epsilon_2]^{(k)} = \sum_{i=1}^{r}\lambda_i^2-\lambda_k^2, \quad k=1,2,\cdots,p.$$

Hence, so far, $\underline{\alpha}^{(1)}$ is attained as the minimum. Now, let $\underline{\alpha}^{(1,2)} = [\lambda_1,\lambda_2,\cdots,0]^T$. Then,

$$[\epsilon_1+\epsilon_2]^{(1,2)} = \sum_{i=1}^{r}\lambda_i^2-(\lambda_1^2+\lambda_2^2)+2\lambda_1\lambda_2.$$

Since

$$\lambda_2^2 \leq \lambda_1\lambda_2,$$
$$[\epsilon_1+\epsilon_2]^{(1,2)} \geq [\epsilon_1+\epsilon_2]^{(1)}.$$

For

$$\underline{\alpha}^{(k,\ell)} = [0,0,\cdots,0,\lambda_k,0,\cdots,0,\lambda_\ell,0,\cdots,0]^T, \quad 1\leq k,\ell\leq p$$
$$[\epsilon_1+\epsilon_2]^{(k,\ell)} = \sum_{i=1}^{r}\lambda_i^2-(\lambda_k^2+\lambda_\ell^2)+2\lambda_k\lambda_\ell \geq [\epsilon_1+\epsilon_2]^{(1)}.$$

For $\underline{\alpha}^{(k,\ell,m)}$, the similar argument can be applied. By continuing these procedures until

$$\underline{\alpha} = [\lambda_1,\lambda_2,\cdots,\lambda_p,0,\cdots,0]^T$$

is reached, one can show that

$$[\epsilon_1+\epsilon_2]^{(1)} = \min\|Q-\underline{d}\underline{d}^T\|^2.$$

Therefore,

$$\alpha_1 = \sqrt{\lambda_1}, \quad \alpha_2=\alpha_3=\cdots=\alpha_N=0 \tag{3.43}$$

will give the optimal vector $\underline{d}$ minimizing $\|Q-\underline{d}\underline{d}^T\|$. But,

$$\underline{d}\underline{d}^T = (\sqrt{\lambda_1}\underline{v}_1)(\sqrt{\lambda_1}\underline{v}_1^T) = \lambda_1 E_1.$$

Hence, the Theorem 3.1 has been proved.

The error resulted from the above approximation is given by

$$\|Q-\underline{d}\underline{d}^T\| = \sum_{i=2}^{r}\lambda_i^2 \tag{3.44}$$

By applying the Theorem 3.1 to $Q^{(i)}$, i=0,1,$\cdots$,N-1 in (3.1), one will get $\hat{Q}^{(i)}$, i=0,1,$\cdots$,N-1 which is nonnegative due to the Perron-Frobenius Theorem [24]. That is, the nonnegativity of the system matrix $\hat{B}$ which is the approximate version of B in (3.11) is maintained, while the each row of the matrix $\hat{B}$ satisfies the conditions (3.4), (3.5) and (3.6) in the Fact 3.1.

By combining the Fact 3.1 and the Theorem 3.1, the image restoration algorithm from the partially coherent system can be obtained as follows:

Step 1) Obtain N×1 vectors $\underline{d}_i$, i=0,1,•••,N−1, by

$$\underline{d}_i = \sqrt{\lambda_{i1}}\,\underline{v}_{i1} \tag{3.45}$$

where λ_{i1} and $\underline{v}_{i1}$ denote, respectively, the dominant eigenvalue and eigenvector of $Q^{(i)}$. Form $N^2\times 1$ vectors $\underline{e}_i$, i=0,1,•••,N−1, by

$$\underline{e}_i = [(D^{(i)})_1,(D^{(i)})_2,\cdots,(D^{(i)})_N]^T \tag{3.46}$$

$$D^{(i)} = \underline{d}_i\underline{d}_i^T. \tag{3.47}$$

Step 2) Obtain the minimum norm solution, $\hat{\underline{x}}$, of (3.11).

Step 3) Obtain N×1 vector $\underline{w}$ by

$$(\underline{w})_i = \begin{cases} \sqrt{<\underline{e}_{i-1},\hat{\underline{x}}>}\,, & <\underline{e}_{i-1},\hat{\underline{x}}> \;\geq\; 0,\quad i=1,2,\cdots,N. \\ 0\,, & \text{otherwise} \end{cases} \tag{3.48}$$

Step 4) Solve N×N linear system $U\underline{f}=\underline{w}$ for $\underline{f}$, where

$$U = \begin{bmatrix} \underline{d}_0^T \\ \underline{d}_1^T \\ \vdots \\ \underline{d}_{N-1}^T \end{bmatrix}. \tag{3.49}$$

Step 5) If the solution vector $\underline{f}$ has negative element, make it zero. Denote it $\underline{f}^*$. Then, $\underline{f}^*$ is the approximate solution.

By applying the above algorithm, one will have the squarred error of

$$\sum_{i=0}^{N-1}[g(i)-\underline{f}^{*T}Q^{(i)}\underline{f}^*]^2 = \sum_{i=0}^{N-1}[g(i)-\sum_{j=1}^{N}\lambda_{ij}\{(\underline{v}_{ij},\underline{f}^*)\}^2]^2 \tag{3.50}$$

where λ_{ij} is the j^{th} eigenvalue of $Q^{(i)}$ and $\underline{v}_{ij}$ is the j^{th} eigenvector of $Q^{(i)}$.

This error results from approximation of the range space of B^T by a space satisfying (3.4), (3.5) and (3.6). Figure-6 will help understanding their relationships. In Figure-6, the

matrix E denotes the matrix resulting from the approximation of the matrix B in (3.11) by applying the Theorem 3.1. The dotted curve represents the nonlinear space which consists of the vector having the form defined in (3.7) and (3.8). Then, solving $U\underline{f}=\underline{w}$ in the step 4) will correspond to seek a vector $\underline{x}$ on the dotted curve so that the projection of $\underline{x}$ on $R(E^T)$ be $\overline{OB}$. But, the true solution $\overline{OD}$ is on the intersection of $\overline{AD}$, which represents the set of all (least squares) solution vectors of (3.11), and the dotted curve. If the true projection of $\overline{OD}$ on $R(E^T)$, that is, $\overline{OC}$, is given, the true solution $\overline{OD}$ can easily be obtained. For the completely coherent case or the completely incoherent case, $R(B^T)$ coincides with $R(E^T)$. Hence, the true projection $\overline{OC}$ can be obtained only by computing the minimum norm solution.

The innerproduct operation in the step 3) includes the projection operation of $\overline{OA}$ on $R(E^T)$, that is, obtaining $\overline{OB}$. This step results in the error because the true projection of $\overline{OD}$ on $R(E^T)$ is $\overline{OC}$. The reason why the innerproduct operation in step 3) includes the projection operation is following.

The projection of $\overline{OA}$ on $R(E^T)$ is represented by

$$\overline{OB} = (E^{\dagger}E)(\overline{OA})$$

since $E^{\dagger}E$ is idempotent and the projection operator on $R(E^T)$ [25]. Suppose, now we want to compute the value $(E)(\overline{OB})$ to establish the system equation in the form of $E\underline{x}=\hat{\underline{g}}$ which is the approximated version of $B\underline{x}=\underline{g}$. Then,

$$(E)(\overline{OB}) = (E)(E^{\dagger}E)(\overline{OA}) = (E)(\overline{OA})$$

since $EE^{\dagger}E=E$ [25]. Since $(E)(\overline{OA})$ represents the innerproduct operation in step 3), this step includes the orthogonal projection operation on $R(E^T)$.

One more thing to be noted is the possible negative values resulting from the innerproduct operations in (3.48). In the proof of the Fact 3.1, the innerproduct result of (3.18) never becomes negative because

$$< (B)_i, \hat{\underline{x}} > = < (B)_i, \underline{x} > = [<\underline{h}^{(i)}, \underline{d}>]^2 \geq 0$$

But, for the partially coherent case, since $R(B^T)$ does not exactly coincide with $R(E^T)$, the first equality in the above expression doesn't hold. That is,

$$< (E)_i, \hat{\underline{x}} > \neq < (E)_i, \hat{\underline{x}} > + < (E)_i, \tilde{\underline{x}} >$$

since $\underline{\tilde{x}}$ may contain the component belonging to $R(E^T)$. Hence, if the error in (3.43) is sufficiently small, then $\underline{\tilde{x}}$ can be said to belong to N(E). Hence, the innerproduct values in step 3) have to be nonnegative.

The 2-D bilinear system representation corresponding to (1.1) is given by

$$y(n_1,n_2) = \sum_{m_1=0}^{N-1}\sum_{m_2=0}^{N-1}\sum_{\ell_1=0}^{N-1}\sum_{\ell_2=0}^{N-1} q_2(n_1,n_2;m_1,m_2,\ell_1,\ell_2)u(m_1,m_2)u(\ell_1,\ell_2). \tag{3.51}$$

Initially the following form of the 2-D DIR is considered.

$$q_2(n_1,n_2;m_1,m_2,\ell_1,\ell_2) = q(n_1;m_1,\ell_1)q(n_2;m_2,\ell_2). \tag{3.52}$$

In the Köhler illumination system [7] with an incoherent square source, the 2-D field's coherence function is of the form,

$$\gamma_2(m_1,m_2,\ell_1,\ell_2) = \gamma(m_1,\ell_1)\gamma(m_2,\ell_2) \tag{3.53}$$

where $\gamma(m,\ell) = C_1 \cdot \mathrm{sinc}[C_2 \cdot (m-\ell)]$ and C_1 and C_2 are constants. It is well-known [7] that the Fraunhofer diffraction pattern for a square aperture results in a product separable form of the coherent impulse response, i.e., the 2-D counterpart of h(n;m) in (1.2) is of the form,

$$h_2(n_1,n_2;m_1,m_2) = h(n_1;m_1)h(n_2;m_2) \tag{3.54}$$

where $h(n;m) = C_3 \cdot \mathrm{sinc}[C_4 \cdot (n-m)]$ and C_3 and C_4 are constants. Hence the optical microscopic imaging system of the square incoherent source will have a DIR of the form in (3.52).

When the 2-D DIR is as in (3.52), (3.51) can be rewritten as

$$\begin{aligned} y(n_1,n_2) &= \sum_{m_1=0}^{N-1}\sum_{m_2=0}^{N-1}\sum_{\ell_1=0}^{N-1}\sum_{\ell_2=0}^{N-1} q(n_1;m_1,\ell_1)q(n_2;m_2,\ell_2)u(m_1,m_2)u(\ell_1,\ell_2) \\ &= \sum_{m_2=0}^{N-1}\sum_{\ell_2=0}^{N-1} q(n_2;m_2,\ell_2)\sum_{m_1=0}^{N-1}\sum_{\ell_1=0}^{N-1} q(n_1;m_1,\ell_1)u(m_1,m_2)u(\ell_1,\ell_2) \\ &= \sum_{m_2=0}^{N-1}\sum_{\ell_2=0}^{N-1} q(n_2;m_2,\ell_2)w(n_1;m_2\ell_2) \end{aligned} \tag{3.55}$$

where

$$w(n_1;m_2,\ell_2) \triangleq \sum_{m_1=0}^{N-1}\sum_{\ell_1=0}^{N-1} q(n_1;m_1,\ell_1)u(m_1,m_2)u(\ell_1,\ell_2). \tag{3.56}$$

The minimum norm solution, $\hat{w}(n_1;m_2,\ell_2)$, $n_1=0,1,\cdots,N-1$, can be obtained via the application of step 2) in the 1-D algorithm. Define,

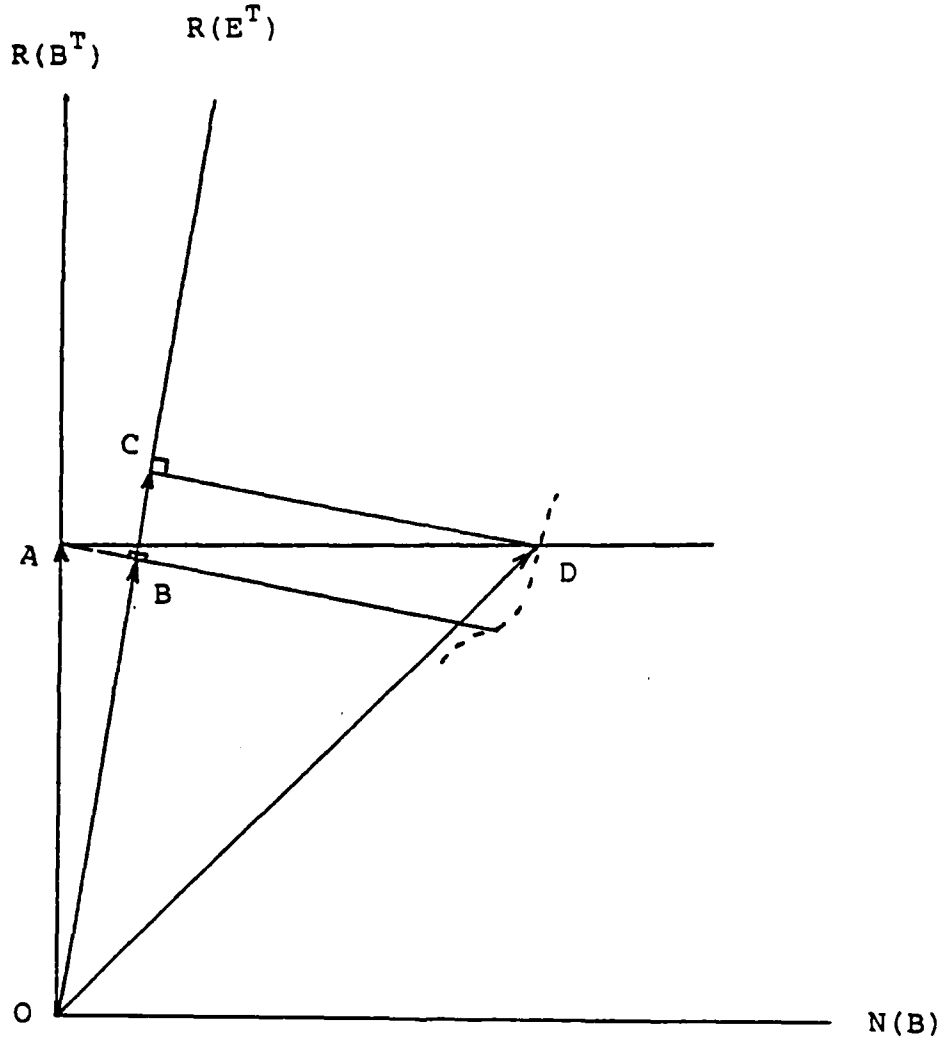

Figure - 6 Range Space Approximation

$$Q^{(n_2)} \triangleq \begin{bmatrix} q(n_2;0,0) & q(n_2;0,1) & \cdots & q(n_2;0,N-1) \\ q(n_2;1,0) & q(n_2;1,1) & \cdots & q(n_2;1,N-1) \\ \vdots & \vdots & \vdots & \vdots \\ q(n_2;N-1,0) & q(n_2;N-1,1) & \cdots & q(n_2;N-1,N-1) \end{bmatrix} \quad n_2=0,1,\cdots,N-1 \tag{3.57}$$

Then, as in (3.45), by obtaining the dominant eigensystem of $Q^{(n_2)}$, the $N\times 1$ vectors $\underline{d}_{n_2}$, $n_2=0,1,\cdots,N-1$, are obtained. For the fixed value of n_1, $y(n_1,n_2)$ can be obtained, from $\underline{d}_{n_2}$ and $\hat{w}(n_1;m_2,\ell_2)$, by

$$\hat{y}(n_1,n_2) = \sum_{m_2=0}^{N-1}\sum_{\ell_2=0}^{N-1} d(n_2;m_2)d(n_2;\ell_2)\hat{w}(n_1;m_2,\ell_2) \tag{3.58}$$

where $d(n;m)$ is the m^{th}-element value of the vector $\underline{d}_n$. By substituting (3.56) for $\hat{w}(n_1;m_2,\ell_2)$, (3.58) can be rewritten as, for $n_1=0,1,\cdots,N-1$,

$$\hat{y}(n_1,n_2) = \sum_{m_1=0}^{N-1}\sum_{\ell_1=0}^{N-1} q(n_1;m_1,\ell_1)\sum_{m_2=0}^{N-1}\sum_{\ell_2=0}^{N-1} d(n_2;m_2)d(n_2;\ell_2)u(m_1,m_2)u(\ell_1,\ell_2) \tag{3.59}$$

Let

$$z(m_1,n_2) \triangleq \sum_{m_2=0}^{N-1} d(n_2;m_2)u(m_1,m_2). \tag{3.60}$$

Then, (3.59) can be rewritten as,

$$\hat{y}(n_1,n_2) = \sum_{m_1=0}^{N-1}\sum_{\ell_1=0}^{N-1} q(n_1;m_1,\ell_1)z(m_1,n_2)z(\ell_1,n_2). \tag{3.61}$$

$y(n_1,n_2)$ is given in (3.58) and $q(n_1;m_1,\ell_1)$ is also known. Hence, (3.61) is the 1-D bilinear expression for the fixed value of n_2, $n_2=0,1,\cdots,N-1$. By applying the 1-D algorithm to (3.61) for each value of n_2, $n_2=0,1,\cdots,N-1$, $z(m_1,n_2)$, $m_1=0,1,\cdots,N-1$, is obtained. Then, $u(m_1,m_2)$ can be solved for in (3.60). The 2-D algorithm with the product separable form DIR is shown on Figure-7.

The algorithm in Figure-7 is implemented with

$$h_2(n_1,n_2;m_1,m_2) = \begin{cases} \text{sinc}[(n_1-m_1)/N_h]\text{sinc}[(n_2-m_2)/N_h], & |n_i-m_i|<N_h,\ i=1,2 \\ 0, & \text{otherwise} \end{cases} \tag{3.62}$$

where $\text{sinc}x=[\sin(\pi x)]/(\pi x)$, and

$$\gamma_2(m_1,m_2,\ell_1,\ell_2) = 1 \quad \text{for all } m_1,m_2,\ell_1,\ell_2. \tag{3.63}$$

Hence, Figure-8(b) shows the image blurred by the completely coherent optical system with $N_h=4$ from the 31×31 original image in Figure-8(a). By applying the algorithm in

Figure-7, the image shown in Figure-8(c) has been obtained. The algorithm results in the exact image restoration. For the partially coherent image restoration, the image in Figure-9(a) has been blurred by the system with $h_2(n_1,n_2;m_1,m_2)$ in (3.62) and

$$\gamma_2(m_1,m_2,\ell_1,\ell_2) = \text{sinc}[(m_1-\ell_1)/N_c]\text{sinc}[(m_2-\ell_2)/N_c]. \tag{3.64}$$

The blurred image is shown on Figure-9(b). N_c has been chosen as 19. The restored image in Figure-9(c) retains a little error since the blurring system belongs to the partially coherent system close to the completely coherent case.

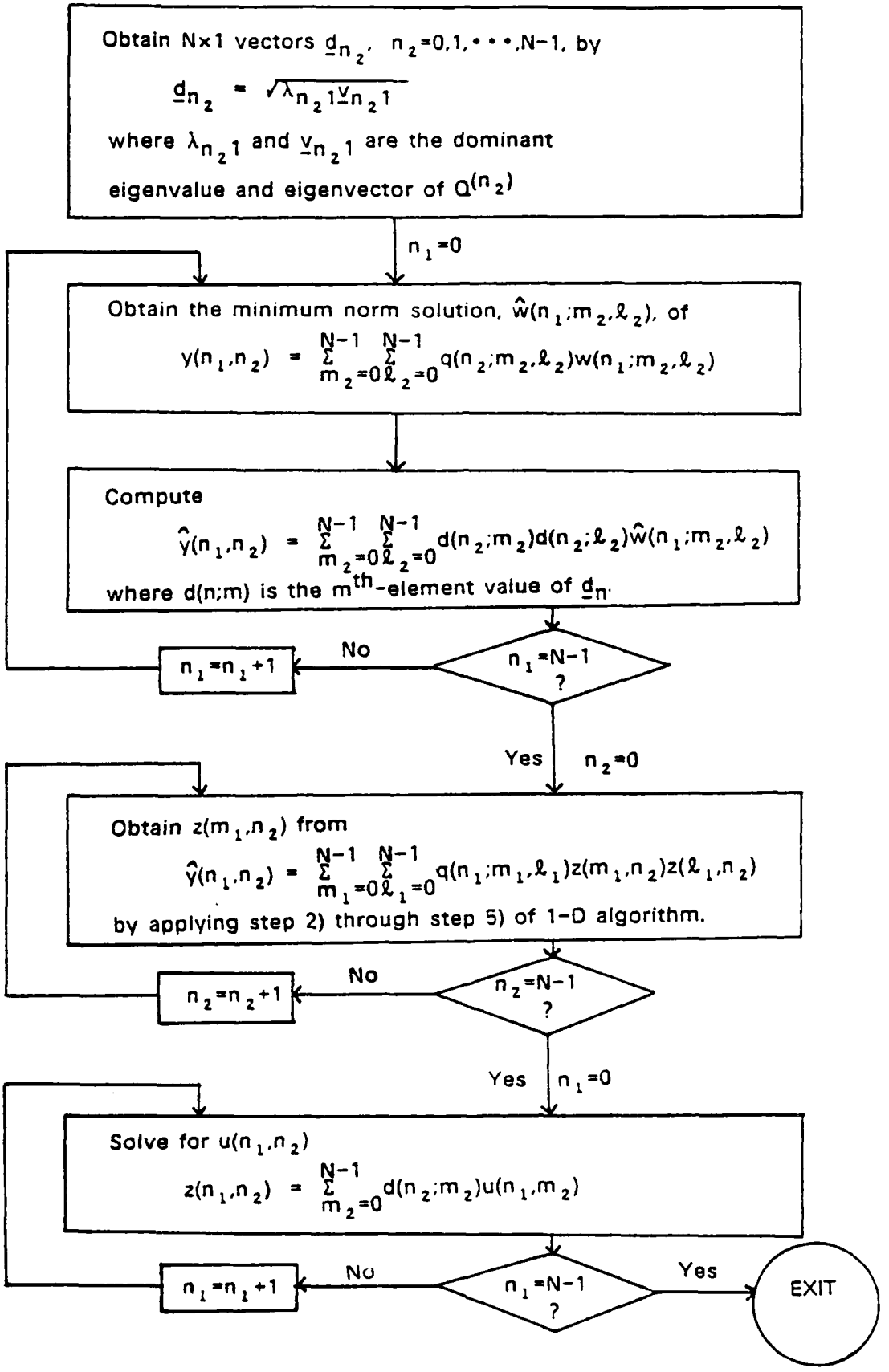

Figure-7. 2-D Product Separable Form Algorithm

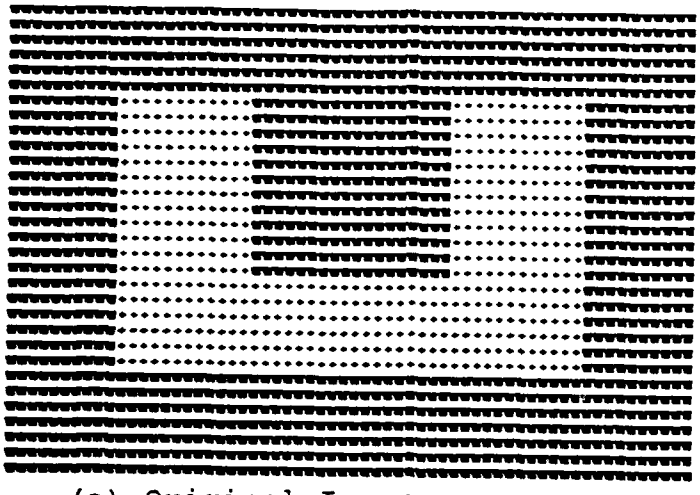

(a) Original Image

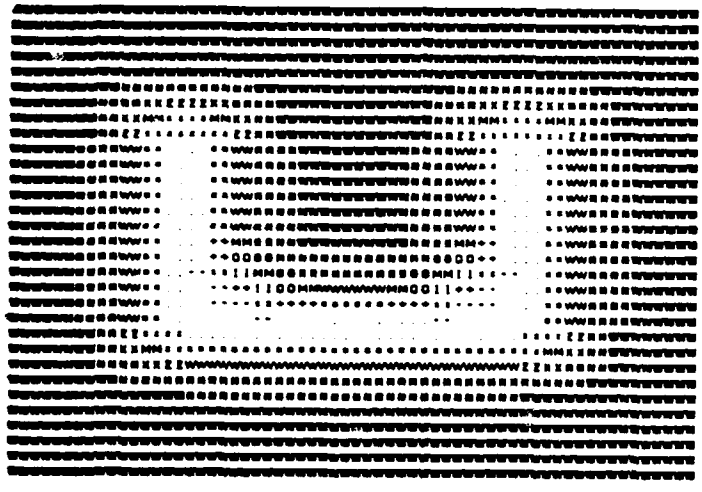

(b) Blurred Image

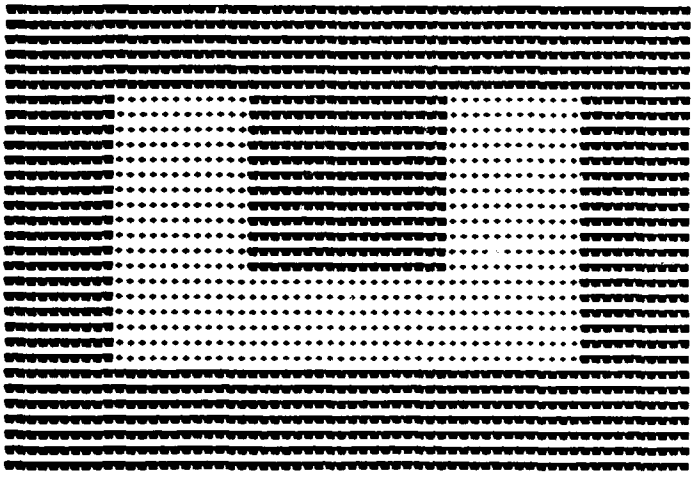

(c) Restored Image

Figure - 8. Completely Coherent Image Restoration Simulation (31x31 Image, N_h = 4)

AD-A158 973 SHIFT-VARIANT MULTIDIMENSIONAL SYSTEMS(U) PITTSBURGH 2/2
UNIV PA DEPT OF ELECTRICAL ENGINEERING N K BOSS
29 MAY 85 AFOSR-TR-85-0724 AFOSR-83-0038

UNCLASSIFIED F/G 12/1 NL

END

FILMED

DTIC

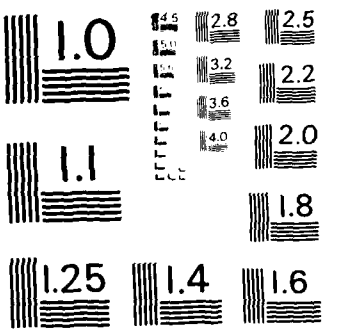

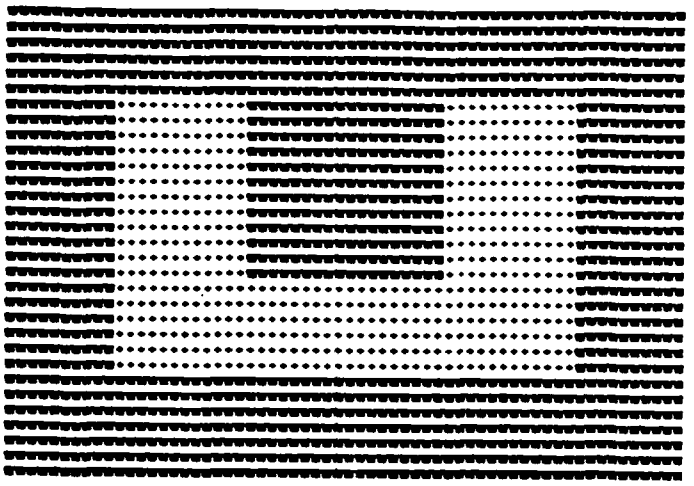

(a) Original Image

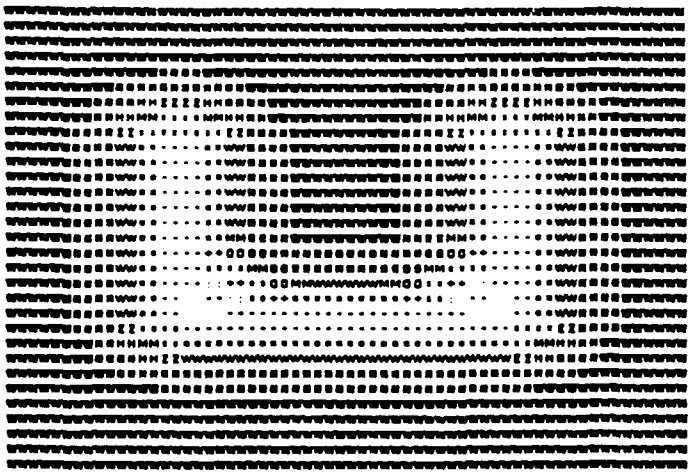

(b) Blurred Image

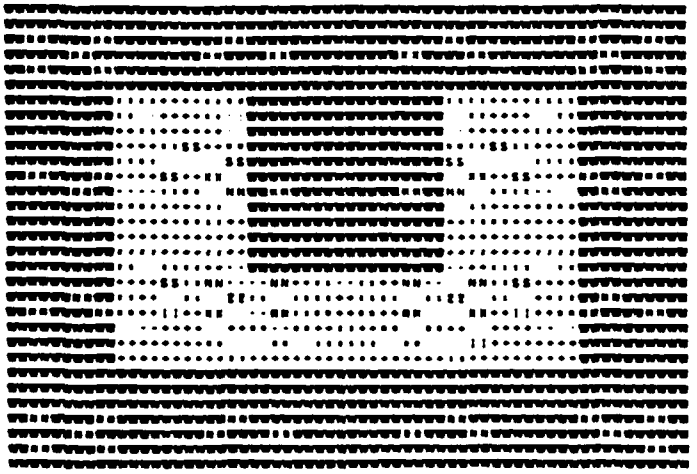

(c) Restored Image

Figure - 9. Partially Coherent Image Restoretion Simulation (31×31 Image, $N_h = 4$, $N_c = 19$)

4. Image Restoration From Noise Added Blurred Image

In this section the original image restoration from the noise added image following bilinear blurring in (2.1) with nonnegative DIR will be considered. The blurred image with additive noise can be described by

$$g(n) = \sum_{m_1=0}^{n} \sum_{m_2=0}^{n} q(n;m_1,m_2)f(m_1)f(m_2) + v(n) \tag{4.1}$$

where v(n) is a zero mean white gaussian noise. The bilinear blurring in (4.1) can be recovered by applying the algorithm in Figure-1. But due to the noise effect the nonnegativity condition in (2.4) may not be satisfied. Then, solving (2.12) recursively might result in two negative solutions, or two complex solutions in addition to a nonnegative solution with a negative one. The algorithm in Figure-1 will be adapted for use in this case.

Suppose that nonnegative values for f(0), f(1),$\cdots$, f(n-1) have been obtained and

$$C_k^{(i)} \geq 0, \quad i=1,2,\cdots,n, \quad k=i,i+1,\cdots,N-1. \tag{4.2}$$

Since $A_n \geq 0$ and $B_n \geq 0$ due to the nonnegativity of $q(n;m_1,m_2)$ and

$$C_n = C_n^{(n)} \geq 0 \tag{4.3}$$

due to (4.2), solving (2.12) for f(n) will result in one nonnegative solution, say s_1, and one negative solution, s_2. Let

$$f^{(1)}(n) = s_1. \tag{4.4}$$

Using $f^{(1)}(n)$ in (4.4), $C_k^{(n+1)}$, k=n+1,n+2,$\cdots$,N-1 can be computed. If

$$C_k^{(n+1)} \geq 0, \quad k=n+1,n+2,\cdots,N-1 \tag{4.5}$$

then

$$f(n) = f^{(1)}(n) \tag{4.6}$$

And one can proceed the algorithm to solve f(n+1).

If any of $C_k^{(n+1)}$ turns out to be negative, say,

$$C_{\ell_1}^{(n+1)}<0, \quad C_{\ell_2}^{(n+1)}<0,\cdots,C_{\ell_r}^{(n+1)}<0, \tag{4.7}$$

then by choosing $C_\ell^{(n+1)}$ as

$$C_{\ell}^{(n+1)} \triangleq \min \{ C_{\ell_1}^{(n+1)}, C_{\ell_2}^{(n+1)}, \cdots, C_{\ell_r}^{(n+1)} \} \tag{4.8}$$

the output index ℓ, say $\ell=\ell_i$, at which the largest modulus occurs among negative $C_k^{(n+1)}$, $k=\ell_1,\ell_2,\cdots,\ell_r$ can be obtained. For $C_{\ell}^{(n+1)}$ to be nonnegative, f(n) has to satisfy

$$C_{\ell}^{(n)} - [\, q(\ell;n,n)f^2(n) + \sum_{m=0}^{n-1}\{q(\ell;n,m)+q(\ell;m,n)\}f(m)f(n) \,] \geq 0 \tag{4.9}$$

where $C_{\ell}^{(n)} \geq 0$ by (4.3). Let $0<\alpha \leq 1$. Then, (4.9) can be rewritten by

$$q(\ell;n,n)f^2(n) + \sum_{m=0}^{n-1}\{q(\ell;n,m)+q(\ell;m,n)\}f(m)f(n) - \alpha C_{\ell}^{(n)}=0. \tag{4.10}$$

Choosing proper value for α and solving (4.10) for f(n) will result in $f^{(2)}(n)$. By using this $f^{(2)}(n)$, the nonnegativity of $C_k^{(n+1)}$, $k=n+1,n+2,\cdots,N-1$, can be rechecked. Note that

$$C_{\ell}^{(n+1)} = (1-\alpha)C_{\ell}^{(n)} \geq 0. \tag{4.11}$$

If all the inequalities in (4.5) are satisfied by $f^{(2)}(n)$, then set

$$f(n) = f^{(2)}(n) \tag{4.12}$$

and proceed the algorithm to obtain f(n+1). If any one or more of inequalities in (4.5) are not satisfied by $f^{(2)}(n)$, then, by repeating the above procedure until all the inequalities in (4.5) can be satisfied, one can obtain a desired nonnegative f(n). It is easy to see that the number of negative $C_k^{(n+1)}$ will be reduced by, at least, one whenever the above procedure is repeated. Hence, by repeating the above procedure at most r times, one can obtain a nonnegative f(n) satisfying (4.5). This scheme is shown on Figure-10.

In the simulation SNR=30dB white gaussian noise is added to the blurred image in Figure-5(b). The resulting noise added image is shown on Figure-11(a). By choosing α=0.5, the restored image in Figure-11(b) is obtained. The resulting SNR is 16dB.

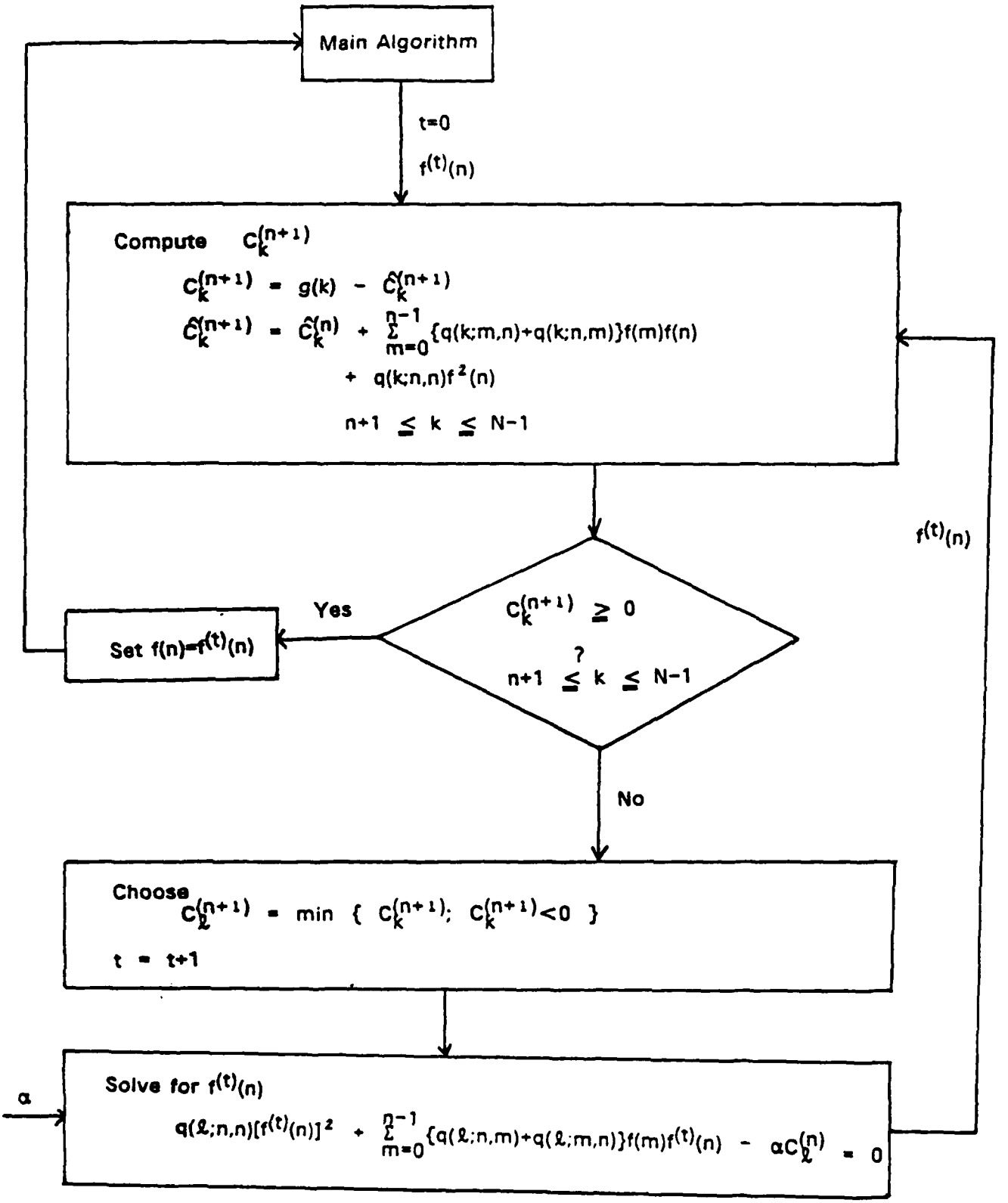

Figure-10. Supplementary Algorithm to Figure-1 to Recover the Noisy Blurred Image

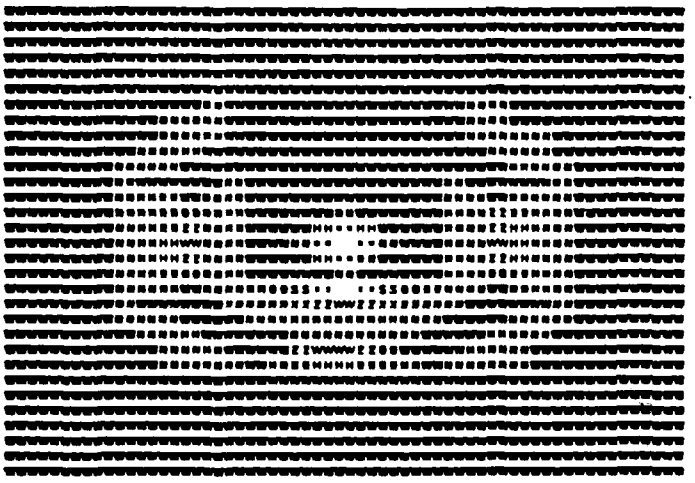

(a) Blurred Image
with Additive Noise (SNR = 30dB)

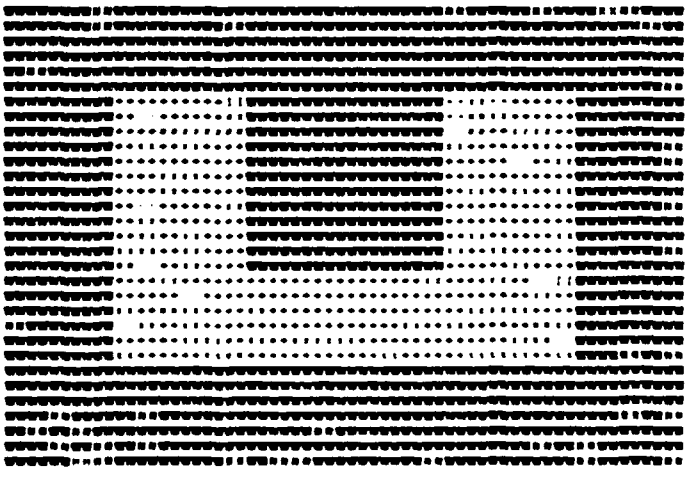

(b) Restored Image (SNR = 16dB)

Figure - 11. Noisy Image Restoration Simulation

References

1. V. Volterra, Theory of Functionals and of Integral and Integrodifferential Equations, Dover Publications, Inc., New York, 1959.

2. N. Wiener, Nonlinear Problems in Random Theory, The M.I.T. Press, Cambridge, Massachusetts, 1958.

3. N. K. Bose, Applied Multidimensional Systems Theory, Van Nostrand Reinhold, Co., New York, 1982.

4. B. E. A. Saleh, "Optical Bilinear Transformations : General Properties", Optica Acta, Vol. 26, No. 6, 1979, pp. 777-799.

5. B. E. A. Saleh & M. Rabbani, "Simulation of Partially Coherent Imagery in the Space and Frequency Domains and by Modal Expansion", Applied Optics, Vol. 21, No. 15, 1982, pp. 2770-2777.

6. B. J. Thompson, "Image Formation with Partially Coherent Light", in Progress in Optics, E. Wolf, ed., North-Holland Publishing Co., Amsterdam, Vol. 7, 1969, ch. IV.

7. M. Born & E. Wolf, Principles of Optics, Pergamon Press, New York, 1965.

8. E. Wolf, "The Radiant Intensity from Planar Sources of Any State of Coherence", J. OPt. Soc. Am., Vol. 68, No. 11, 1978, pp. 1597-1605.

9. A. V. Lugt, "Coherent Optical Processing", Proc. of IEEE, Vol. 62, No. 10, 1974, pp. 1300-1319.

10. Y. Yamakoshi & T. Sato, "Transfer Characteristic for a Projection-Type Imaging System With an Extended Incoherent Source", J. Opt. Soc. Am., Vol. 1, No. 1, 1984, pp. 11-17.

11. Y. Yamakoshi, K. Kitamura & T. Sato, "Magnification-Type X-Ray Imaging System : Optimum Design and Image Restoration", Applied Optics, Vol. 23, No. 23, 1984, pp. 4292-4298.

12. Y. Yamakoshi & T. Sato, "Linear Restoration of Projections Obtained By an Extended Incoherent Source", Applied Optics, Vol. 23, No. 14, 1984, pp. 2271-2274

13. D. S. Goodman & G. W. Johnson, "Bilinear Noncoherent Imaging of Patterns on Translucent Scattering Substrates", J. Opt. Soc. Am., Vol. 1, No. 12, 1984, pp. 1158-1162.

14. B. E. A. Saleh, "Bilinear Processing of 1-D Signals by Use of Linear 2-D Coherent Optical Processors", Applied Optics, Vol. 17, No. 21, 1978, pp. 3408-3411.

15. E. W. Kamen, "On the Relationship Between Bilinear Maps and Linear Two-Dimensional Maps", Nonlinear Analysis, Vol. 3, No. 4, 1979, pp. 467-481.

16. R. K. Raney, "Quadratic Filter Theory and Partially Coherent Optical Systems", J. Opt. Soc. Am., Vol. 59, No. 9, 1969, pp. 1149-1154.

17. H. M. Valenzuela-Neumann, Modeling of Multidimensional Linear Shift-Variant Systems With Applications, PhD dissertation, University of Pittsburgh, 1983.

18. B. E. A. Saleh & M. Rabbani, "Restoration of Bilinearly Distorted Images : II. Bayesian Methods", J. Opt. Soc. Am., Vol. 73, No. 1, 1983, pp. 71-75.

19 B. E. A. Saleh & S. I. Savegh, "Restoration of Partially Coherent Images by Use of a Second-Degree Nonlinear Filter, Applied Optics, Vol. 20, No. 23, 1981, pp. 4089-4093.

20. B. E. A. Saleh & M. Rabbani, "Restoration of Bilinearly Distorted Images : I. Finite Impulse Response Linear Digital Filtering", J. Opt. Soc. Am., Vol. 73, No. 1, 1983, pp. 66-70.

21. B. E. A. Saleh & W. C. Goeke, "Linear Restoratin of Bilinearly Distorted Images", J. Opt. Soc. Am., Vol. 70, No. 5, 1980, pp. 506-515.

22. B. E. A. Saleh, "Wiener Restoration of Defocused Partially Coherent Images", Applied Optics, Vol. 19, No. 21, 1980, pp. 3646-3650.

23. G. M. Robbins & T. S. Huang, "Inverse Filtering for Linear Shift-Variant Imaging Systems", Proc. of IEEE, Vol. 60, No. 7, 1972, pp. 862-872.

24. A. Berman & R. J. Plemmons, Nonnegative Matrices in the Mathematical Sciences, Academic Press, Inc., New York, 1979.

25. A. Albert, Regression and the Moore-Penrose Pseudoinverse, Academic Press, Inc., New York, 1972.

26. A. Albert, Regression and the Moore-Penrose Pseudoinverse, Academic Press, Inc., New York, 1972.

4. Publication Citations

(a) Books and Special Issue

1. N.k. Bose, ed. "Multidimensional Systems: Theory and Applications," IEEE Press, New York, 1979.
2. N.K. Bose, "Applied Multidimensional Systems Theory, Van Nostrand Reinhold, New York, 1982.
3. N.K. Bose (Guest Editor), "Aspects of Spatial and Temporal Signal Processing, Circuits, Systems and Signal Processing, Birkhauser Boston, June 1984.
4. N.K. Bose et al, "Multidimensional Systems: Progress, Directions and Open Problems," D. Reidel Publishing Co., Dordrecht, Holland, 1985.

(b) Reviewed Journal Articles

1. N.K. Bose and K.A. Prabhu, "2-D discrete Hilbert transform and computational complexity aspects in its implementation," IEEE Trans. ASSP, Aug. 1979, pp. 356-361.
2. N.K. Bose, "Multivariate polynomial positivity test efficiency improvement," Proc. IEEE, Oct. 1979, pp. 1443-1444.
3. N.K. Bose and S. Basu, "2D matrix Pade approximants: existence, nonuniqueness and recursive computation," IEEE Trans. Auto. Control, June 1980, pp. 509-514.
4. N.K. Bose and J.P. Guiver, "Multivariate polynomial positivity invariance under coefficient perturbation," IEEE Trans. ASSP, Dec. 1980, pp. 660-665.
5. N.K. Bose, "2-D rational approximants via 1-D Pade technique, "Signal Proc: Theory and Appliciations, ed. by Professors Kunt and de Coulon, North-Holland Publishing Co., EURASIP 1980, pp. 409-411.
6. J.P. Guiver and N.K. Bose, "On test for zero-sets of multivariate polynomials in non-compact polydomains," Proc. IEEE, April 1981, pp. 467-469.

7. K.A. Prabhu and N.K. Bose, "Impulse response arrays of discrete-space systems over a finite field," IEEE Trans. ASSP, Feb. 1982, pp. 10-18.

8. S. Basu and N.K. Bose, "Stability of 2-D matrix rational approximants, "IEEE Trans. Auto Control, April 1981, pp. 467-469.

9. J.P. Guiver and N.K. Bose, "Polynomial matrix primitive factorization over arbitrary coefficient field and related results," IEEE Trans. CAS, Oct. 1982, pp. 649-657.

10. J.P. Guiver and N.K. Bose, "Strictly Hurwitz property invariance of quartics under coefficient perturbation," IEEE Trans. Auto. Control, Jan. 1983, pp. 106-107.

11. S. Basu and N.K. Bose, "Matrix Stieltjes series and network models" SIAM J. Math. Anal., March 1983, pp. 209-222.

12. H.M. Valenzuela and N.K. Bose, "Maximally flat rational approximants in multidimensional filter design," Circuits, Systems, and Signal Processing, vol. 2, #1, 1983, pp. 119-128.

13. N.K. Bose, "Properties of the Q_n - matrix in bilinear transformation," Proc. IEEE, Sept. 1983, pp. 1110-1111.

14. N.K. Bose, "Properties of Pade approximants to Stieltjes series and systems," invited paper in book entitled, "Rational Approximation and Interpolation", ed. by P.R. Graves-Morris, E.B. Saff and R.S. Varga, Springer-Verlag, 1985, pp. 182-188.

15. N.K. Bose, "Applications for multidimensional systems theory," invited article in Encyclopedia of Systems and Control, Pergamon Press Ltd., England, scheduled for publication in 1985.

16. N.K. Bose, "Multidimensional Systems stability," invited article in Encyclopedia of Systems and Control, Pergamon Press Ltd., England, scheduled for publication in 1985.

17. N.K. Bose, "Multivariate realization theory," invited article in Encyclopedia of Systems and Control, Pergamon Press Ltd., England, scheduled for publication in 1985.

18. N.K. Bose, "Symbolic and algebraic computations in multidimensional systems theory," invited article in "Papers on the Future of Computer Algebra," SIGSAM Bulletin, ACM, vol. 18, #2, pp. 31-32.

19. N.K. Bose, "A system-theoretic approach to stability of sets of polynomials," invited article in Contemporary Mathematics series, AMS, scheduled to appear in 1985.

e. List of Personnel Associated with the Research Effort

1. N.K. Bose

Dr. N.K. Bose, Professor of Electrical Engineering and Professor of Mathematics at the University of Pittsburgh served as the Principal Investigator. He was responsible for initiating the research, conducting it to its successful completion and supervising the graduate student researchers who worked on this project.

2. Hector M. Valenzuela

Served as a graduate student researcher for eight man-months, from March 1, 1983 to October 31, 1983. He completed his Ph.D. dissertation entitled, "Modeling of Multidimensional Linear Shift-Variant Systems with Applications," in October 1983. The research for this dissertation was supervised by Professor N.K. Bose.

3. H.M. Kim

Served as a graduate student researcher for 13 man-months. Mr. Kim is currently a candidate for the Ph.D. degree in Electrical Engineering. He has been performing his research in the area of restoration of bilinearly degraded images, under the supervision of Professor N.K. Bose.

f. Interactions of Principal Investigator

. Was invited to be a member of the Technical Program Committee of the International Symposium on Circuits and Systems (ISCAS) held at Newport Beach, California, May 2-4, 1983.

2. Was chairman and organizer of a Special Session on "Multidimensional Systems: Spatio-Temporal Filtering" at ISCAS, Newport Beach, California, May 2-4, 1983.

3. Delivered a talk on "Modeling of 2-D LSV systems with applications," based on work co-authored with Hector M. Valenzuela at ISCAS, Newport Beach, California May 2-4, 1983.

4. Invited to give a seminar on "Rational approximants in systems theory," at the U.K. - U.S.A. Conference on Rational Approximation and Interpolation, University of South Florida, Tampa, Florida, December 16, 1983.

5. Invited to give a seminar on "A system-theoretic approach to stability of sets of polynomials," at the NSF sponsored Conference on "Linear Algebra and its Role in Systems Theory," Bowdoin College, Brunswick, Maine, July 29-August 4, 1984.

6. Invited to give a talk entitled, "Novel interpretations in multidimensional systems theory," at the Special Session on "Two-Dimensional Circuits and Systems Theory with Applications," ISCAS, Montreal, May 10, 1984.

7. Invited to give a seminar on "Basic tutorial in multidimensional systems," at Lehrstuhl fur Theoretische Elektrotechnik und Messtechnik, Universitaet Karlsruhe, West Germany, July 19, 1984.

8. Invited to give a seminar on "Aspects of multidimensional Systems theory" at Rutgers University, New Brunswick, New Jersey, on March 21, 1985.

9. Invited to serve as a member of program committee of European Conference on Computer Algebra (Symbolic and Algebraic Manipulation), Linz, Austria, April 1-3, 1985.

10. Invited to give a seminar on "Restoration of bilinearly degraded images," at ISCAS, Kyoto, Japan, June 7, 1985.
11. Invited to present a series of seminars and also to chair a session on "Multidimensional digital signal processing 2," at the Seventh European Conference on Circuit Theory and Design, September 1985.
12. Invited to give a talk on "Status of recent results on image restoration in Multidimensional Systems theory," at the 24th IEEE Conference on Decision and Control, Fort Lauderdale, Florida, December 1985.

8. Specific Applications Stemming from Research Report

Principal Investigator: Dr. N.K. Bose

(a) Primitive Factorization of Bivariate Polynomial Matrices Over an Arbitrary Field of Coefficients: Similar to the widespread use of irreducible matrix fraction descriptions in the 1-D case, such representations in the 2-D case are known to have great potentials. An important outcome of the research conducted has been the presentation of a primitive factorization theorem for matrices of bivariate polynomials over an arbitrary but fixed field of coefficients [1]. This, in turn, leads to a method for obtaining an irreducible matrix fraction description for a matrix of bivariate rational functions over an arbitrary field. In fact the factorization results hold not just for matrices over K[z,w] (K a field), but for matrices over D[w], where D is an arbitrary Euclidean domain (or in theory, over a Principal Ideal Domain). Importantly, the computations required to obtain the factors in K[z,w] depend neither on any extension field nor on the restriction of algebraic closure, in contrast to earlier approaches.

The matrix fraction descriptions obtained are then used to study stability of 2-D feedback systems where the plant and compensator each corresponds to discrete 2-D causal or weakly causal multi-input/multi-output systems. In particular, necessary and sufficient conditions are obtained for an unstable plant to be stable and a classification of the stabilizing compensators are given [2]. These results have proven and potential applications since multidimensional feedback systems have been proposed for various purposes like iterative image processing and restoration [3,4]. Such image processing systems that contain feedback loops are sometimes known to oscillate in space and time and these undesirable oscillations can only be avoided if proper stability conditions are imposed on the feedback systems.

(b) Multidimensional Linear Shift-Variant (LSV) Systems: For any n-D discrete positive cone causal (or weakly causal) LSV system, whose impulse response is approximated by a K-th order degenerate sequence, a K-th order state-space model is obtained [5]. This recursive state-space model is based on a (2^n-1)-points recurrence formula, which for the causal case uses the (2^n-1)-closest neighboring "past" points in addition to the input in order to compute any current output state. For the weakly causal case, the (2^n-1) computed points required are not, in general, the closest neighbors to the present output, which is being computed. Models for the 2-D LSV system and its inverse can be used to perform analysis and deconvolution problems very efficiently. Examples of physically motivated applications making use of the theoretical results have been worked out. These applications include effects of 1-D LSV motion blur and the blurring due to Seidel aberrations of a lens; in particular, the 2-D LSV coma aberration was studied in detail. The reconstruction of the original object from the LSV blurred image was carried out successfully by means of the state-space model for the inverse system. There are several advantages of the approach adopted in this research. First, any impulse response sequence can be approximated arbitrarily closely by a K-th order degenerate sequence by increasing K. The

recursive implementation is associated with reduced space-time computational complexity, so that it is conceivable that degraded images may be processed in real time, when necessary. Though, all types of point-spread functions cannot be modeled via the recursive state-space model, the flexibility provided by the weak causality condition broadens considerably the scopes for applications. Sometimes even a noncausal point-spread function (as illustrated by coma aberration [5]) can be decomposed suitably, the recursive model applied to each part, and the results carefully superimposed to yield the correct solution. Extensions and applicability of the results to image restoration subject to nonlinear (especially bilinear) degrading phenomena in the presence of nonstationary noise is currently being investigated.

References

[1] J.P. Guiver and N.K. Bose, "Polynomial matrix primitive factroization over arbitrary coefficient field and related results," IEEE Trans. Circuits and Systems, 30, Oct. 1982, pp. 649-657.

[2] J.P. Guiver and N.K. Bose, "Causal and weakly causal 2-D filters with applications in stabilization," Chapter 3 of book, "Multidimensional Systems Theory: Progress, Directions and Open Problems," D. Reidel Publishing Co., scheduled to appear in 1984.

[3] G. Ferrani and G. Hausler, "TV optical feedback systems," Optical Engineering, 19, July/Aug. 1980, pp. 442-451.

[4] G. Hausler and N. Streibl, "Stability of spatio-temporal feedback systems," Optica Acta, 1983, pp. 171-187.

[5] H.M. Valenzuela and N.K. Bose, "Linear shift-variant multidimensional systems," Chapter 5 of book, "Multidimensional Systems Theory: Progress, Directions and Open Problems," D. Reidel Publishing Co., scheduled to appear in 1984.

(c) Restoration of Bilinearly Degraded Images: Explained in adequate detail in Section c entitled "Details of Research Results Obtained," of this report.

END

FILMED

11-85

DTIC